POLITECNICO DI MILANO

School of Industrial and Information Engineering

Master of Science in Electrical Engineering

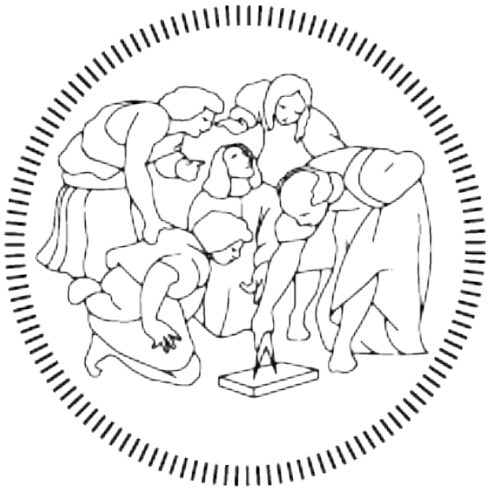

Modelling and Validation in OpenModelica®
Of Utility Scale Battery Energy Storage System Model

Supervisor:

Prof. ***Marco Merlo***

Company co-supervisor:

Ing. ***Ferdinando Parma***

Master's Thesis of:

Ahmed Hasaballah

ID n. 918046

Academic year 2019/2020

Acknowledgment

I would like to thank my supervisors, Professor Merlo and Ing. Parma, for providing guidance and feedback despite the difficult times the whole world was going through.

I would like to dedicate this work to my family and friends for their constant understanding, tolerance, and support.

Finally, I would like to express my sincere gratitude to my former Professor Seif Fatein even though his physical absence his legacy of truth, dedication and academic perseverance still reside among us.

Abstract

Energy has always been linked to fossil fuels but recently this link is being shifted away towards renewable energy sources (RES). Despite their advantages, RES specially wind and photovoltaic are characterized by intermittency and weather dependence, hence making the complex process of generation-load balancing more complex to the network operator. Energy Storage systems (ESS) present a solution to the beforementioned problems and are argued to provide better performance than conventional power plants. In this context, a proper reliability study through software simulation is important to assess the performance of the ESS and evaluate their suitability for maintaining the network's security and quality of service. Modelica® language has been introduced by ENTSO-E to be used in coordinating data exchange in dynamic modelling as it complies with the Common Grid Model Exchange Specifications. CESI S.p.A as a consultant for Terna has implemented the Modelica language in the description of the electric power system components through a library called "Basic Power System". The library has been employed in the proprietary network analysis software TESEO. The aim of this study is to expand the beforementioned library through developing a preliminary standard model of ESS. The first stage is to investigate the pragmatic ESS technologies and their available services provided. The second stage is concerned with the modelling where the structure of the model is founded along the services provided. Finally, the model is tested and validated in TESEO/DYANA through a test grid. The model is found capable of performing active/reactive power control and frequency stabilization services successfully. It will be proposed to ENTSO-E as a basis for the realization of CGMES standard models.

Sommario

L'energia è sempre stata legata ai combustibili fossili, ma recentemente il portafoglio di generazione si sta spostando verso le fonti di energia rinnovabile (FER). Nonostante i loro vantaggi, le FER, in particolare il vento e il fotovoltaico, sono caratterizzati dall'intermittenza e dalla dipendenza dalle condizioni atmosferiche, rendendo così più complesso per il gestore della rete il complesso processo di bilanciamento del carico di generazione. I sistemi di immagazzinamento dell'energia (ESS) rappresentano una soluzione ai problemi sopra citati ,in particolare è possibile regolare tali apparati cosi da avere prestazioni migliori rispetto alle centrali elettriche convenzionali. In questo contesto, un adeguato studio di affidabilità attraverso la simulazione software è fondamentale per valutare le prestazioni degli ESS e valutare la loro idoneità a mantenere la sicurezza della rete e la qualità del servizio. Il linguaggio Modelica® è stato introdotto dall'ENTSO-E per essere utilizzato nel coordinamento dello scambio di dati nella modellazione dinamica in quanto conforme alle Specifiche di scambio del modello di rete comune (Common Grid Model Exchange Specifications). CESI S.p.A in qualità di consulente di Terna ha implementato il linguaggio Modelica nella descrizione dei componenti del sistema elettrico attraverso una libreria denominata "Basic Power System". La libreria è stata impiegata nel software proprietario di analisi di rete TESEO. L'obiettivo di questo studio è quello di ampliare la suddetta libreria attraverso lo sviluppo di un modello standard preliminare di ESS. La prima fase consiste nello studio delle tecnologie ESS pragmatiche e dei servizi disponibili. La seconda fase è invece stata dedicata alla codifica dei servizi erogati dai sistemi di accumulo. Infine, il modello viene testato e convalidato in TESEO/DYANA attraverso un'apposita procedura di prova. Il modello ha dimostrato di essere in grado di eseguire con successo servizi di controllo della potenza attiva/reattiva e di stabilizzazione della frequenza. In ragione degli incoraggianti risultati ottenuti, il modello sarà proposto all'ENTSO-E come base per la realizzazione dei modelli standard CGMES.

Contents

List of Acronyms

ACE	Area Control Error
ARERA	Autorità Di Regolazione Per Energia Reti E Ambiente (Italian Regualtory Authority for Electricity, Gas, And Water)
ASM	Ancillary Services Market
BESS	Battery Energy Storage Systems
BMS	Battery Management System
BPS	Bulk Power System
CAES	Compressed Air Energy Storage
CGMES	Common Grid Model Exchange Standard
CSP	Concentrated Solar Power
DCC	Demand Connection Codes
DER	Distributed Energy Sources
DRES	Distributed Renewable Energy Sources
DSO	Distribution System Operator
ECM	Equivalent Circuit Model
EDLC	Electrochemical Double Layer Capacitor
ENTSO-E	European Network of Transmission System Operators for Electricity
EPRI	Electric Power Research Institute

ESS	Energy Storage Systems
EV	Electric Vehicles
FERC	Federal Electricity Regulatory Authority
FES	Flywheel Energy Storage.
FFR	Fast Frequency Response
FSM	Frequency Sensitive Mode
HVDC	High Voltage Direct Current
ISO	Independent Service Operator
LFSM-U/O	Limited Frequency Sensitive Mode-Underfrequency/Overfrequency
Li-ion	Lithium Ion
Na-S	Sodium Sulphur Battery
NERC	North America Electric Reliability Cooperation
Ni-Cd	Nickel Cadmium Battery
Ni-MH	Nickel Metal Hydride Battery
OCV	Open Circuit Voltage
PCS	Power Conversion System
PFR	Primary Frequency Response
PHS	Pumped Hydro Storage
PPM	Power Park Modules

PV	Photovoltaic
RED	Renewable Energy Directive
RES	Renewable Energy Sources
RfG	Requirements for Generation
ROCOF	Rate of Change of Frequency
SMES	Super-Conducting Magnetic Energy Storage
SOC	State of Charge
SOH	State of Health
TSO	Transmission System Operator
VRB	Vanadium Redox Battery
WECC	Western Electricity Coordinating Council

List of Tables

List of Figures

1. Energy Storage Systems

Energy is the cornerstone of the economy, development and welfare of societies; it has always been linked to fossil fuels but recently this link is being shifted away from fossil fuels towards renewable energy sources (RES). With their falling investment costs [1] RES are introducing new green features to the energy equation that their fossil fuels counterparts failed to achieve. Renewable energy sources now can offer sustainable solutions to Fossil fuel challenges such as: greenhouse gases emissions, air pollution, water contamination, strategic energy dependence, and rural electrification expansion.

In the past 20 years Photovoltaic and Wind energy have had the biggest share in the annual worldwide renewable energy growth [2] with ratios 36.5% and 24.5% respectively. Despite their advantages, renewable sources specially wind and PV are characterized by intermittency and weather dependence, which make the complex process of generation-load balancing even more complex to the network operator.

Fortunately, Energy Storage systems (ESS) present a solution to the beforementioned problem and can perform the continuous generation-load balancing procedure from a scale of few millisecond up to several hours [3], even with better performance than conventional power plants. As reported in Figure 1-1 by selecting the correct technology, ESS can help to solve the power quality, intermittency, and uncontrollability challenges related to renewable energy power production.

Combining the previous mentioned drawbacks of renewables and the latest technological advancements in the energy storage field with the new limits set by the European Union for the renewable energy consumption and greenhouse gas savings in RED II [4], only reveals that energy storage systems are playing a crucial role in the future of the electric power systems.

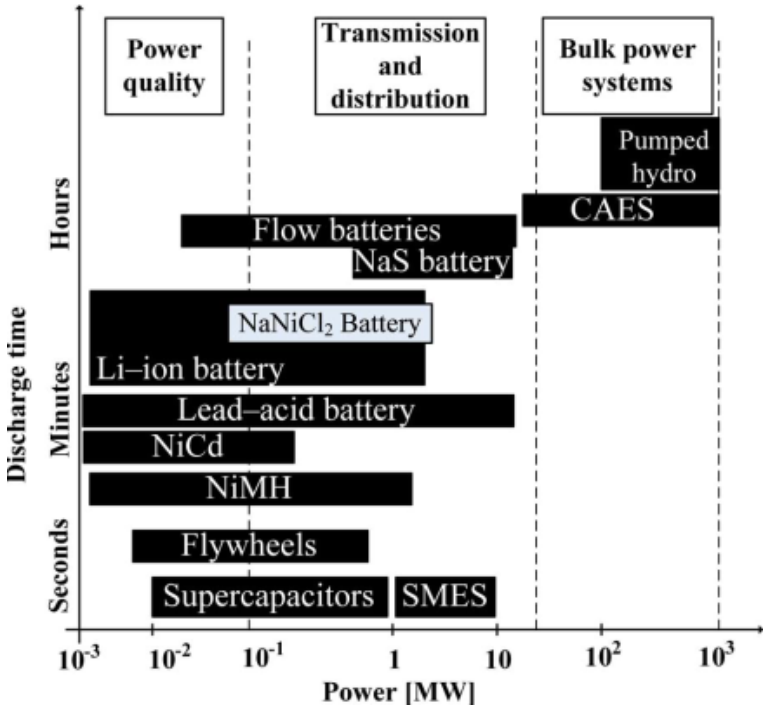

Figure 1-1 Storage technologies for power systems [3]

Energy storage systems are categorized into 5 main categories [5]:

- Mechanical storage systems which store energy in the form of mechanical energy such as pumped hydro storage (PHS), compressed air energy storage (CAES), and flywheel energy storage (FES).

- Chemical storage systems which store energy in the form of a chemical such Hydrogen gas for fuel cells.

- Thermal storage systems which store energy in the form of thermal energy such sensible heat storage of fluids in concentrated solar power (CSP) plants.

- Electrochemical storage systems which store the energy in the form of electrochemical reactions such battery energy storage systems (BESS).

- Electrical storage systems which store energy in the form of electrical charges such as super-conducting magnetic energy storage (SMES), and super capacitors.

1.1. Energy storage technologies

For an energy storage system to work properly for a specific application the suitable technology must be selected depending on various criteria[5], [6]:

- Power density [W/Kg].
- Energy density [Wh/kg].
- Self-discharge rate.
- Lifetime.
- Cycle efficiency.
- Response time.
- Power capital cost.
- Energy capital cost.

– **Pumped hydro storage system (PHS)** is relatively an old energy storage technology, where the system stores the electrical energy in pumping water from a low-altitude reservoir to a high-altitude reservoir. PHS systems have the highest share in the installed storage power worldwide [7] with 125 GW installed. They are characterized by high power ratings from 1 to 3000 MW, very long life, and theoretically infinite cycle numbers. However, PHS systems have several drawbacks: high investment cost, site specific, slow response time, and long construction duration. For these reasons PHS systems are suitable for bulk energy services.

– **Flywheel energy storage system (FES)** utilizes the angular momentum of a rotating disc to store electrical energy thus converting electrical energy into kinetic energy and vice versa. FES systems are characterized by high efficiency 85% to 90%, high power density, and a high response rate [3], [7]. Unfortunately, they suffer from high self-discharge rate, low energy density, and high specific costs which make them an immature technology that have high potential for improvement by research.

– **Compressed air energy storage (CAES)** systems store the energy in the form of compressed air aboveground or underground where it can be converted to electrical energy by heating and expanding the air via a turbine-generator system. CAES systems exhibit grid scale potential, long life, and low self-discharge rate but they are limited by geographical site constraints, and relatively low efficiency [3], [5], [7].

Battery energy storage systems (BESS) are the earliest energy storage technology established, as they date back to the 18th century, which store the energy in the form of electrochemical redox reactions. BESS are extremely versatile, cost efficient, and include various families of technologies that could be found in almost everyday applications.

- **Lead acid batteries** invention dates to the 19th century hence they are considered mature technology. They exhibit fast response time, low specific cost, low self-discharge rate, and good cycle efficiency. On the other hand, they suffer from low energy and power density, lifetime dependency on charging/discharging rate, temperature degradation and environmental hazards. Lead acid batteries are used in stationary applications and have been the main choice for telecommunication systems and emergency power supply in the past years. [3], [8].
- **Lithium ion (Li-ion) battery** is a cluster of battery technologies emerged in the 1970s employing lithium in layered graphite sheets in the anode and a lithium metal oxide in the cathode [9]. Li-ion batteries are characterized with high energy density compared to lead acid, low self-discharge rate, long life cycle, fast response rate, fast charge/discharge, high power density, high efficiency, and maintenance free. Because of their advantageous features, Li-ion batteries have gained a large share in the portable electronics industry, electric vehicles, and grid applications.[3], [8]

Table 1-1 summarizes the specification of the beforementioned energy storage technologies along with additional technologies which are less commercial. On the other hand Figure 1-2 and Figure 1-3 present a comparison of different energy storage technologies regarding their power and energy density, and cycle life and efficiency.

Table 1-1 Comparison Energy Storage Systems

Type	Energy Efficiency (%)	Energy Density (Wh/kg)	Power Density (W/kg)	Cycle Life (cycles)	Self Discharge
Pb-Acid	70–80	20–35	25	200–2000	Low
Ni-Cd	60–90	40–60	140–180	500–2000	Low
Ni-MH	50–80	60–80	220	< 3000	High
Li-Ion	70–85	100–200	360	500–2000	Med
Li-polymer	70	200	250–1000	> 1200	Med
NaS	70	120	120	2000	–
VRB	80	25	80–150	> 16000	Negligible
EDLC	95	< 50	4000	> 50000	Very high
Pumped hydro	65–80	0.3	–	> 20 years	Negligible
CAES	40–50	10–30	–	> 20 years	–
Flywheel (steel)	95	5–30	1000	> 20000	Very high
Flywheel (composite)	95	> 50	5000	> 20000	Very high

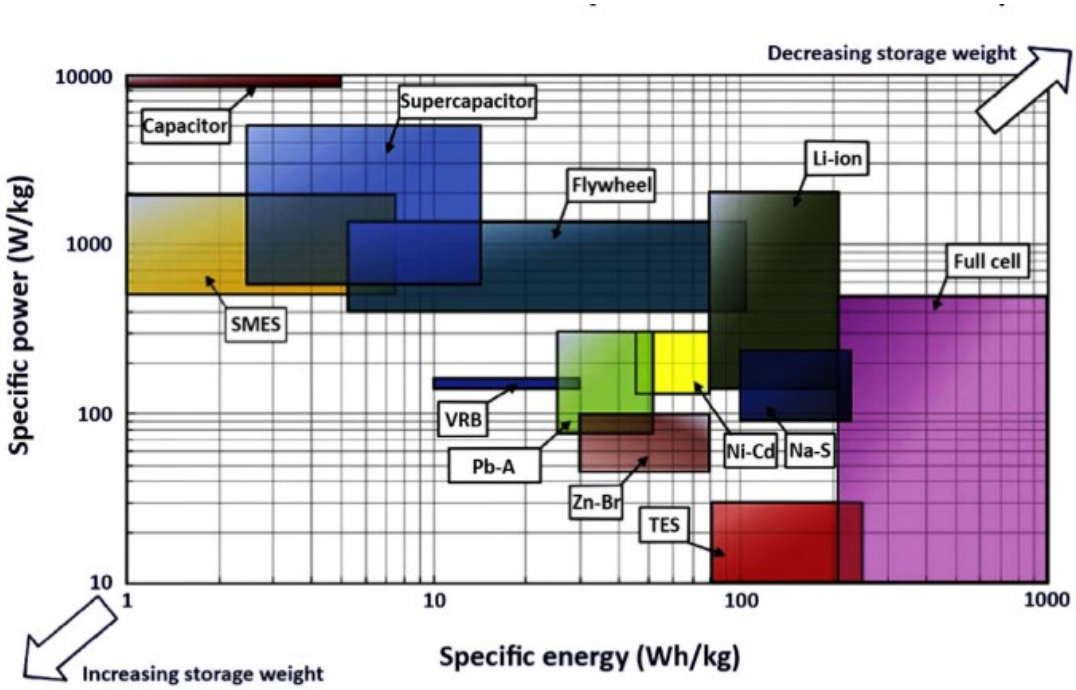

*Figure 1-2 Comparison of different **ESS** with respect to energy and power density*

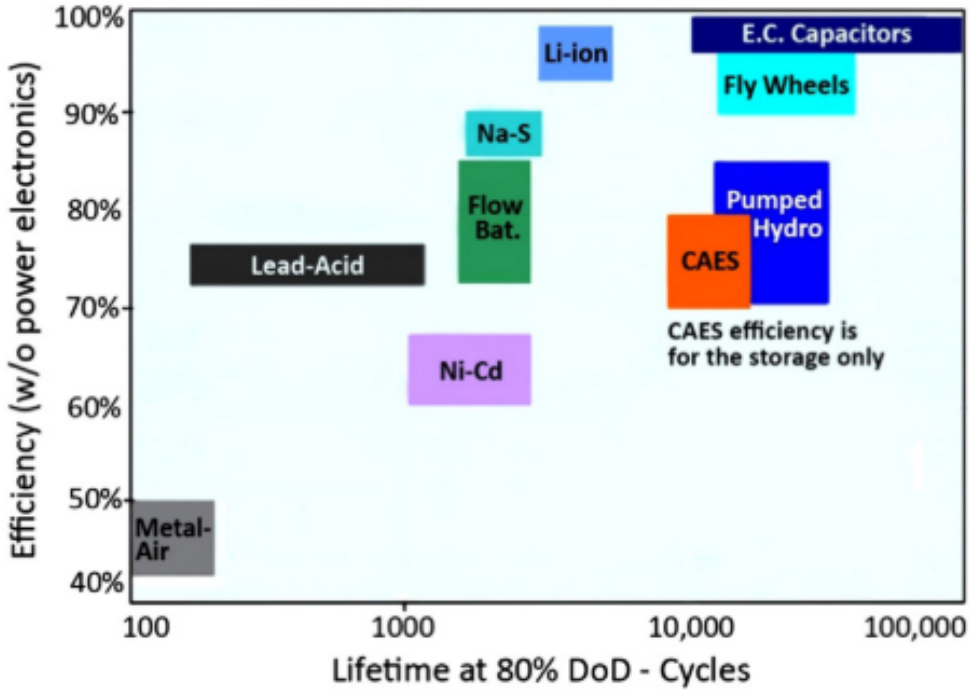

*Figure 1-3 Comparison of different **ESS** with respect to cycle life and efficiency.*

Figure 1-4 represents a comparison between different utility-scale ESS technologies costs and estimated forecasts based on a system of 4 hours duration at rated power.

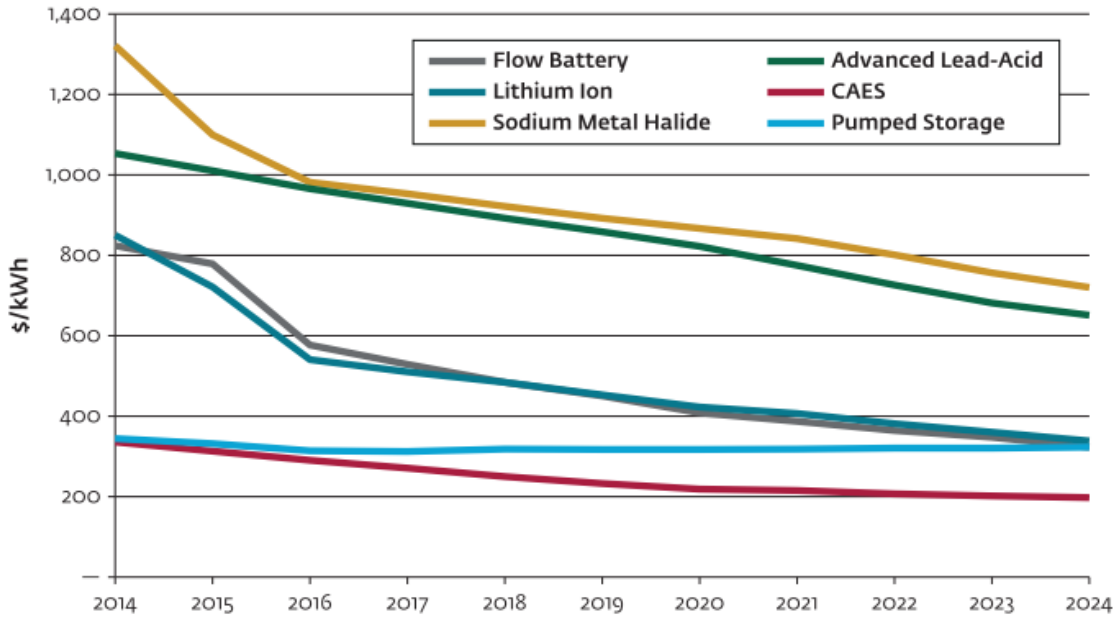

Figure 1-4 Utility-Scale Energy Storage System Cost Trends by Technology

1.2. Energy storage systems for grid applications

1.2.1. Transition to smart grid architecture

The increasing capacity of intermittent renewable energy sources [9], mostly wind and solar in Figure 1-5, along with the challenging attributes of the smart grid architecture where microgrids are the key role figures, have created a technological need for the completion of the transition as the operation and planning of the grid would become difficult with the traditional market players.

The new advancements in the energy storage systems (ESS) have made it possible for ESS to satisfy that technological need. ESS can perform bulk energy services as absorbing excess energy from the PV power plants in low demand times and injecting them back in peak hours. ESS can participate in the Ancillary services market (ASM) through frequency regulation, spinning reserve, and black start-up. ESS can help in energy management services through demand side management and peak shaving. The detailed structure of the services which could be provided by energy storage systems are described in Figure 1-6.

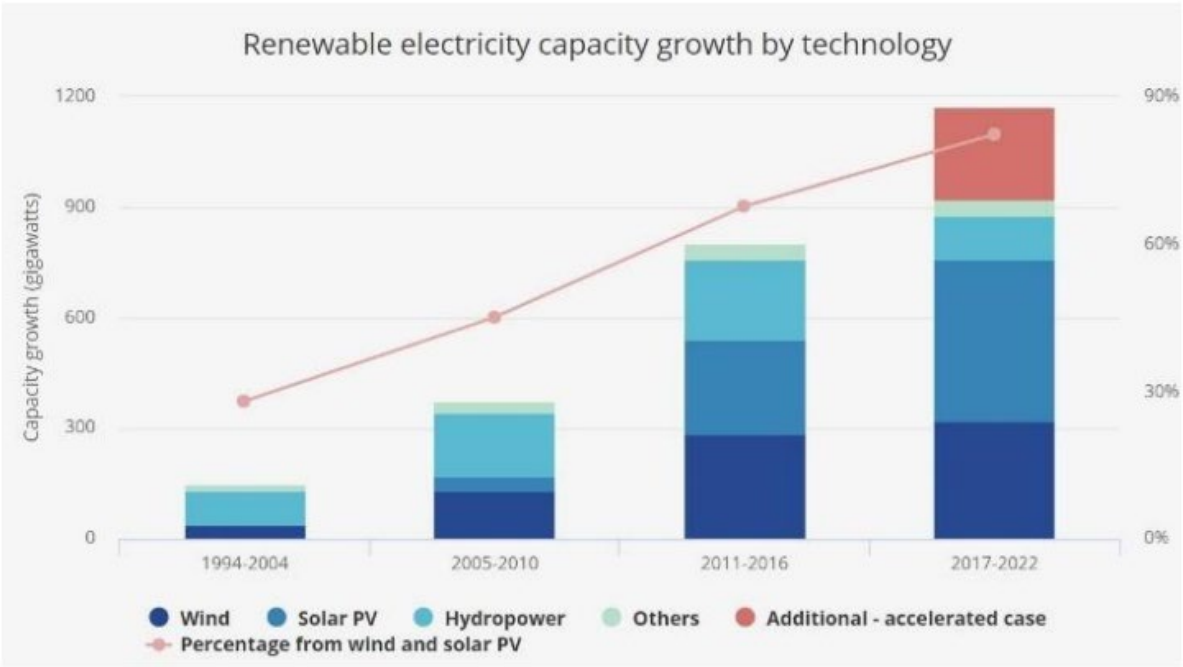

Figure 1-5 Capacity growth of renewable energy sources

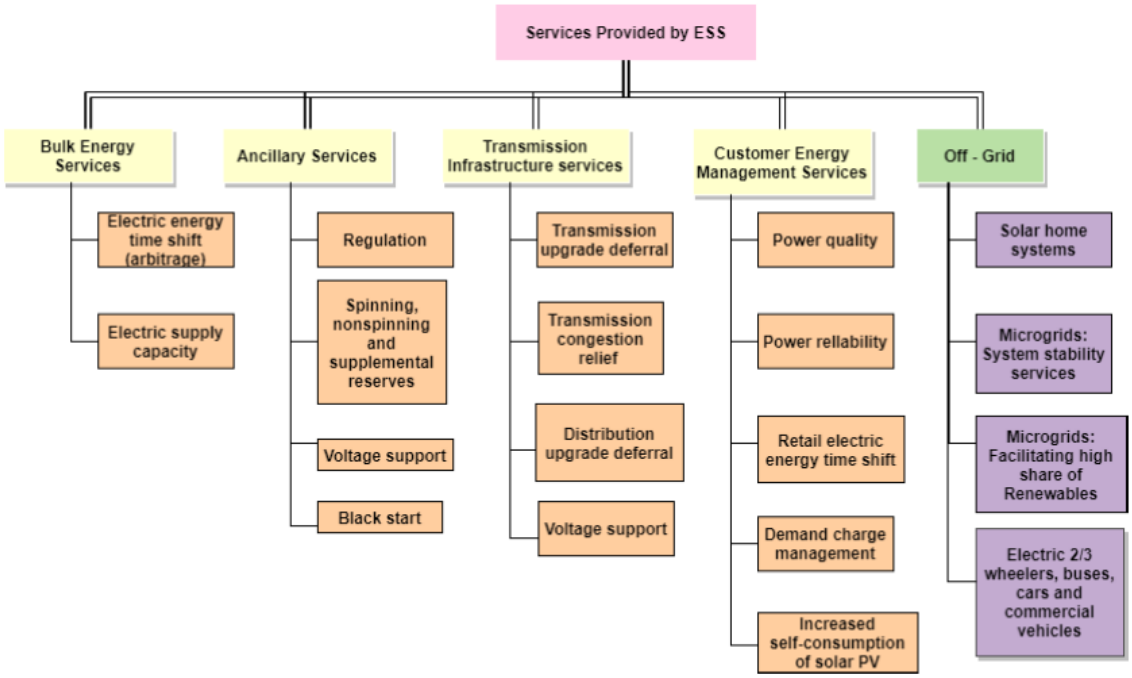

Figure 1-6 Grid services offered by ESS

1.2.2. Trends in utility scale energy storage systems

Utility scale energy storage systems are stationary storage systems which provide different energy services for the system operation. Utility scale energy storage systems can either be connected to the national transmission/distribution grid or to a private islanded microgrid system. They span from few megawatt-hours for pilot projects up to hundreds of megawatt-hours for transmission service provider's (TSO) projects.

Pumped hydro storage (PHS) systems accounts for almost 96% of the world energy storage power capacity [9], but PHS is a matured technology which suffer from environmental and restricted geological implantation thus constraining the future of its future development. Since 2003 the United States of America have almost excluded PHS systems from its new utility scale energy storage systems [10].

As previously mentioned, Lithium-ion batteries exhibit high power/energy density, high cycle efficiency, and fast response which added this to the drastic decrease of their cost have made Li-ion battery a good candidate for utility scale energy storage systems. In the past few years Li-ion batteries share in the global battery storage new installation had been increasing as seen in Figure 1-7 [11].

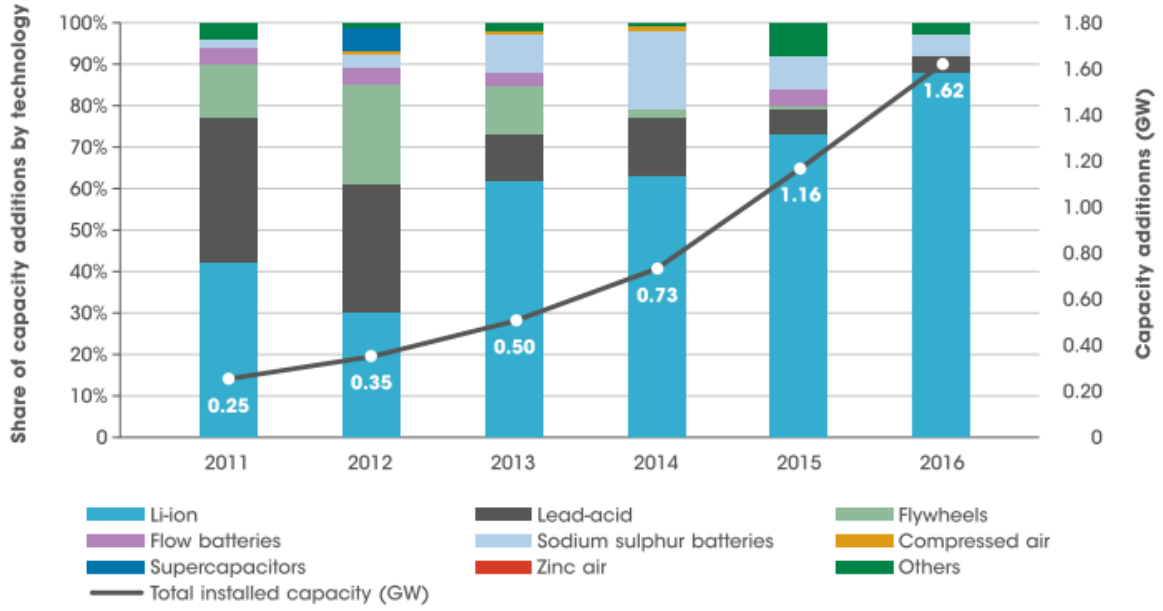

Figure 1-7 Global increase of the share of Li-ion in the annual global battery installation

In addition, Li-ion technology offers the highest estimated fuel savings, highest average roundtrip efficiency, and lowest instalment cost compared to other technologies in remote microgrids as shown in Table 1-2 [12].

Table 1-2 Estimated fuel savings and system costs of BESS in remote microgrids

Battery Type	Installed Cost ($/kW)	Est. Annual O&M Cost ($/kW)	Avg. Round-Trip Efficiency	Est. Annual Fuel Savings (L/kW)	Est. Annual Fuel Savings ($/kW)
Flow Battery: Utility-Scale	2,300.2	31.1	70%	1,680	1,831.2
Flow Battery: Distributed	2,874.4	34.5	70%	1,680	1,831.2
Advanced Lead-Acid: Utility-Scale	2,903.5	66.2	80%	1,920	2,092.8
Advanced Lead-Acid: Distributed	3,284.5	66.8	80%	1,920	2,092.8
Lithium Ion: Utility-Scale	2,062.0	47.3	90%	2,040	2,223.6
Lithium Ion: Distributed	2,150.3	50.8	90%	2,040	2,223.6

1.2.3. Battery energy storage system role in frequency regulation

An ideal electric power system operates at a constant frequency 50/60 Hz where the active power generated is equal to the active power consumed at every time step of the day. But ideal conditions do not occur in real life because of the unpredictability of weather conditions for RES systems, constant change of loads, and contingencies. Therefore, the electric power system operates in a dynamic equilibrium state with a 60 milli-Hz window [13] around the nominal 50Hz frequency, for European Union, through the frequency regulation services.

Frequency control maintains the momentary supply-demand balance of the system hence keeping the frequency of the system within the acceptable range. In the past thermal and hydro powerplants were the only players allowed to participate in the regulation through the turbine governor control, but it gave rise to inefficient operation of the thermal units as some of them were left on standby or operated at inefficient setpoints hence increasing the production cost of electricity. The slow response time of thermal units is an additional crucial drawback where units may take up to minutes to respond to TSO/ISO signal for frequency regulation.

On the contrary of conventional units, battery energy storage systems can provide frequency regulation with response time up to milliseconds. BESS can provide solution to fuel volatility of thermal units with more profitability. The BESS can provide other services to the system with better performance than thermal units such: spinning reserve, voltage/reactive power support, load following, and peak shaving hence increasing the system stability and security. In 2016 the transmission system operator in the UK, through a technology neutral auction, contracted 200 MW of battery energy storage systems for frequency regulation [11].

The United States energy administration has reported that more than 80% of the utility scale battery energy storage systems installed provide frequency regulation as presented in Figure 1-8.

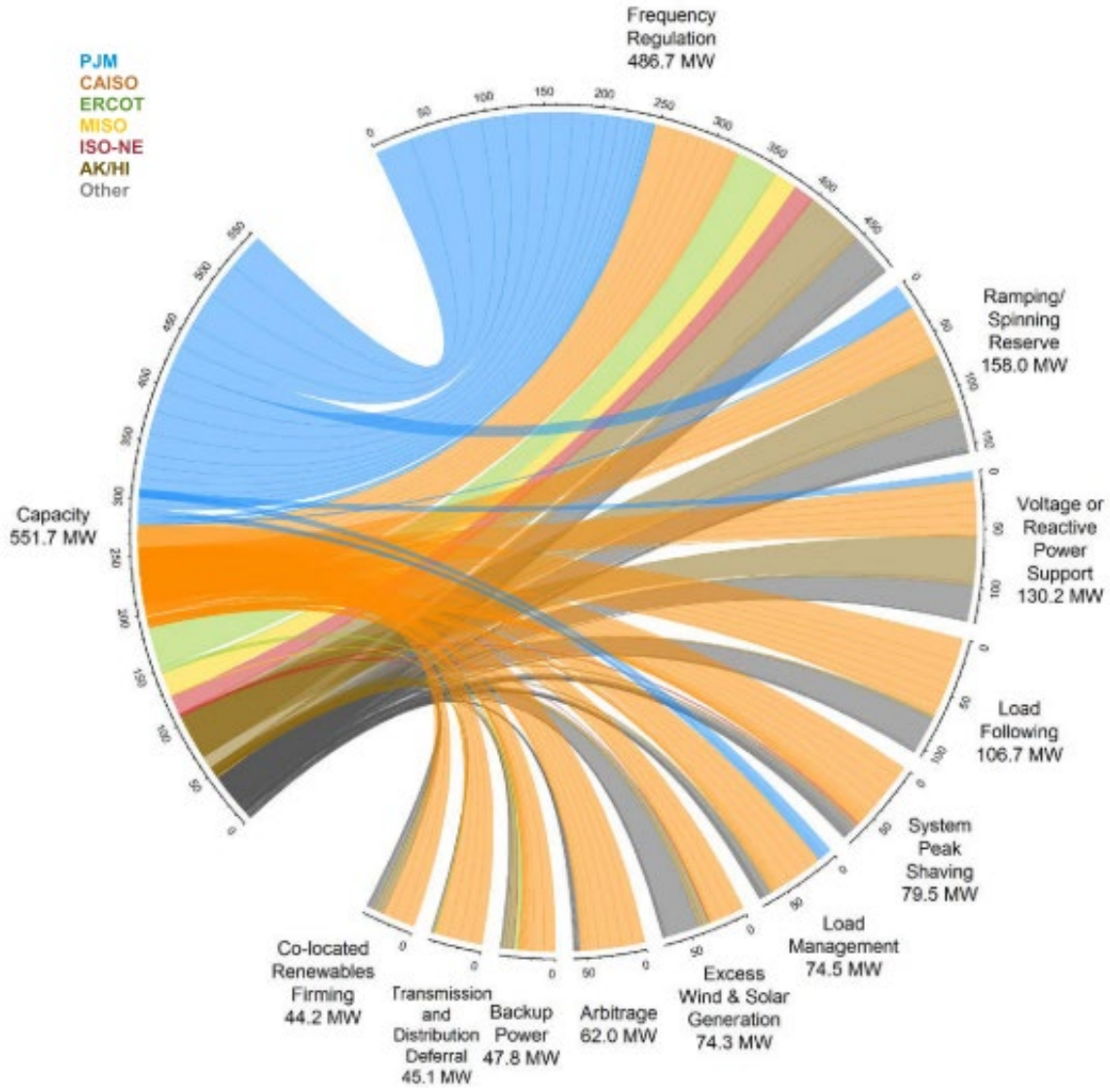

Figure 1-8 U.S utility scale BESS capacity and applications provided

2. Frequency regulation services

The frequency regulation process is a multistage process in which network codes define the role of each component and how these components interact with each other as shown in Figure 2-1 [14].

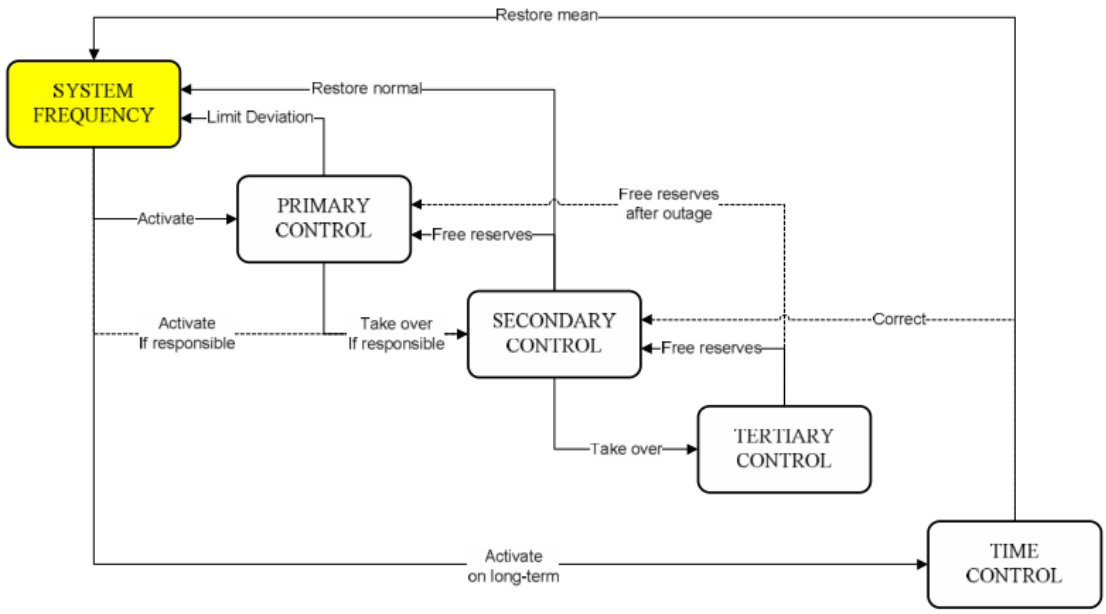

Figure 2-1 Frequency regulation process components

- Primary Frequency response (PFR)/Frequency containment process is the process where actions provided by active units aim to stabilize and arrest the network frequency as a reaction to frequency deviation signals. Traditionally PFR comes from automatic generator governor response based on local signals [15].
- Secondary Frequency response/Frequency Restoration process is the process where actions provided by active units aim to restore both the system frequency to its nominal value and the primary frequency reserves to its scheduled limits. Secondary frequency response can be automatic based on local signals or manual based on a system operator signal [15], [16].
- Tertiary Frequency response/Reserve replacement process is the process where actions provided by active units aim to zero the area control error (ACE) and restore the secondary frequency reserves to their scheduled limits. Tertiary frequency response are manually activated by the system operator's signals [15], [16].

Figure 2-2 [16] shows the link between the frequency real time value and the distinct components of the frequency regulation process.

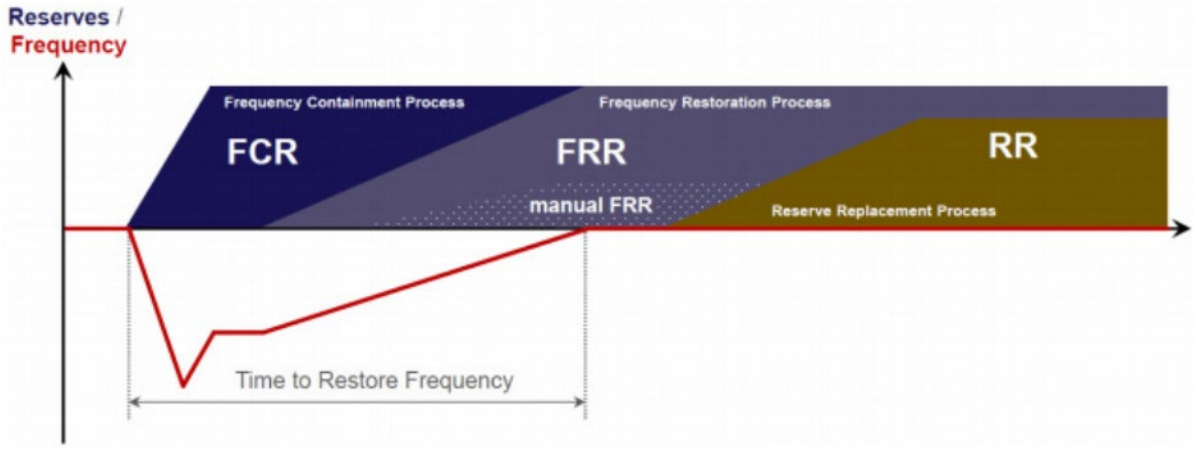

Figure 2-2 Frequency regulation processes operation through a frequency deviation

2.1. Primary Frequency regulation

Primary frequency control is a crucial fragment in the process of maintaining the electrical network's stability and reliability. Primary Frequency control is the first responder to a frequency deviation operating within seconds from the trigger signal aiming to arrest the variation and stabilize the frequency. Primary frequency control is automatic based on local signals but coordinated on a centralized scale to ensure its efficiency and avoid unwanted instabilities [15].

In the electrical power system, the sudden event of a generation power loss is first met by the tendency of the system to resist this change, also known as the system's inertia, where the rotating machines connected to the system utilize the kinetic energy stored in them to make up for the generation loss causing a decline of the system frequency from the nominal value. Upon hitting a specific underfrequency threshold primary frequency control automatically operates and increases the generating power to meet the demand to arrest the frequency deviation. As a result, the primary frequency control re-establishes the electric power equilibrium, stabilizing the system frequency but does not restore it to its nominal value [15].

The process is shown in Figure 2-2, the frequency deviation was assumed to be based on a generation loss as the probability of generation loss event is higher than a similar load loss. In the loss of load event the same logic is used but the kinetic energy stored in the rotating machines will increase hence increasing the frequency of the system and the primary frequency

control will act on decreasing the output power of the generating unit. Consequently, units participating in the primary frequency control must keep a power margin between the operating point and the maximum feasible power and the declared minimum technical power. In rotating machines, the primary response is performed by the governors operating on the generators' valves based on the assigned generator droop while in electronically coupled units it is done by the electronics' controller.

2.1.1. Generator Droop

The droop of a generator is a dimensionless ratio usually expressed in percentage between the relative variation of frequency and the relative variation of the generator power [13] :

$$\sigma\_p\ (\%) = -\frac{\left(\frac{\Delta f}{50}\right)}{\frac{\Delta P_e}{P_{eff}}} \times 100$$

Where the variation of the system frequency is defined as follows, where (f) is the measured frequency:

$$\Delta f = f - 50$$

The relative variation of the output power is defined as the ratio between the variation of output power of the generator (ΔP_e) (at steady state given that the primary control output has not been depleted) and the maximum active power that the unit can produce continuously (P_eff) [13].

Figure 2-3 [14] shows how generating units with the same primary control reserve react differently to the same frequency disturbance as a result of the different droop value setting. For a small disturbance ($Frequency\ disturbance\ < \Delta f\_b$) the contribution of generator 'a' ,which has the smaller droop coefficient, will be larger than that of 'b'. The frequency deviation (Δf_a) at which generator 'a' will deliver its maximum power will be less than that of 'b' (Δf_b) even though both have the same primary reserve. For a large disturbance ($Frequency\ disturbance\ > \Delta f\_b$) both generators will be delivering the same output power.

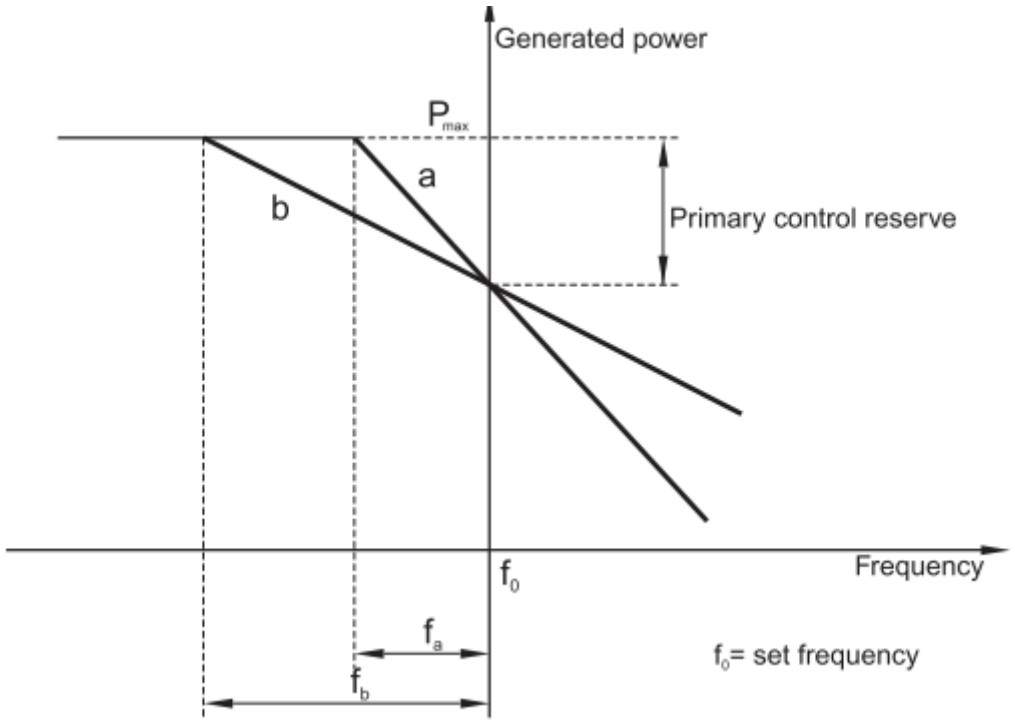

Figure 2-3 The effect of different droop values on the same primary control reserve

The regulating energy [MW/Hz] of a generating unit is defined as the ratio between the variation of the electrical power delivered by the unit (ΔP_e) to the frequency variation that caused this variation (Δf) [13]:

$$K_r = -\frac{\Delta P_e}{\Delta f} \left[\frac{\text{MW}}{\text{Hz}}\right]$$

2.2. Grid Codes for Primary frequency response in Italy; Terna

In Italy Primary frequency regulation is obligatory for all units whose nominal power is greater than 10 MVA excluding non-programmable renewable energy units.

2.2.1. Minimum Primary Reserve

In the case of continental Italy and Sicily, in the case it is programmed to be connected to continental Italy, all the units participating in the primary control must guarantee a minimum of 1.5% of its effective power where the maximum and the minimum operating points are as follows [13]:

- $P_{min} = P_{MT} + 1.5\% P_{eff}$
- $P_{max} = P_{max\ deliverable} - 1.5\% P_{eff}$

Where P_{MT} is the minimum technical power.

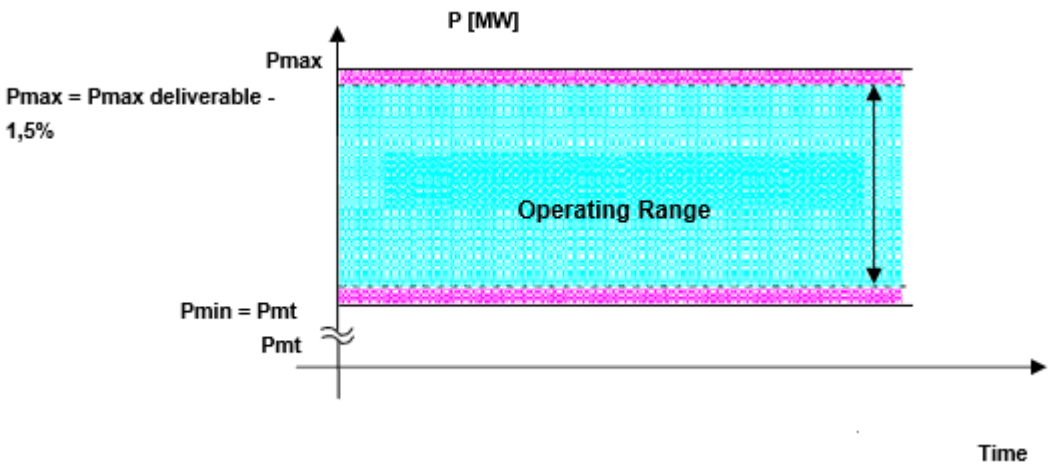

Figure 2-4 Admissible operating range for the participating units in continental Italy and Sicily in the case it is connected to the continental Italy.

For Sardinia, always, and Sicily, only in the case that it is scheduled that Sicilia will be disconnected from continental Italy, all the units participating in the primary control must guarantee a minimum of 10% of its effective power where the maximum and the minimum operating points are as follows [13]:

- $P_{min} = P_{MT} + 10\% P_{eff}$
- $P_{max} = P_{max\ deliverable} - 10\% P_{eff}$

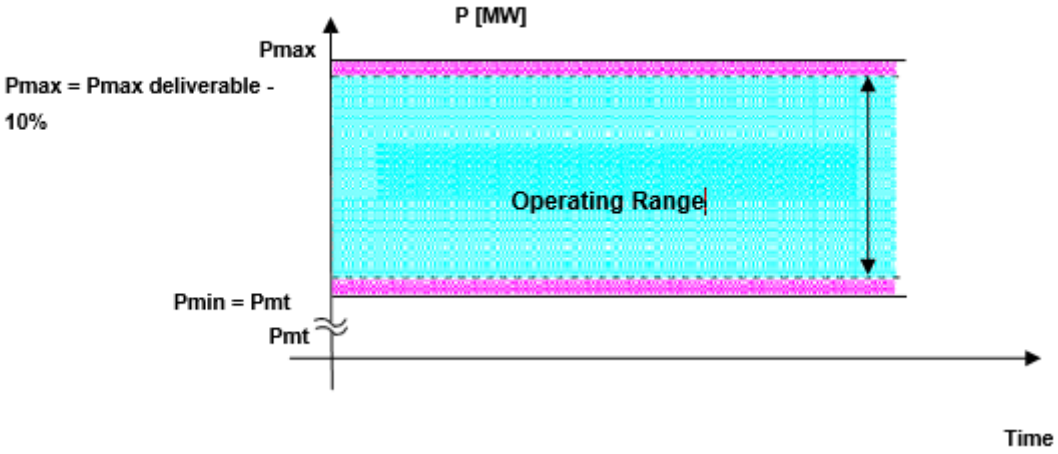

Figure 2-5 Admissible operating range for the participating units in Sardinia, always, and Sicilia in the case it is disconnected to the continental Italy.

2.2.2. Deadband and Droop Value

Terna describes the droop requirements for generators as follows [13]:

Parameter	Range
Droop	• For Hydroelectric units, the droop value must be equal to 4%. • For Thermal units, the droop value must be equal to 5%.
Deadband	• For Hydroelectric units and steam units of simple cycle, the intentional deadband must not exceed ±10 mHz. • For steam units of combined cycle and gas turbine units, the deadband must not exceed ±20 mHz.

For all types of systems, the frequency response sensitivity of the regulator must be less than ±10 mHz. An adaptation is made for old plants whose regulator's sensitivity surpasses ±10 mHz, where the intentional deadband is combined with the regulator's sensitivity and together they do not exceed ±30 mHz.

2.2.3. Service provision modalities

- In the normal grid operating conditions and for units operating in the admissible operating range indicated in Figure 2-4 and Figure 2-5, every unit must supply a (ΔP_e) amount of power for the frequency variation (Δf) according to the equation :

$$\Delta P\_e = -\frac{\Delta f}{50} . \frac{P_{eff}}{\sigma_p(\%)}$$

- Within 15 seconds from the start of the frequency variation Δf, at least 50% of the required power ΔP_e must be delivered by the participating unit.
- Within 30 seconds from the start of the frequency variation Δf, 100% of the required power ΔP_e must be delivered by the participating unit.
- Once the service is initiated and the required power ΔP_e has been supplied, the participating unit must be able to supply the new power setpoint for at least 15 consecutive minutes.

2.3. Fast Frequency regulation

2.3.1. Consequences of green energy revolution

Traditional thermal units have always been the corner stone of the ancillary services markets, ensuring the reliability and security of the bulk electrical power system operation. However, in the past few years the electric power sector has been going through an extensive transformation by abandoning conventional power plants and adopting renewable energy sources. The shortcomings of this transformation and how it is impacting the security of the power system have now begun to be observed. In the future it is expected that these effects will be more evident as more conventional units will be replaced by renewable energy powered units.

Through the last decade the European Union has been trying to comply with the renewable energy directive target for 20% of the total energy coming from renewables by 2020 and 32% of the total energy coming from renewables by 2030 [4]. Hence the impacts of increasing shares of renewables are more visible and can be demonstrated by the following trends [17], [18]:

– Reduction of the available regulating power required for keeping the bulk power system operating securely. Renewable energy sources are intermittent and cannot provide regulating power adding up with their displacement of traditional units, the availability of power reserve for frequency and voltage regulation has decreased accompanied by a demand increase for power. Figure 2-6 illustrates more the problem [19].

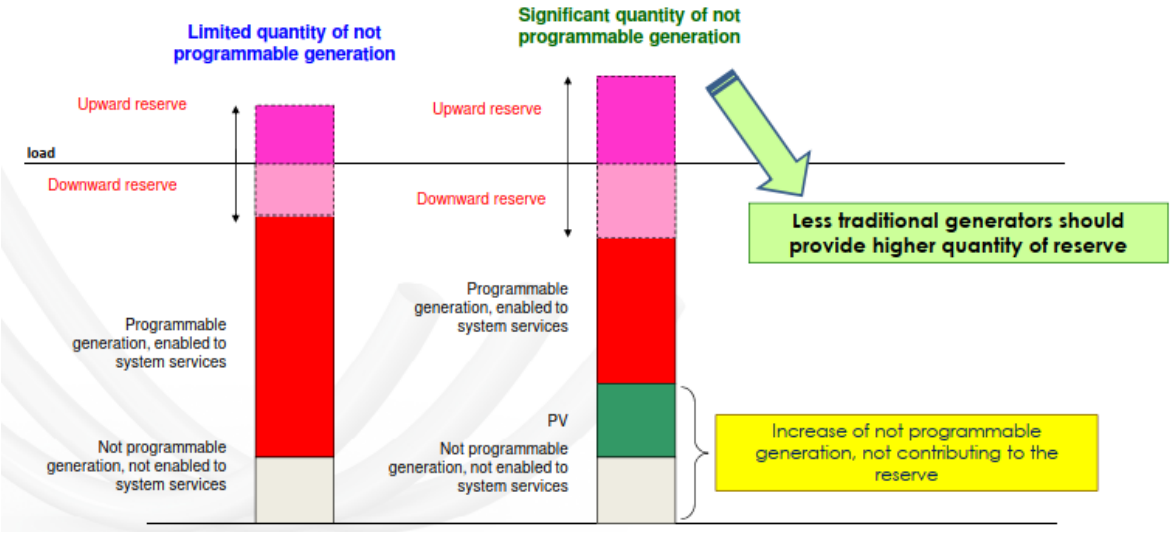

Figure 2-6 Impact of the increase of RES units on the BPS security

– Reduction of the bulk power system inertia. With the increase of inverter based renewable energy sources more thermal units were displaced from the system, as shown in Figure 2-6, thus decreasing the overall kinetic energy stored in the rotating masses of the units. The significant loss of the system's inertia can affect the frequency response and the security of the system during transient period after the loss of bulk generation. Figure 2-7 demonstrates a traditional frequency response of a system after generation loss, the blue curve represents the system with lower inertia. It can be concluded that the system with lower inertia experiences a steeper rate of change of frequency (ROCOF), and a greater frequency minima that occurs sooner than that of the other system [17].

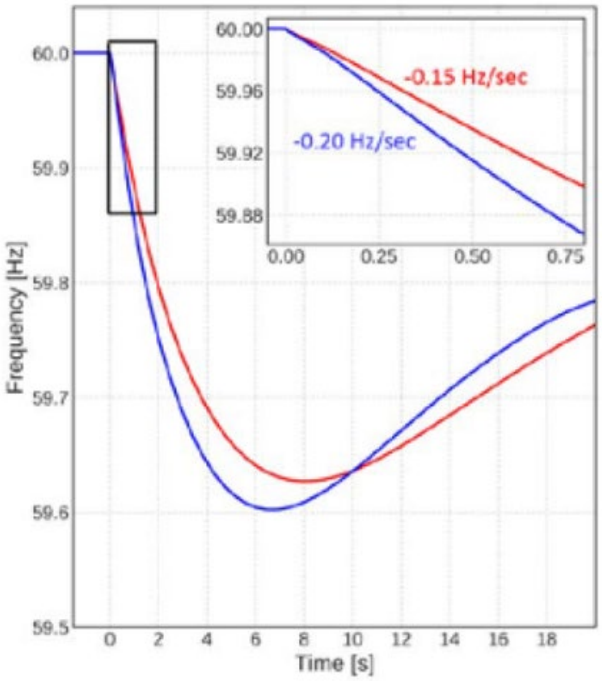

Figure 2-7 Impact of the system inertia on the frequency minima and ROCOF after generation loss

– The possibility that the largest single contingency is no longer because of the tripping of a single large unit but rather because of the tripping of multiple renewable distributed energy resources (DER) within the same perimeter because of a fault or multiple DER dispersed because of ride through ROCOF protection [17].
– Increase in the probability of network congestion as renewable energy sources like wind and solar often are site specific, due to weather conditions, and are located far from consumption zones.

– Increase in the steepness of the evening ramp of the duck shaped residual load curve because of the increase in deployment of photovoltaic powerplants and increase in the RES overgeneration time period where excess power is curtailed, both represented in Figure 2-8 [18].

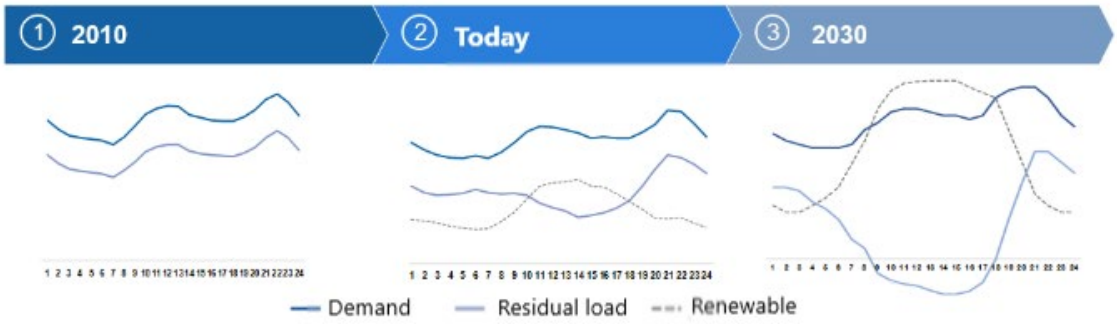

Figure 2-8 Evolution of the residual load curve with the increase of RES

2.3.2. The need to define new grid services.

Figure 2-9 shows a standard system response following a sudden loss of relatively large generation where primary, secondary, and tertiary control collaborate into containing the event and restoring the system to its normal state [17]. At time t=0 the event occurs, and the rotating machines of the system start supplying the system with their kinetic energy as an act to oppose the change: system inertia. The speed of the rotating machines begins to decline and consequently the frequency of the system, after some time the primary frequency control is initiated and starts supplying the system with reserve power leading to stopping the frequency deviation and the system frequency hits a minimum point. This minimum point is defined as the nadir and the period from the event start to the nadir is called the arresting period. As illustrated before in Figure 2-7 the frequency nadir and the ROCOF are influenced by the system inertia which is dependent on the amount of rotating machines operating in the system during the event.

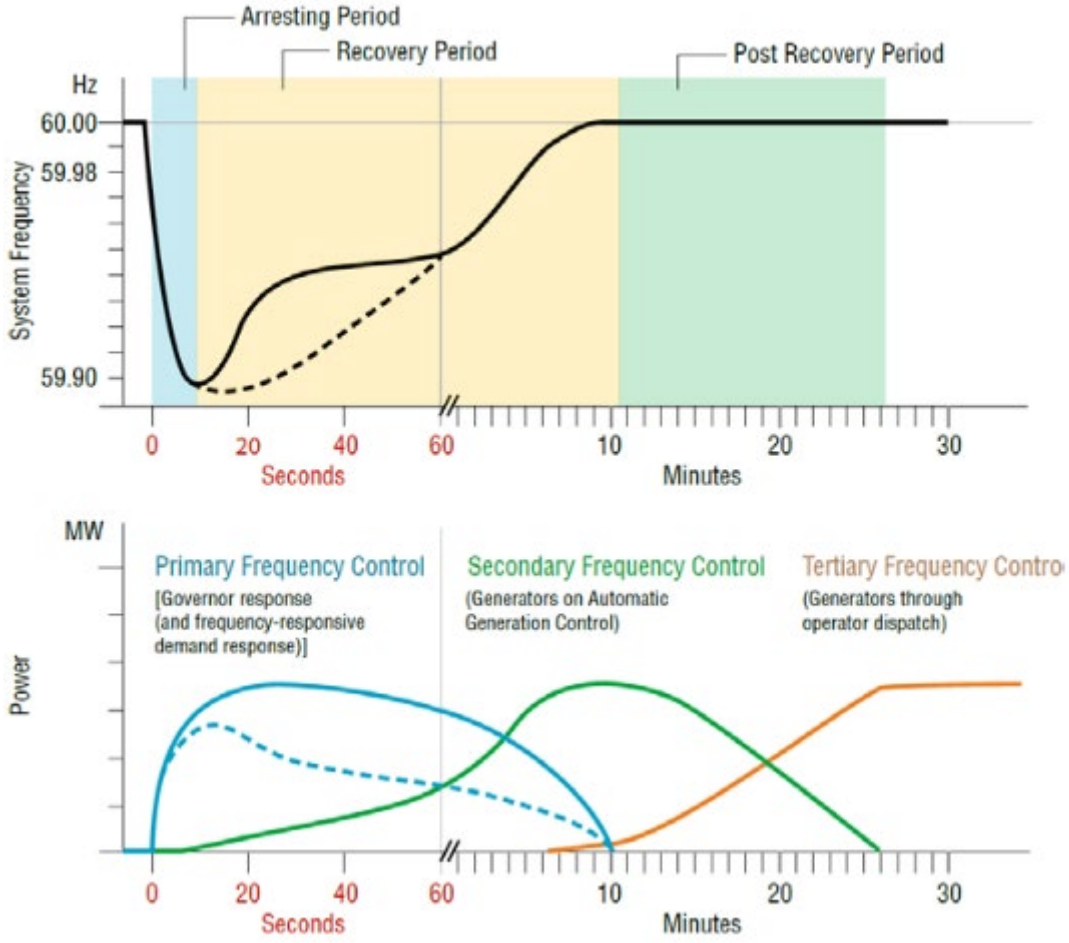

Figure 2-9 System frequency response with the respective time frames

The Italian national energy and climate plan (NECP) compares the number of hours where 50% of the loads are covered by synchronous machines in 2017 and the predicted values in 2025 and 2030 as a result of complying by REDII requirements in Figure 2-10 [18]. The number of hours decline from approximately 8700 hours/year in 2017 to 7900 hours/year in 2025 and 5900 hours/year in 2030. This declination will translate in the future into a loss of the system inertia and the ability of the system to resist sudden power imbalances as inverter-based units offer almost zero to the system's inertia.

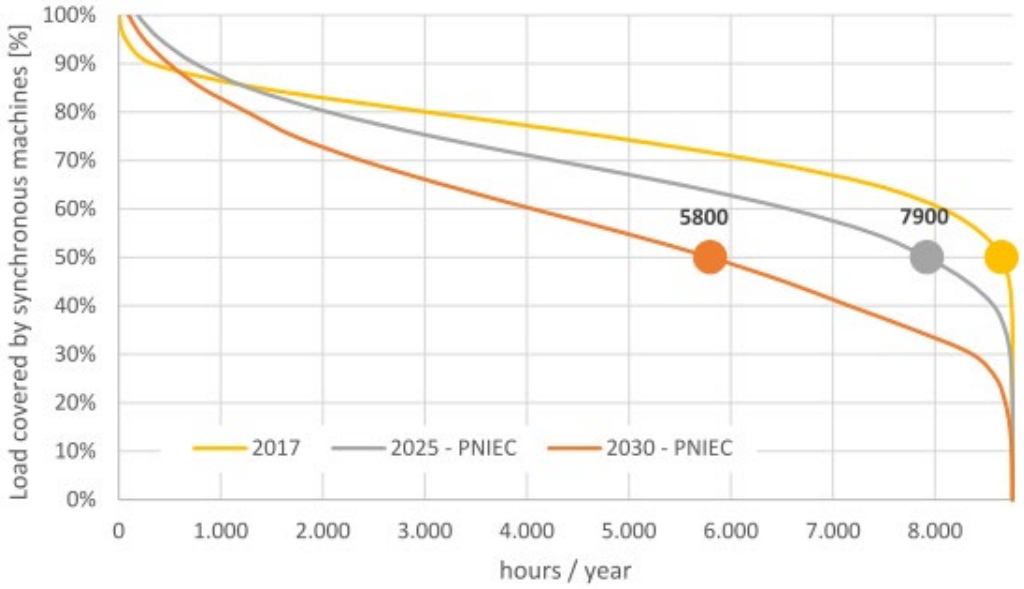

Figure 2-10 Load coverage by synchronous machines

Grid operators have decided to define a new grid service simply focusing on the frequency response of the bulk power system following a sudden power imbalance to counteract the effects of the further future loss of system's inertia and operate in the time period prior to primary frequency response.

This new grid service is called Fast Frequency Response (FFR) which is defined by NERC as " Power injected to/absorbed from the grid in response to changes in measured frequency during the arresting phase of a frequency deviation event to improve the frequency nadir or initial rate of change of frequency "[17].

The fast reserve should be fully activated before the primary reserve thus complementing its operation not replacing it. Fast response can occur in several forms such as inertial response of rotating machines, part of the turbine governor response, battery energy storage systems, load

resource, and even renewable energy sources like wind turbine generator, and photovoltaic systems.

Fast frequency response control techniques vary differently according to the capabilities of the service unit, the characteristics of the local electric grid, for example [17]:

- Power injection is proportional to the measured frequency.
- Power injection is a constant step response when frequency hits a specific threshold.
- Power injection is proportional to the measured ROCOF.
- Power injection is a constant step response when ROCOF hits a specific threshold.
- Load Power Rejection is proportional to the measured frequency.
- Load Power Rejection is a constant step response when ROCOF hits a specific threshold.

Figure 2-11 [17] provides only a visual demonstration of the implementation of the previous techniques without taking into consideration any technical restrictions, which must be set by each grid operator according to the predefined studies, such as:

- Magnitude of the response.
- Speed of the response
- Type of control.
- Sustaining time.
- Availability and repeatability of response.

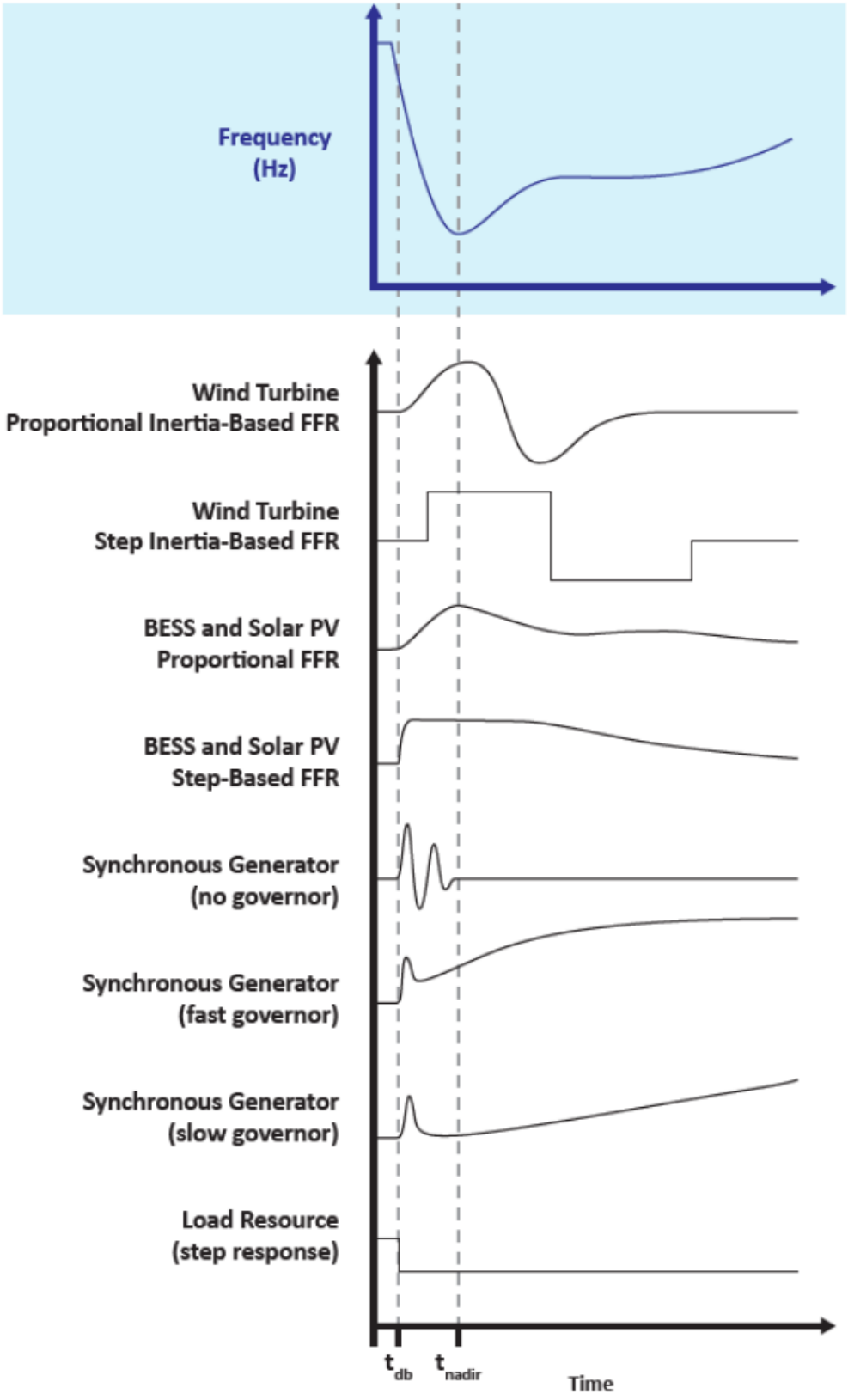

Figure 2-11 Demonstration of FFR from different units.

2.3.3. Terna's proposed fast frequency control

Terna has the intention to launch a pilot project within the context of ARERA Resolution 300/2017/R/eel [20] as a provisional regarding the new grid service "Fast Reserve". The fast reserve response will not replace the primary response but rather complement it and it is characterized by the following features [18]:

- Fast reserve is a technology neutral service.
- Fast reserve unit participating capacity must lie between 5 and 25 MW.
- Fast reserve is a bidirectional service consists of injecting active power proportional to the frequency variation.
- Fast reserve unit must have sufficient energy capacity to supply 15 minutes of service either upwards or downwards every 2 hours.
- The full activation time of the service is 1 second after the frequency trigger event. The response must be maintained for 30 seconds and decreased gradually within 5 minutes as linear ramp as illustrated in Figure 2-12.

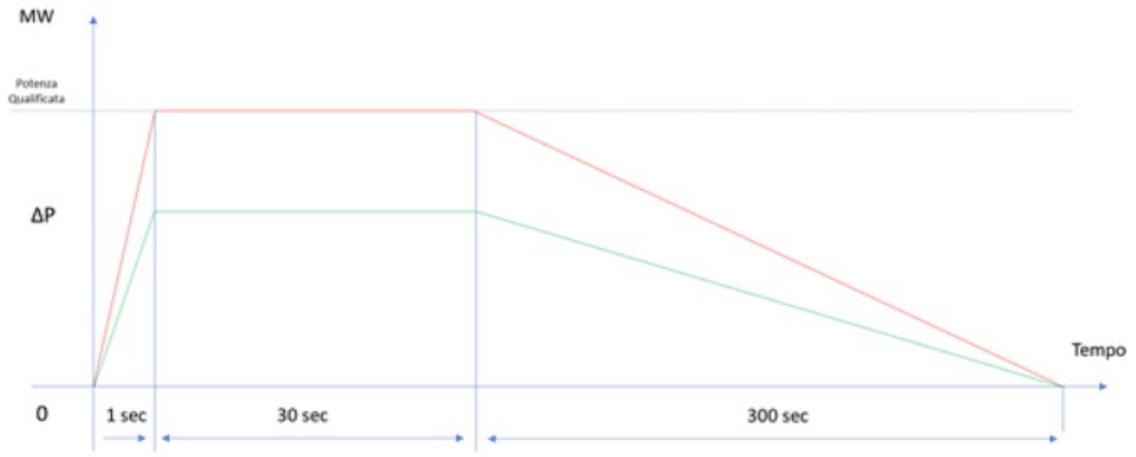

Figure 2-12 FFR service activation dynamics.

- The service can be provided by both stand-alone resources connected to a single point of delivery or by an aggregation of resources.
- Fast reserve units must guarantee 1000 hours of availability per year.

3. BESS grid services and connection codes

In the past the main philosophy of the electric power system operators was that supply should always follow the demand the whole time and reinforce the system by investing in generation, transmission, and distribution capacity to meet the peak demand. Nowadays as the green revolution gains momentum throughout the world and distributed renewable energy resources (DRES) deployment increase, a new philosophy has emerged; the demand should too try to follow the supply and the new renewable units' generation constraints. The former philosophy is pushed by the constraint of the uncontrollability of customers' electrical consumption habits while the latter is pushed by the constraint of the uncontrollability of renewable energy production hours. Energy storage systems can serve as a bridge between the two viewpoints as it can [21], [22] : meet the sudden demand events, provide grid services, store the excess energy produced by DRES, defer investments in peak demand units and bulk power system reinforcement, and enable a higher penetration of RES.

3.1. BESS available grid services

At the end of chapter1 we have briefly mentioned all the grid services which can be provided by ESS, here we shall dig deeper into some of these services which have been expected to contain a promising potential either now or in the future.

Services provided by utility scale ESS can be put together into four main categories [11] as illustrated in Figure 3-1

- System Operation.
- Investment deferral.
- Solar PV and wind generators.
- Mini grids.

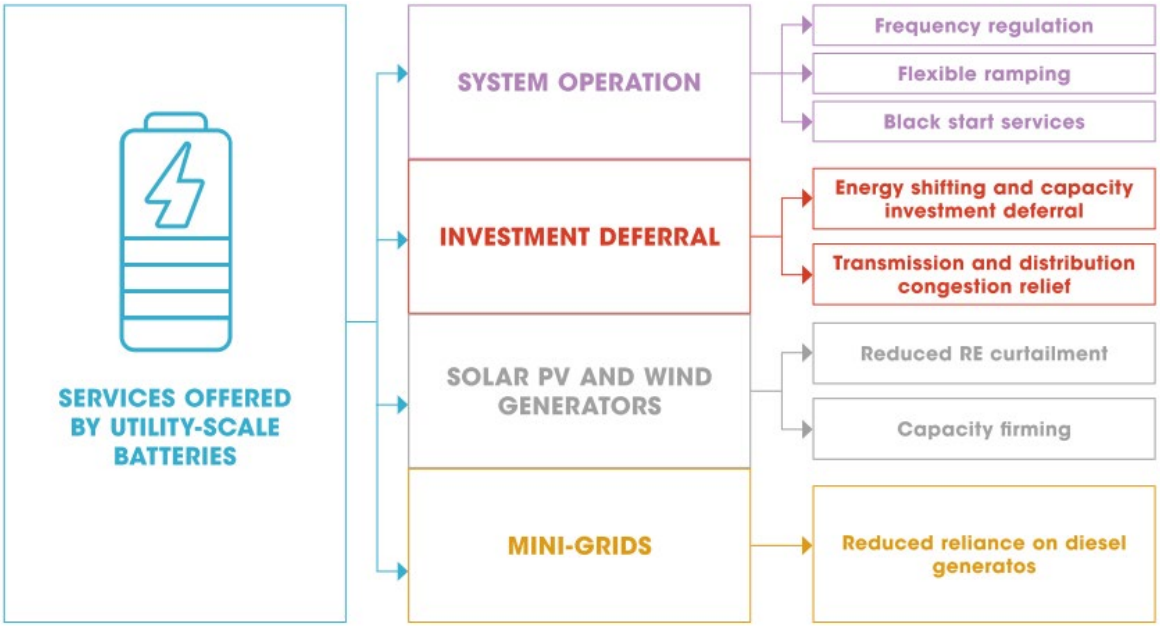

Figure 3-1 Services provided by ESS

3.1.1. System Operation

Frequency regulation

The imbalance between power supply and demand leads to a dip or rise of the system frequency, this change can be tolerable if it lies within a specific range else the operator must act to ensure the system's stability through a process called frequency regulation. In the past only conventional units could perform frequency regulation and often units were forced to be either on standby or operate at inefficient operating point thus increasing the cost of the service. BESS can perform frequency regulation more precise and better than conventional units since the respond time of BESS is in milliseconds range while that of conventional units can be up to several minutes.

In South Australia, Tesla has commissioned a Li-ion BESS of 100MW/129MWh at the 315MW Hornsdale wind farm to provide frequency regulation services and contingency reserves. The Australian energy market operator has reported that the services provided by the BESS compared to the services provided by the conventional units are rapid and precise [23].

In the United States, the Federal Electricity Regulatory Authority (FERC) has authorized a different compensation structure for the fast-acting units such as BESS than for slower conventional units. This mandate has incentivised many system operators to use batteries for frequency regulation services [10], [24].

In the United Kingdom, the national transmission system contracted 200 MW of BESS to provide the grid with frequency regulation services. The tender was technologically neutral which implies that BESS are becoming more suited for the frequency regulation application [25].

Flexible ramping

At high penetration levels of DRES and particularly solar PV technology the shape of the standard load curve begins to transform into the new duck curve shape. Solar PV units produce excess energy at low demand time periods and cease production at high demand period creating a very high ramping load curve. The power system is ought to ramp downwards in the morning period where excess solar power is produced and ramp upwards in the evening when the PV units cease production and the demand increase [11]. BESS offer a direct solution to the problem by absorbing the excess power at low demand periods and injecting it at high demand period hence flattening the duck curve.

In the United States, California Independent System Operator (CAISO) has installed 150 MW of BESS for providing flexible ramping service [11]. Figure 3-2 illustrates the expected effects on the duck curve due to flexible ramping services provided by BESS. The study expects a reduction of 59% at the peak ramp rate and a 14% load peak reduction.

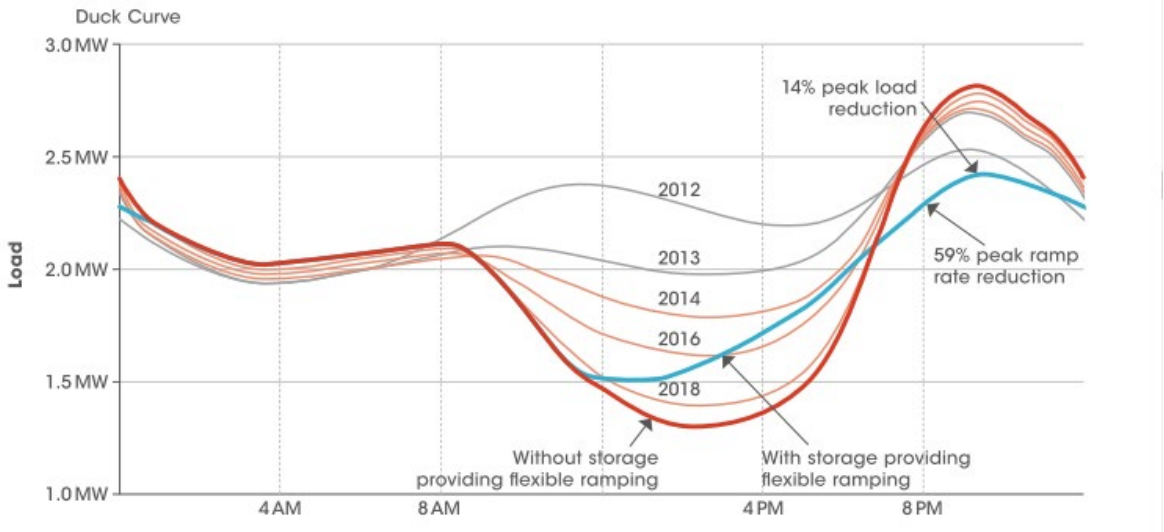

Figure 3-2 The impact of BESS flexible ramping services on the duck curve using a 3 MW feeder.

Black-start services

The black start services refer to the restoration of the generation plants following a grid failure event. Black start services have been typically provided by diesel generators located in the same facility of the generating units. BESS can provide black start services in the same manner as diesel generators along with other ancillary services in the market since BESS theoretically have no minimum loading point thus providing extra revenue to the owner [11].

3.1.2. Investment Deferral

Energy shifting and capacity investment deferral

BESS can be employed as peak power plants hence acting as a capacity reserve unit by discharging in peak load hours. This scheme can defer more capacity investments by acting as a peak load capacity unit.

In the United Kingdom, a 6 MW/10MWh BESS is operated for capacity reserve services in Bedfordshire along with other ancillary services [26].

In the United states, the electricity supplier Southern California Edison has constructed a 20 MW BESS unit for capacity reserve services to meet peak hours demand. The system is designed to supply the nominal power for 4 hours thus having a nominal storage of 80 MWh [27].

Transmission and distribution investment deferral

Network congestion phenomenon occur when the power flow through the transmission/distribution network exceed the designed nominal capacity, often during peak hours. In most of the cases the power system operator solves the congestion problem by investing in transmission and distribution assets such as: powerlines, transformers, and substations. However, in a few cases the congestion event does not occur periodically but only for limited dispersed hours throughout the year. Further investment in the grid in these cases will be waste of resources and will be considered overbuilding of the grid.

BESS offer a solution to this problem by acting as a “virtual power line” to increase the reliability of the system and relieve congestion hence deferring investment in distribution and transmission assets.

In Italy, transmission system operator Terna has deployed 35 MW of BESS at the 150 kV level of the grid to relieve congestion in southern Italy when the wind production exceeds the transport capacity of the network [28].

3.1.3. Services provided for DRES

Reduced renewable energy curtailment

Renewable energy sources aim to generate the maximum available power based on the instantaneous weather conditions, this results in their uncontrollability and fluctuation. In certain situations, the power produced by RES becomes high during peak sun/wind hours compared to the local demand and the local network capacity prevents the transportation of this excess RES power. This will lead to some RES power curtailment to maintain the power system stability and reliability thus forbidding the RES units from utilizing the full available power they possess and halt the progress of the grid towards sustainability. BESS may offer a solution as it can store the excess energy during peak RES hours and low demand time then injecting the energy back into the grid at peak demand.

In Germany, by the end of 2018 around 120,000 households and commercial venues have invested in PV battery systems which helped reduce the production cost of electricity below purchasing prices while increasing self-consumption from 35% to 70% on average [29].

Capacity firming

As stated earlier, RES units are characterized by their uncertainty and fluctuating output power. A slight weather event like cloud movements or variability in wind speed is amplified and can cause a serious variation in the output power for large RES power plants. When paired with RES, BESS offer a chance of reducing the variability in the output power and control the ramp rate associated with weather events enabling the RES to behave as controllable dispatchable units therefore facilitating their integration into the electric power system and the traditional supply and demand market structure.

In Spain, Acciona Energy has employed an experimental BESS comprised of 2 units the first is of 1 MW/ 0.39 MWh and the second is 0.70 MW/0.70 MWh. Both units are to be coupled with a wind farm in Navarra to store the produced energy when required. In addition to storing the required energy the BESS will aim to improve the quality of the energy delivered to the grid [30].

3.1.4. Services provided to Mini Grids

Reduction of reliance on diesel generators

For the existence of mini grids systems in rural and islands, they have been always been relying on conventional units like diesel for energy supply. Nowadays, as the price of electricity produced by RES is becoming cost competitive more units are being employed in remote areas aiming to save on the conventional units' fuel cost. Unfortunately, the process of balancing the supply and demand has become more tedious on the mini grid operators because of the RES's uncertainty in power production hence limiting their penetration into the mini grids. BESS can offer help to the mini grids' operator by smoothing the output of the RES and reducing the ramp rate therefore supporting the high penetration of RES into the mini grids.

In the United States, Solar city, recently acquired by Tesla, has commissioned a 1.4 MW solar PV supported by a BESS of 0.75 MW/6 MWh to enable the Ta'u island to run exclusively on solar energy [30].

3.2. Grid code requirements

Network codes are a set of rules which detail the technical requirements that must be met by a market player that wish to connect to the transmission system. Grid codes aim to develop a harmonised electricity grid connection regime that will support a more efficient and secure system operation.

Grid codes can either be solely established by the local national Transmission System Operator in the case of local transmission systems not belonging to a bigger entity, or can be drafted by a regional entity, as ENTSO-E for Europe or NERC for North America, and locally appropriated by national/independent transmission system operators, like Terna in Italy and CAISO in the United States, to meet local technical specifications of the grid in the case of transmission systems belonging to a bigger entity.

Despite the increasing interest in BESS as a key enabler in increasing the renewable energy sources' penetration and smoothen the transition toward the smart grid architecture, most of the countries grid codes have not yet been updated with BESS specific technical prescriptions. BESS are mentioned in different situations in grid codes, but they frequently might fall under distributed energy resources category. In this section we will try to demonstrate the available connection codes on national and regional levels and the state of ongoing assessments.

3.2.1. ENTSO-E

ENTSO-E, the European Network of transmission System Operators for Electricity, represents 42 electricity transmission system operators from 35 countries throughout Europe, established in 2009 by the EU's third legislative package for the internal energy market [31]. ENTSO-E aims at improving the cooperation between Europe's TSOs to support the implementation of the European energy policy and climate agenda, ensuring proper integration of renewable energy sources into the power system while retaining a secure and reliable electric power supply to all users in presence of an transparent and non-discriminatory internal energy market.

Figure 3-3 ENTSO-E association logo

ENTSO-E provides European network codes, the set of rules that applies to the sections of the energy sector and the definition of cross border issues, like:

- Connection to the grid.
- Integration of markets and congestion management between grids.
- Security and Interoperability of transmission grids.

3.2.2. Terna S.p.A

Terna is the owner of the Italian national transmission system grid for high and extra high voltage power, operating as a monopoly through the guidelines set by the Italian Regulatory Authority (ARERA). Terna performs national transmission grid development, planning, and maintenance activities ensuring constant supply of electricity throughout every second of the year. Around 90% of Terna's activities are conducted on the regulated market through ARERA's predefined rules.

Figure 3-4 Terna group logo

According to Terna, the national Grid Code should define transparent and not-discriminatory rules for [32]:

- Access to the grid and its technical regulations.
- Development of the grid and its management and maintenance.
- Issue of dispatching services.
- Provision of metering.
- Regulation of economic items connected with various services.
- Security of the Italian national electrical system.

3.2.3. Proposed European Grid Codes

In general, there is no explicit mention of connection codes regarding the ESS in the current European electrical energy regulations or legislations. However, on 11th of June 2018 the Grid Connection European Stakeholder Committee (ESC) was established to consider the suitability of the three European connection codes requirements for generation (RFG), high voltage direct current (HVDC), and demand connection code (DCC) to energy storage technologies. The expert group was held on two phases were they started by first the proper definition of energy storage devices, technologies, and capabilities then in part they would investigate the behaviour in low frequency, electric vehicles, and how (RFG, HVDC, and DCC) should be updated to include storage [33], [34].

For the first phase the objectives were:

- Identify storage technologies, applications, and topologies.
- Categorize storage devices (if reasonable).
- Investigate the possibility of useful definition of storage devices.

The second phase continued from options produced from phase 1 and the objectives were:

- Revise the relevant articles of the Connection Network Codes according to phase 1 results and observations.
- List and asses the possible implications that these revisions might have on other network codes.
- List any possible doubts that could be addressed by other network guidelines.
- Involve some specifications regarding Electric Vehicles.
- Identify possible grid modes of operations and grid connection configurations.
- Asses the consequences on connection requirements.

In the following paragraphs the major outcome recommendations of the group regarding continental Europe will be demonstrated:

The Energy Storage modules shall be categorized according to their maximum capacity and the voltage of the connection point as follows per continental Europe:

- Type A: The voltage of the connection point is below 110 kV and maximum capacity of 0.8 kW.
- Type B: The voltage of the connection point is below 110 kV and maximum capacity of 1 MW.
- Type C: The voltage of the connection point is below 110 kV and maximum capacity of 50 MW.
- Type D: The voltage of the connection point is equal to or above 110 kV and maximum capacity of 75 MW.

For type A generating modules the following shall be adopted:

Operational Frequency

- Energy storage modules shall be capable of remaining connected to the network and operate within the frequency ranges listed in Table 3-1.

Table 3-1 Minimum time periods for which a Energy Storage module has to be capable of operating on different frequencies, deviating from a nominal value, without disconnecting from the network..

Synchronous area	Frequency range	Time period for operation
Continental Europe	47,5 Hz-48,5 Hz	To be specified by each TSO, but not less than 30 minutes
	48,5 Hz-49,0 Hz	To be specified by each TSO, but not less than the period for 47,5 Hz-48,5 Hz
	49,0 Hz-51,0 Hz	Unlimited
	51,0 Hz-51,5 Hz	30 minutes

Limited Frequency Sensitive Mode- Over-frequency (LFSM-O)

- Regarding limited frequency sensitive mode- over-frequency (LFSM-O), the Energy Storage module shall be capable of activating the provision of active power frequency response according to Figure 3-5 at a frequency threshold and droop settings specified by the relevant TSO;
- In Figure 3-5, in the case of electricity storage modules, Pref could be the maximum capacity or the maximum consumption capacity at the moment the LFSM-O threshold

is reached or the maximum capacity or maximum consumption capacity as agreed with the relevant system operator.

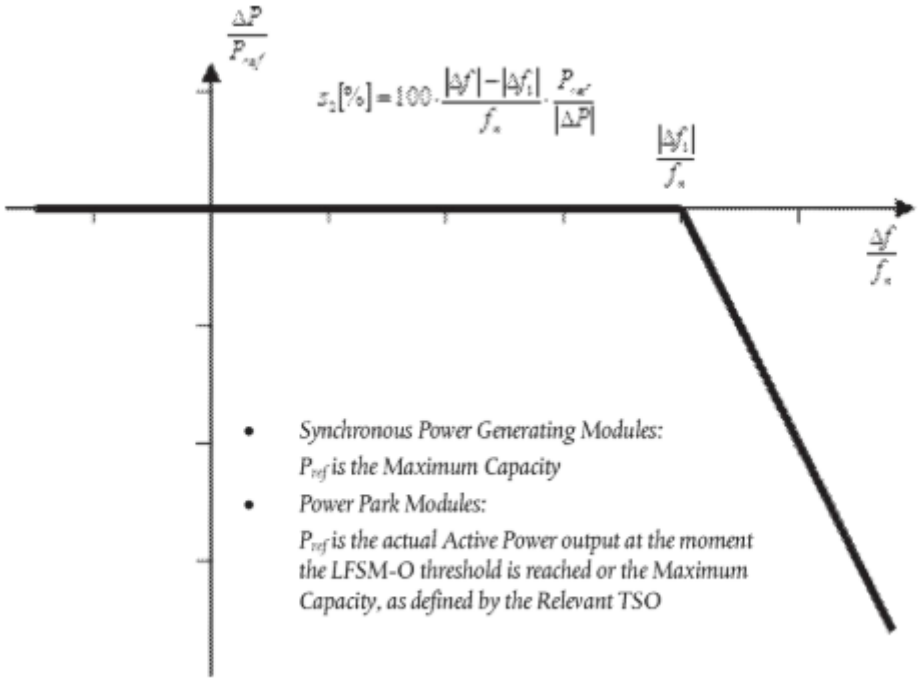

Figure 3-5 Active power frequency response capability in LFSM-O

– An electricity storage module which is absorbing active power during an over-frequency event shall increase the level of active power absorbed according to the LFSM-O characteristic which shall be considered in terms of the power variation rather than the absolute value. The electricity storage module will absorb power up to filling the maximum energy that it is able to store, then it will cease consumption. The TSO can define a different characteristic or establish that the electricity storage module when absorbing active power will maintain the absorption level even during the over-frequency event.

Capability at low system frequency

– When an electricity storage module is operating in a consumption mode (absorbing power) and prior to the activation of the automatic low frequency demand disconnection scheme, each electricity storage module shall be capable of automatically switching to a generation mode (generating power) in accordance Figure 3-6. The parameters for this capability shall be specified by the TSO within the range specified in Table 3-2.

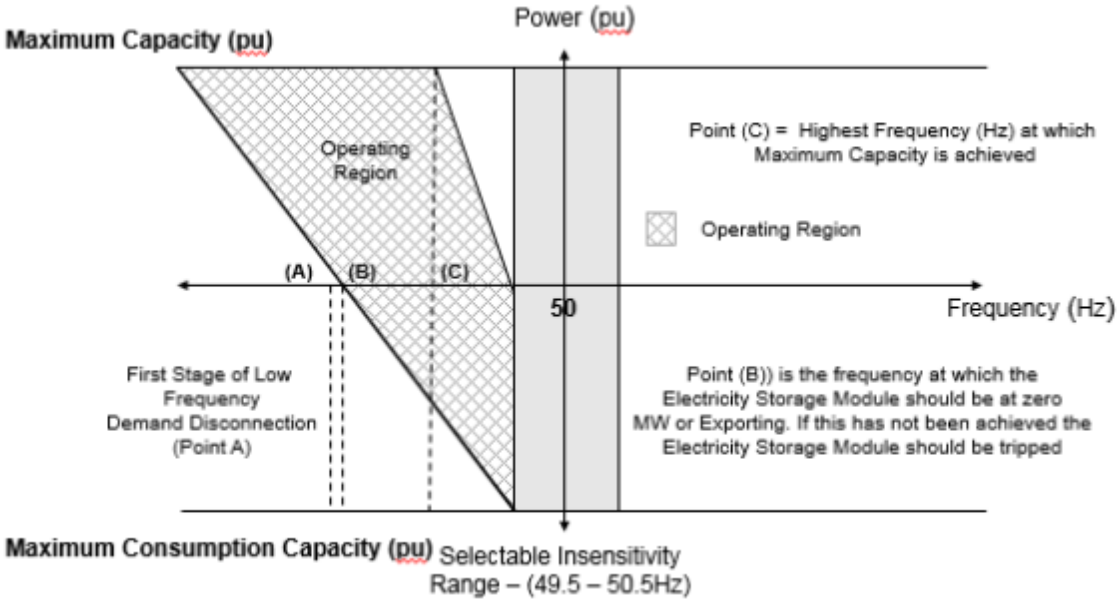

Figure 3-6 Low frequency capability of ESS

Table 3-2 Low frequency capability parameters range.

TSO defined Parameter	Unit	Range
Insensitivity	Hz	49.5-50.5 Hz
Power Gradient	MW/Hz or pu/Hz	Within operating range of Figure 3-6
Point A - First Stage of Low Frequency Demand Disconnection	Hz	TSO defined according to the E&R (EU 2017/2196) code
Point B – Frequency at which the Electricity Storage Module should be at zero	Hz	TSO defined according to the E&R (EU 2017/2196) code
Point C – Frequency at which Maximum Export Capability can be reached	Hz	49.6-49.0 Hz
Time t1 – Maximum Operating time for complete characteristic	s	TSO defined in the range 1 – 25 s
Time t2 – Initiation time from inception of frequency fall	s	TSO defined in the range 0 – 5 s
Final Loading Point following frequency fall	MW	0 – Maximum Capacity

– If the electricity storage module is not capable of switching from a consumption mode (absorbing power) to an injection mode (generating power) within a time limit specified by the TSO, it shall be tripped at a system frequency to be defined by the TSO.

For type B generating modules the beforementioned shall be fulfilled by the Energy Storage module in addition to:

Fault-ride-through

– Each TSO shall specify a voltage-against-time-profile in line with Figure 3-7 at the connection point for fault conditions, which describes the conditions in which the Energy Storage module is capable of staying connected to the network and continuing to operate stably after the power system has been disturbed by secured faults on the transmission system.

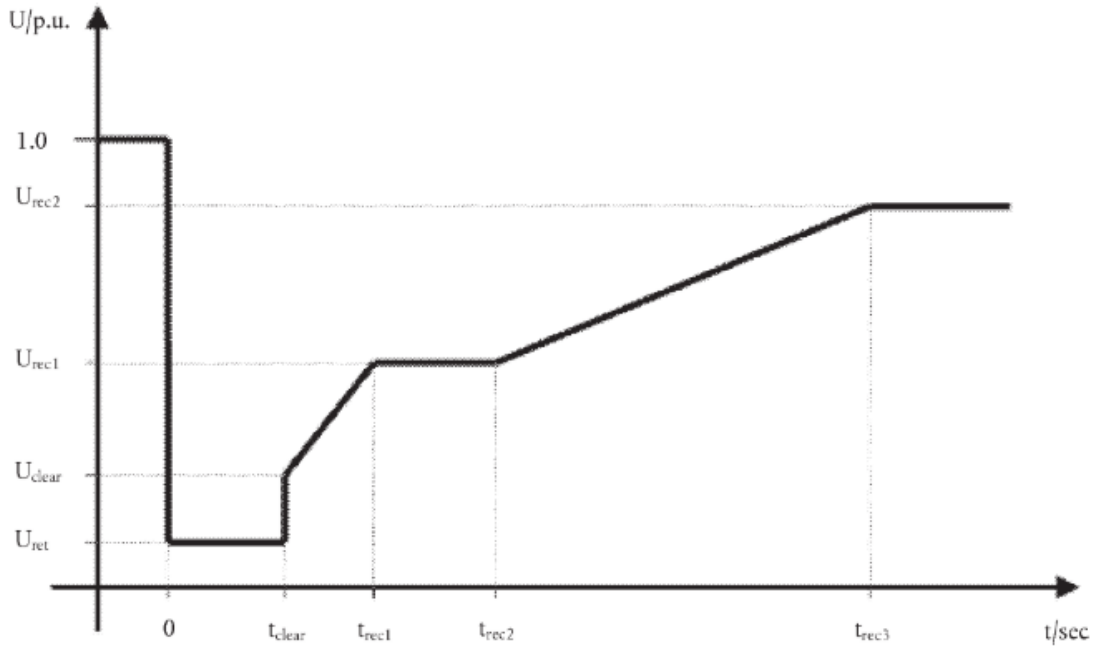

Figure 3-7 Fault-ride-through profile.

For type C and type D generating modules the beforementioned shall be fulfilled by the Energy Storage module in addition to:

Limited Frequency Sensitive Mode- Underfrequency (LFSM-U)

– The power-generating module shall be capable of activating the provision of active power frequency response at a frequency threshold and with a droop specified by the relevant TSO in coordination with the TSOs of the same synchronous area as in Figure 3-8 with the frequency threshold and droop specified by the TSO.

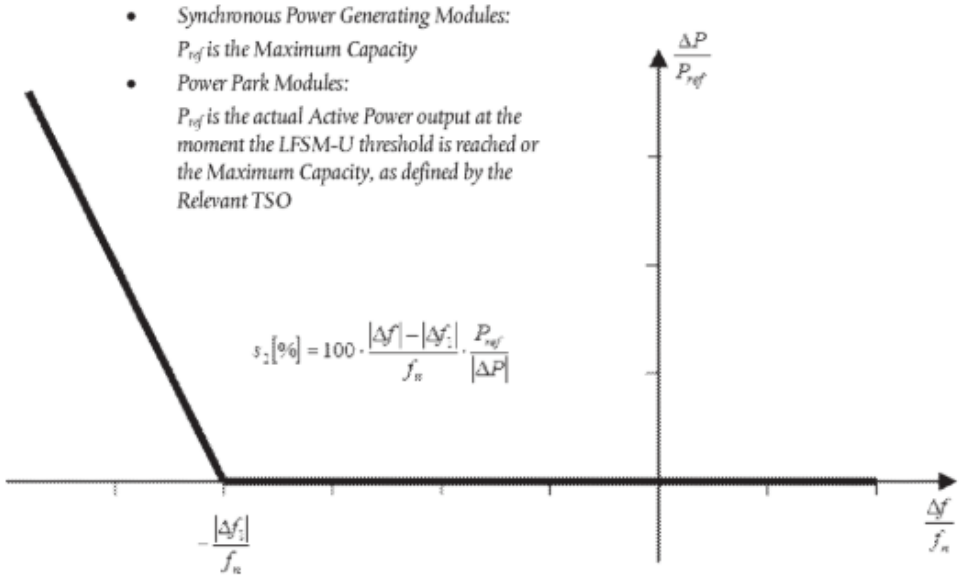

Figure 3-8 Active power frequency response capability in LFSM-U

– In Figure 3-8, in the case of electricity storage modules, Pref could be the maximum capacity or the maximum consumption capacity at the moment the LFSM-U threshold is reached or the maximum capacity or maximum consumption capacity as agreed with the relevant system operator.

Frequency Sensitive mode FSM

– The Energy Storage module shall be capable of providing active power frequency response as illustrated in Figure 3-9 according to the parameters identified by each TSO within the ranges displayed in Table 3-3.

Table 3-3 Active power frequency response parameters in FSM

Parameters		Ranges
Active power range related to maximum capacity $\frac{\lvert\Delta P_1\rvert}{P_{max}}$		1,5-10 %
Frequency response insensitivity	$\lvert\Delta f_1\rvert$	10-30 mHz
	$\frac{\lvert\Delta f_1\rvert}{f_n}$	0,02-0,06 %
Frequency response deadband		0-500 mHz
Droop s_1		2-12 %

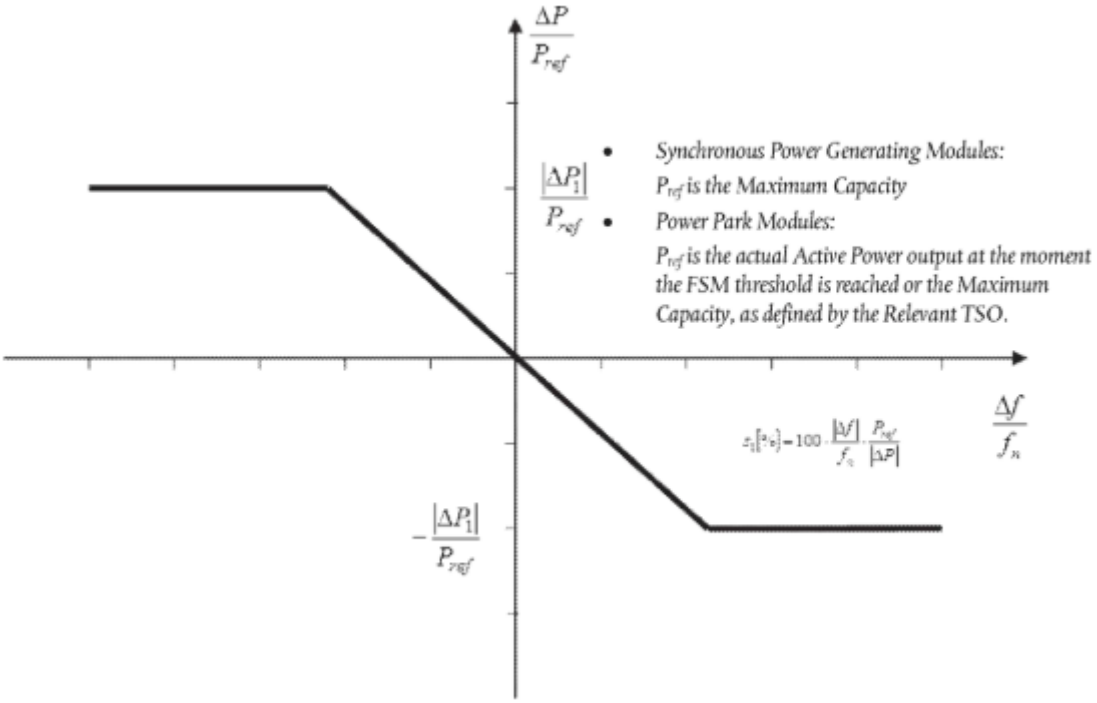

Figure 3-9 Active power frequency response in FSM in the case of zero dead-band and insensitivity.

- In the case of over-frequency, the active power frequency response may be limited by the minimum regulating level or maximum consumption capacity, or the maximum energy content that the electricity storage module can store or as agreed between the power generating facility and the TSO.
- In the case of underfrequency, the active power frequency response is limited by the maximum consumption capacity or maximum energy content of the electricity storage module or as agreed between the power generating facility and the TSO.

3.2.4. Available National Grid Codes

As indicated before all members of the European Union and other European countries have their own Network codes which operate under the supervision of ENTSO-E. In terms of network codes regarding Energy Storage systems Member states stand differently with different timelines as follows:

- Most of the members have no explicit definitions or Codes regarding Energy storage systems.
- Some have started developing their own codes and ongoing projects to integrate Energy Storage systems.
- Few have developed explicit definitions and Network codes regarding Energy storage systems.

France and Netherlands

In Netherlands there is no recorded work on connection requirements for energy storage.

In France, the work on the connection requirements for energy storage technologies has just begin. Only battery energy storage systems connected to the network through inverters have been identified as this technology is comparable to Photovoltaic plants. The plan is to start from RfG requirements and engage in similar technicalities.

Italy

In Italy, the technical requirements regarding the connection to the network are governed by three main documents: CEI 0-21 for Low Voltage (LV) systems, CEI 0-16 for Medium Voltage (MV) systems, and Terna Grid Code for High Voltage (HV) systems.

The technical requirements for storage systems are explicitly described in CEI 0-16 and CEI 0-21 including definitions and testing[35], [36] while in Terna there is still pilot projects and focus groups working on the development of network codes.

Ireland and Northern Ireland

EriGrid the TSO for Ireland and SONI the TSO of Northern Ireland have developed an implementation note that seeks providing definitive guidance for Battery Energy Storage Systems and illustrate some specific cases regarding each TSO's Grid Codes. Battery Energy Storage Systems are categorized as Power Park Modules (PPM) and are considered to be non-RfG units in the EriGrid and SONI Grid Codes. In the following sections some of the technical criteria connection codes will be demonstrated [37]–[39]:

Operational Limits

BESS shall be capable of satisfactory operation in the range of 0 – 120% per unit for the minimum time periods listed in Table 3-4.

Frequency nominal operating range:

- For SONI 49 Hz — 51 Hz.
- For EriGrid 49.5 Hz — 50.5 Hz.

Table 3-4 Minimum operational time periods

Voltage Range (U/Un) %	Minimum Time requirement
115% — 120%	2 seconds
110% — 115%	10 seconds
90% — 110%	Continuous operation
0% — 90%	As per Fault-Ride-Through capability in Figure 3-10

Fault-Ride-Through

The BESS must remain connected to the transmission system for voltage dips measured on on any or all phases, and must remain Stable where the transmission system phase voltage measured at the HV side of the grid connected transformer stays above the heavy black line indicated in Figure 3-10.

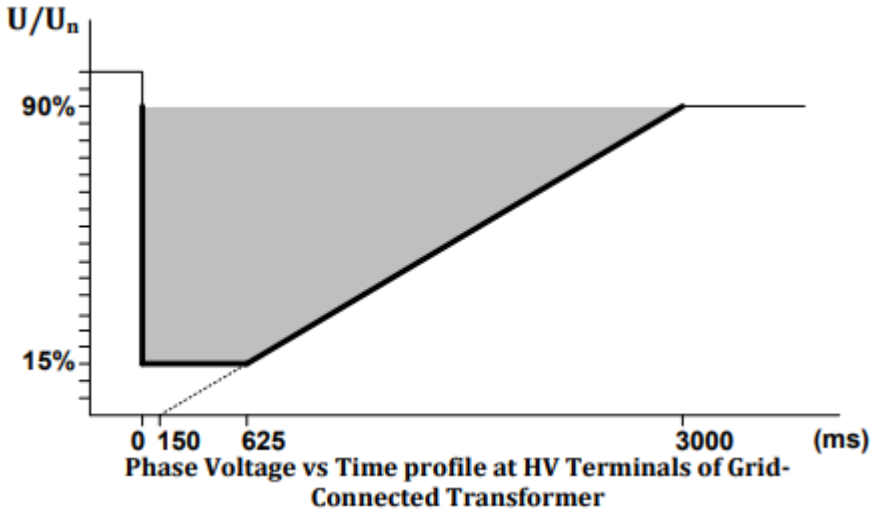

Figure 3-10 Fault ride through capability of BESS

Capacity Limited ramp rate

Capacity limited ramp rate is the technical requirement which dictates how BESS must control their active power generation/consumption when it approaches the limits of its capacity. The requirement dictates the following behaviours:

- Discharging BESS, indicated in Figure 3-11, in response to an active power setpoint or frequency response and reaches a capacity limit indicated as “A”, must not exceed the discharging ramp rate indicated by the line “A-B” until reaching 0 MW output.
- Charging BESS, indicated in Figure 3-12, in response to an active power setpoint or frequency response and reaches a capacity limit indicated as “A”, must not exceed the charging ramp rate indicated by the line “A-B” until reaching 0 MW output.

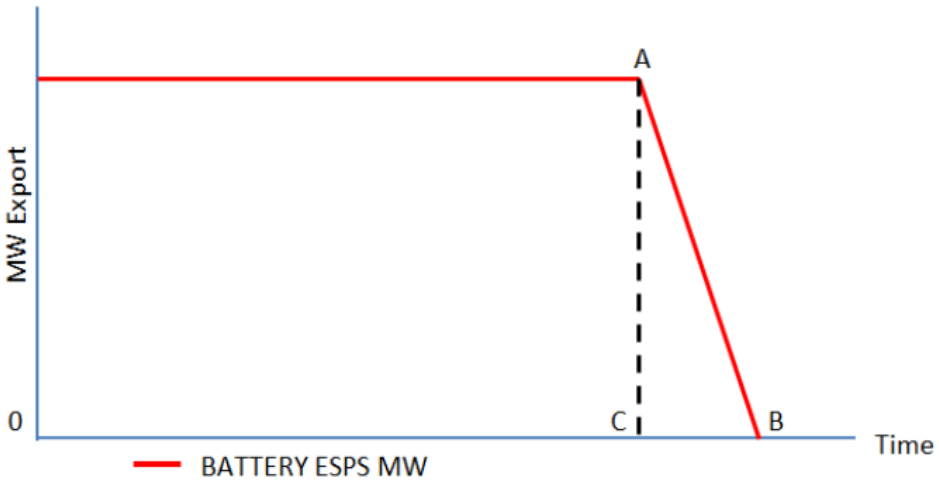

Figure 3-11 Capacity limited ramp rate for discharging

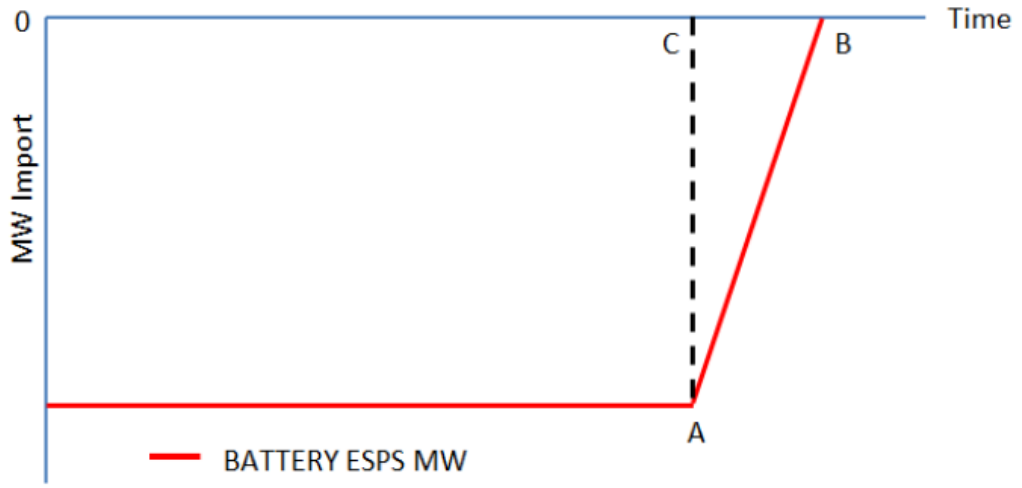

Figure 3-12 Capacity limited ramp rate for charging.

Frequency Response

BESS must be capable of contributing to control of the system frequency through active power modulation according to the characteristics and parameters presented in Figure 3-13, Table 3-5, and Table 3-6.

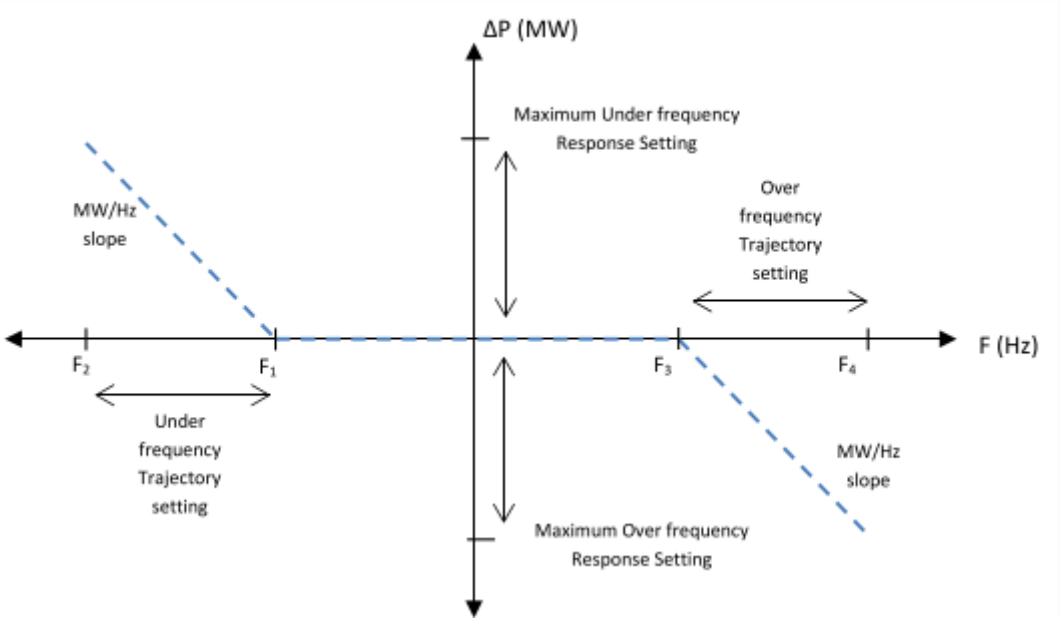

Figure 3-13 BESS frequency response characteristics.

Table 3-5 BESS frequency response parameters description.

Characteristic	Description
F	System frequency at any given time
ΔP	Change in active power output, due to change in system frequency
Under frequency trigger frequency (F_1)	Frequency at which the unit begins to provide under frequency response
F_2	Frequency at which the unit would achieve its maximum under frequency response setting (F1 - Under frequency trajectory setting)
Over frequency trigger frequency (F_3)	Frequency at which the unit begins to provide over frequency response
F_4	Frequency at which the unit would achieve its maximum over frequency response setting (F3 + Over frequency trajectory setting)
Under frequency trajectory	The magnitude of the change in Frequency over which the unit would deliver its Maximum Under frequency Response Setting (if it was not limited by capacity or availability)
Over frequency trajectory	The magnitude of the change in Frequency over which the unit would deliver its Maximum Over frequency Response Setting (if it was not limited by capacity or availability)
Maximum Under frequency Response	Maximum increase in active power which the unit will provide in response to under frequency
Maximum Over frequency Response	Maximum reduction in active power which the unit will provide in response to over frequency

Table 3-6 BESS Frequency Response parameters definitions

Parameters	EriGrid	SONI
Under frequency trigger F1	49.5Hz – 50Hz	49Hz – 50Hz
Under frequency trajectory F1-F2	1Hz – 5Hz	1Hz – 10Hz
Maximum Under Frequency Response	0 MW – Operating Range	
Over frequency trigger F3	50Hz – 50.5Hz	50Hz – 51Hz
Over frequency trajectory F3-F4	1Hz – 5 Hz	1Hz – 10Hz
Maximum Over Frequency response	0 MW – Operating Range	

3.3. Designated Model services

3.3.1. Model's characteristics selection process

With the increase in the deployment of large BESS through tenders and pilot projects, a need for a standard model has risen in which the BESS interaction with the grid can be carefully studied without much reliance on the battery's vendor. However, the selection of a battery model depends on the simulation time frame in which the model will be used and the anticipated services/functionalities. The services which can be provided by BESS are numerous as stated in chapter 1 and 3 depending on the BESS technology.

The reasoning behind the model definition process is demonstrated in the following steps:

- Sort the available BESS technologies according to market and technology maturity.
- List the advantages and disadvantages of the filtered technologies.
- State the available services provided by each technology.
- Investigate the economical aspect of the services.

During section 1.1 we discussed some technological properties of some of the available BESS technologies and came to several conclusions according to [6], [8], [10], [40], [41]:

- According to technological maturity Pumped hydro, Lead acid, Nickel cadmium, lithium-ion, sodium-sulphur, and flywheel are shortlisted.
- All are characterized by high response time.
- High efficiency is achieved by flywheel, lithium-ion, and sodium-sulphur of the shortlist.
- High power density is achieved by flywheel, and lithium-ion of the shortlist.
- High self-discharge rates are achieved by flywheel of the shortlist.
- Pumped hydro storage is site specific and has almost been saturated globally.

From the shortlisted technologies only lead-acid, nickel-cadmium, and lithium-ion can be considered for grid investments. Directive 2006/66/EC prohibits the sale of portable batteries even supplied inside appliance that contain more than 0.002% cadmium by weight [42] thus ruling out cadmium batteries. Lead acid batteries are cost efficient and mature technology but undergo thermal failure when subjected to rapid high power applications along with the environmental toxicity of lead [8].

Lithium-ion technology is characterized by high power and energy density, high roundtrip efficiency, milliseconds respond time, low self-discharge rate, and estimated high lifetime [9], [41], [43] hence making it a pragmatic candidate for the model's characteristics definition process.

Lithium-ion based BESS are physically capable of performing: frequency regulation, spinning reserve, voltage/reactive power support, load following, peak shaving, and investment deferral [9], [10]. Frequency regulation services provided by large BESS have been showing promising outcomes recently as 86% of the large BESS installed in the United States are performing frequency regulation with positive profit according to the new tariff scheme [10], [11]. Additionally, in the United Kingdom BESS have won a 200 MW project for frequency regulation to the national grid through a technology neutral system [25].

3.3.2. Nominated model characteristics

Since differences between BESS technologies is vast, creating a generic model that would capture the complete dynamics of the system would be tedious however, a middle ground was found for the sole of this study.

This study will focus on creating a generic battery energy storage model which would provide frequency regulation services and reactive power support services to the grid. The selected services will be operating in the transient stability analysis which will simplify the modelling selection process constraints. The model should be able to be tailored to Lithium-ion technology as it is the most promising technology for BESS worldwide. The beforementioned points are the minimum key aspects that the BESS model created in this study should abide by.

4. Modelling Environment

The modern-day electrical power system architecture has been growing much complex than before with the introduction of renewable energy sources, electric vehicle charging stations, HVDC, and energy storage systems hence restricting the effectiveness of the traditional power system solvers. Moreover, the smart grid vision of continental Europe networks demands efficient data exchange between transmission system operators, distribution systems operators, and generation companies. ENTSO-E has adopted d regulation EC 714/2009 for cross-border exchanges in the electricity network to ensure coordination of "data exchange and settlement rules, network security and reliability rules, interoperability (IOP) rules, and transparency rules" [44].

To comply with the futuristic network vision and sustain the conventional power systems' reliability a great attention is focused on the simulation tools for performing the coordination task between the grid's various participants. The International Electrotechnical Committee (IEC) has developed the Common Information Model (CIM) to provide standard modelling semantics for power system information exchange [44]. The information exchange is currently concentrated on static model of the network, but a dynamic model is of huge interest as it will be a necessity for tomorrow. Modelica® language has been introduced by ENTSO-E to be used in coordinating data exchange in dynamic modelling as its compliance with the Common Grid Model Exchange Specifications.

CESI S.p.A, consultant of the Italian TSO (Terna), has implemented the Modelica language in the description of the power system models in the dynamic simulator TESEO. In the Past years CESI has been developing a library called "Basic Power System' consisting of passive elements, conventional generators, and some renewable energy sources in Modelica to be used in TESEO. The object of this work is to further extend the library with the inclusion of a basic standard model of battery energy storage system to be utilized in transient stability studies.

4.1. The Modelica® language

The Modelica language is an equation based, object oriented, opensource, multidomain modelling language to efficiently model complex physical systems comprising of mechanical, electrical, electronic, hydraulic, thermal, control, or electric power subcomponents [45]. It is founded and developed by a non-profit organisation known as The Modelica Association.

Figure 4-1 The Modelica Association logo

The four most important features of the Modelica language are [46]:

- Acausal modelling; Modelica is based on equations instead of assignments which allows better reutilization of classes as equations do not require a specific data flow direction. Therefor a class written in Modelica language can handle different data flow framework.
- Multidomain modelling; Modelica can handle the interaction between components originating from different physical domains. As an example, electrical, mechanical, and thermal can be designated in the same environment and connected.
- General class concept/Templates; Modelica is an object-oriented language that enables the usage of general class concept. This trait simplifies components reusage and complex evolution of models.
- Straightforward model connection; Modelica has a strong software component model which qualifies the language for complex physical systems description and to some extent software systems description.

Furthermore, Modelica offers a powerful software component model which increases the flexibility in modelling and classes reusage.

4.2. The OpenModelcia® Environment

To unlock the full power of the Modelica modelling language a modelling and simulation environment are essential which should appropriately enable the definition of a Modelica model using a graphical user interface while translating the graphical model into a textual description model in the Modelica format. Additionally, the modelling and simulation environment should visualise the results of the simulated model in a suitable interactive fashion.

OpenModelica® environment is the first open source Modelica based modelling and simulation environment intended for the academic and the industrial usage. Its development is supported by The Open Source Modelica Consortium which was created in 2007 [47].

OpenModelica main goals are:

- Provide an open source complete Modelica-based industrial strength implementation of the Modelica language including system modelling, simulation, optimization, and additional capabilities in the modelling environment.
- Provide an interactive computational environment for the Modelica language.

The architecture of the OpenModelica environment is shown in Figure 4-2.

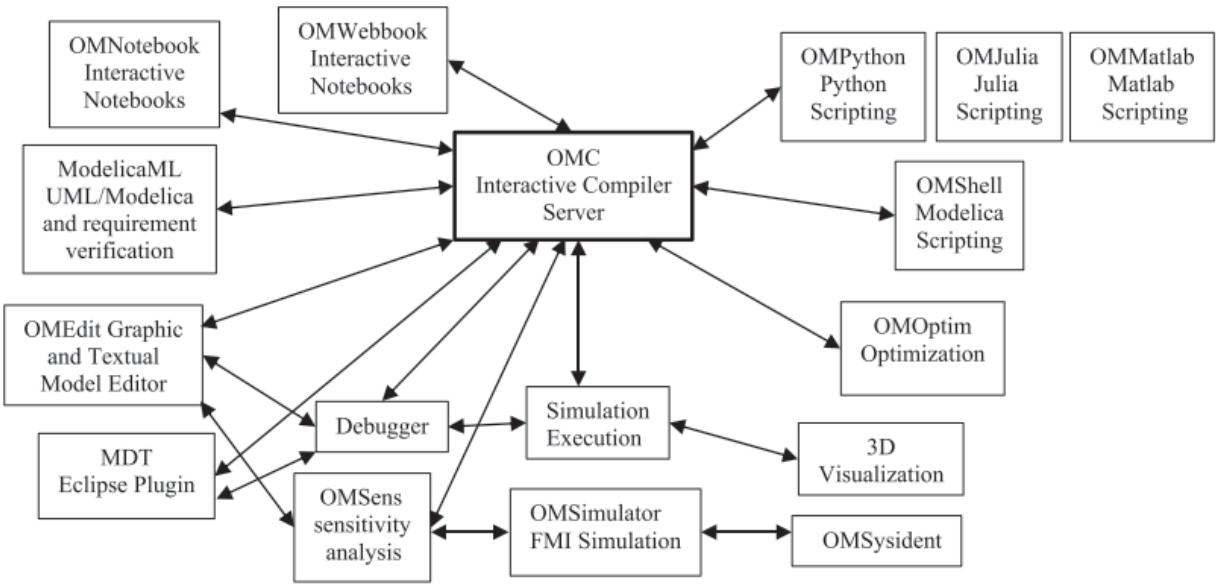

Figure 4-2 The architecture of the OpenModelica simulation environment, the arrows represent the data flow.

OMEdit is a graphical and textual model editor which enables graphical component-based model design by simply connecting instances of Modelica classes. OMEdit GUI also provides graphical user interface to the simulation and plotting of the results OMPlot.

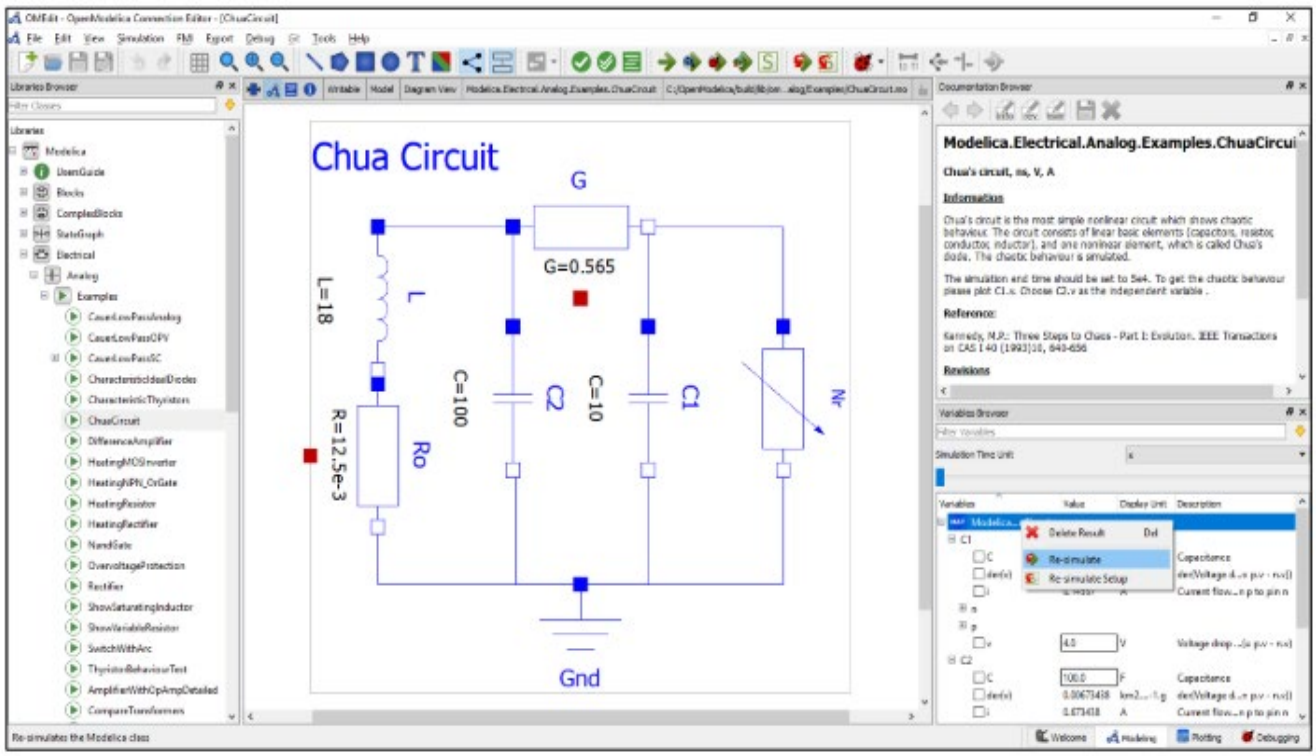

Figure 4-3 OMEdit on the Modelica Electrical Analog. Example: Chua Circuit model.

In Figure 4-3 the OMEdit window is shown for the electrical analog example ChuaCircuit. In the centre of the window is the model connection diagram, left is the Modelica library browser, upper right is the information widow, and lower right is the plot variable browser. Figure 4-4 depicts the results visualisation in OMPlot.

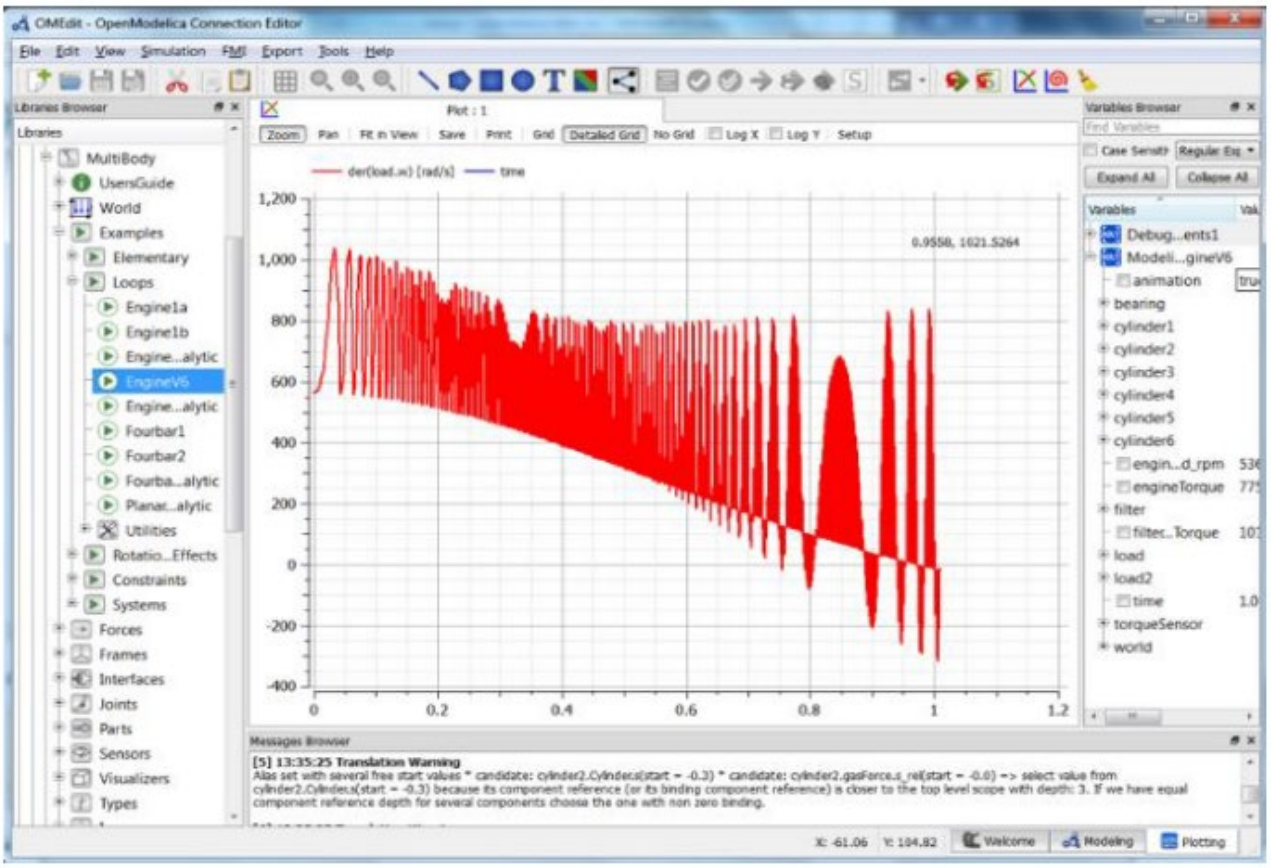

Figure 4-4 OpenModelica simulation of the V6Engine, results visualisation using OMPlot.

4.3. TESEO environment

The main objective of the model is to be able to perform a dynamical simulation inside 'Terna Sistemi Elettrici Ottimizzati' (TESEO) software. TESEO is a software package developed by CESI for Terna, designed for performing electrical network numerical analysis aimed to replace SICRE, another tool developed by CESI for Terna, which was written in an outdated language "Pascal" around 30 years ago. The inputs for TESEO are Dava/Dadir, Italian data structure format, which contain fixed data as network structure and variable data as position of circuit breakers, and from CIM sources. TESEO can perform various steady state functionalities as:

- Load flow calculation.
- Editing parameters of the network structure.
- Verification of grid status.
- Graphical representation of the network.
- Analysis of network situation.

Through TESEO the user may interact with the grid graphically and modify or add new elements/generators easily, a plug and play functionality that was absent in SICRE.

Within TESEO exists the dynamic analyser "Dyana" functionality, a dedicated tool for performing dynamic simulation which inherit some TESEO's steady state simulation attributes as the graphical interface, and input of Dadir/Dava/CIM data.

4.3.1. The Dyana tool

The plug and play functionality of TESEO is inherited by Dyana which originates from how the components are described in the network. Each component in the network is described as a system of differential algebraic equations DAEs that is defined by specific inputs and outputs. The DAEs system is then discretized and solved numerically by Newton-Raphson. The architecture of the dynamic system is divided into two main components as seen in Figure 4-5:

- Generators/Loads also known as injectors.
- Electric Power Grid.

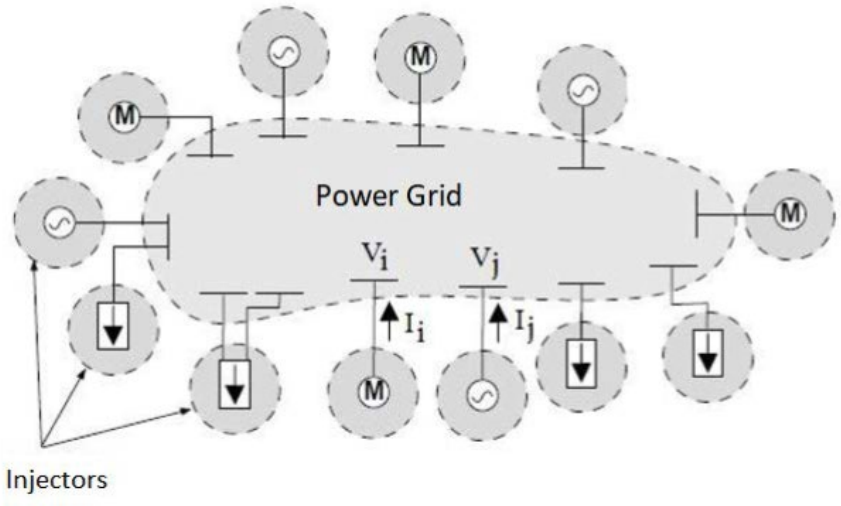

Figure 4-5 General architecture of the dynamic environment.

The injectors are interfaced with the electric grid using real and imaginary currents as outputs, I_i where the subscript "i" refers to the connection node. Afterwards the electric grid receives the nodal currents I_i as inputs and calculates the nodal voltages V_i, real and imaginary parts, which are in turn passed to the injectors as input variables. Analogously, the electrical grid can be viewed as an admittance matrix consisting of the electrical lines and transformers in the network that connects the inputs from the injectors to the outputs by the well know admittance equation $I = Y \cdot V$.

The mathematical model of the generators is developed as FMU (Functional Mock-up) module by using the GUI interface OMEdit in Modelica with special care taken into designating the outputs and inputs interfaces. Figure 4-6 shows the main interface of the BESS developed in OMEdit.

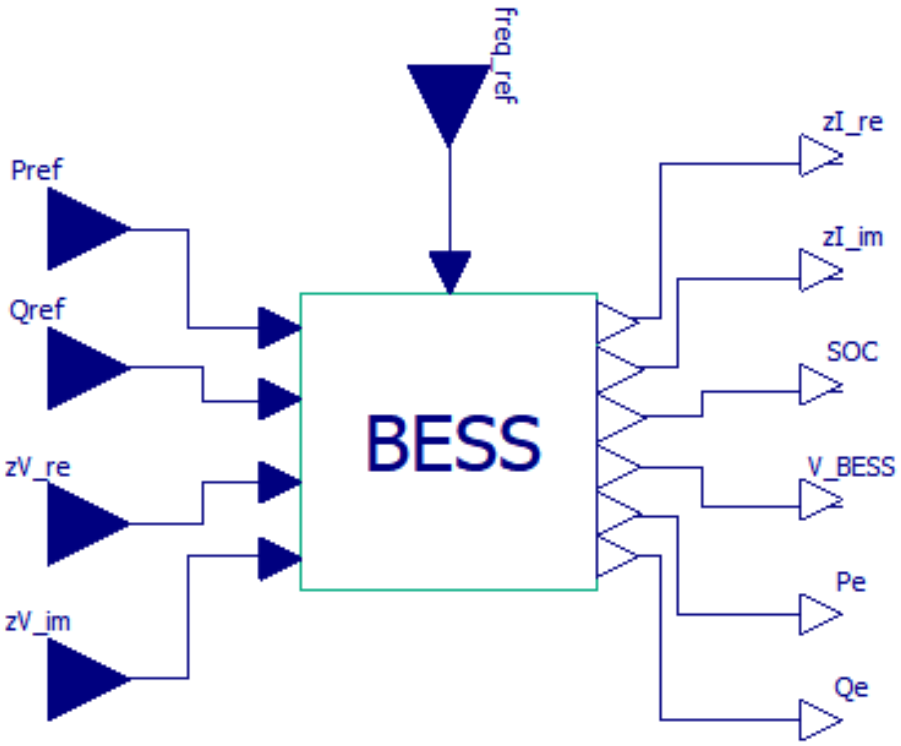

Figure 4-6 BESS Model

The dynamic simulation procedure can be demonstrated briefly in the following steps:

I. Load flow.

Load flow analysis is performed in the beginning by an internal function in TESEO to obtain the reference parameters of the nodal voltages and injected active/reactive power ($V_{mod\_Loadflow}$, $V_{arg\_Loadflow}$, $P_{Loadflow}$, $Q_{Loadflow}$).

II. Initialization.

The dynamic model is initialized with the data acquired from the load flow. The internal state-variables of the model are also estimated by zeroing the

derivatives of the DAE system.

III. Transient calculation.

Eventually the dynamic simulation is commenced, and input and output data are exchanged between different models to simulate load variation and grid status.

5. BESS Modelling

A generic BESS model that is able to represent all technologies and capture the complete dynamics of the system is hard to obtain, because of the huge differences between different technologies and the variations within a single a technology. This study is focused on establishing a standard BESS model able to be used in transient stability studies (typically primary/fast frequency response) in the RMS dynamic environment and, required to fit the voltage/current response of Lithium-ion batteries in case it is needed (since it has been observed to be the most promising technology available).

The BESS consists of 3 main components, as shown in Figure 5-1:

- **Battery Cell Arrays**: Inside this component several battery cells are connected in series and parallel to compose a battery module which are connected to form strings inside a battery stack. Alongside lies the battery management system which monitors the cell voltages, state of health, and performs heat management
- **Power Conversion System (PCS):** The PCS is a bidirectional AC-DC converter where it inverts the DC power to feed the grid (discharge) or rectifies the AC power to feed the BESS (charge). The PCS is controlled through the control and monitoring system.
- **Control and Monitoring System**: The control circuit is the main element which acquires raw measurement data, performs computations, controls the PCS functionality and system protection.

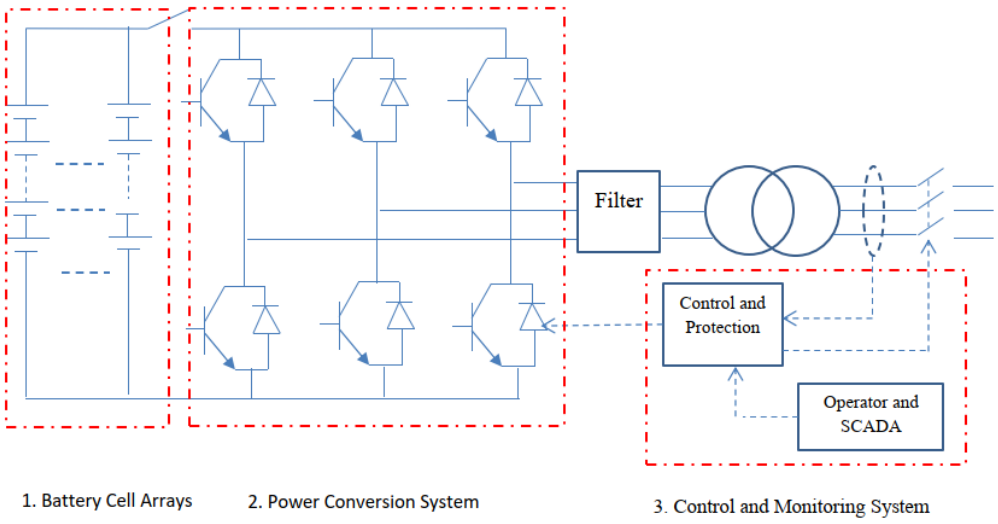

Figure 5-1 BESS main components

There are four main challenges facing the BESS model:

1) Use a battery cell model which can capture as much as possible dynamic characteristics of the battery accurately without being too complex.
2) Acquiring measurement data or parameters from battery manufacturers needed for model employment.
3) Modelling the inverter's inputs, outputs, and controls.
4) Adapting the model to produce the required inputs for TESEO simulation environment.

This chapter will discuss how each obstacle is tackled and possible simplifications adopted to help reach the final goal of the model. It is organised as follows:

- The different approaches of modelling battery cells are discussed.
- The inverter model, control scheme and how it interacts with TESEO are discussed.
- Commercial BESS modelling attempts and the final description of the model used.

5.1. Battery cell modelling

An important functionality of the battery management system (BMS) is to compute/estimate some fundamental properties of the battery:

- The state of charge (SOC).
- Available power. Residual energy.
- Temperature.
- State of health (SOH).

The proper way to calculates these estimations is through high accuracy mathematical set of equations of cell model that can predict the input/output relations. There are two basic different kinds of models that can be utilized to perform these estimations: physical based electrochemical models and equivalent circuit models (ECM) [48].

Physics based models

Physics based models, Figure 5-2, employ set of partial differential equations and algebraic equations (DAEs) that model the cell operation through accurate description of chemical and physical phenomena. The phenomena include but not limited to:

- Ohm's law.
- Diffusion and migration of the active electrodes' ions.
- The electrochemical reactions occurring on the active electrodes' surfaces.
- Charge and energy conservations laws.

After solving the system of DAEs equations the cell voltage is then computed along with the other parameters as state of charge, aging, and temperature of the cell [49].

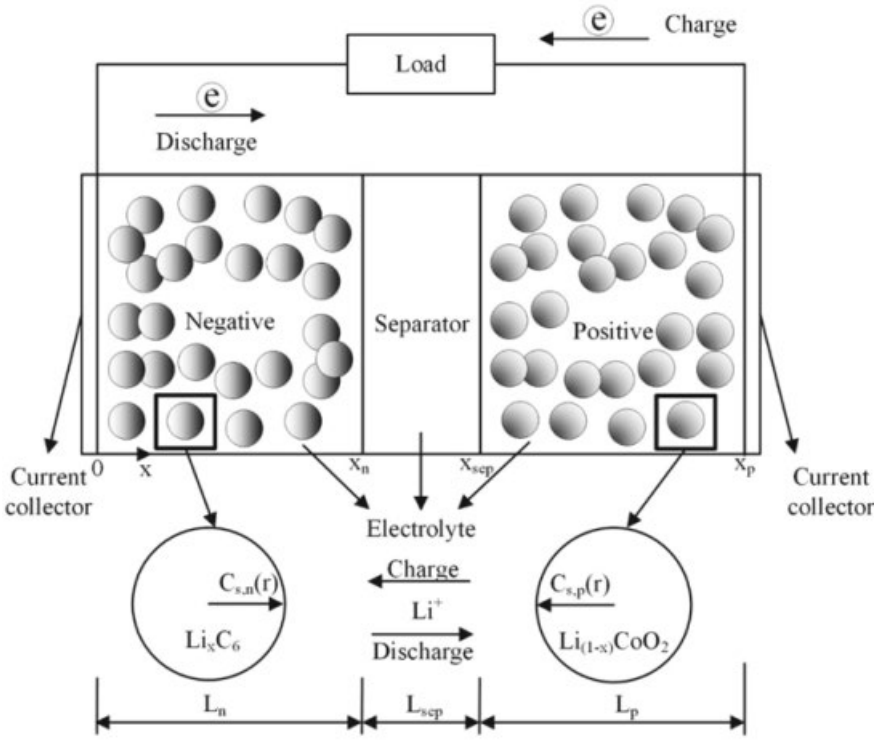

Figure 5-2 Schematic of physics based models

Physics based model can operate over a wide range of operating conditions, can be extended to almost any BESS chemistry given the parameters, and can give insights to how improve the cell design. However, it consists of complex coupled partial differential equations and large number of electro-chemical parameters (Table 5-1) which require high computational power and yield slow simulations that suffer from robustness and convergence issues.

	Mathematical expression	Boundary conditions
Li-ion diffusion in the electrolyte phase	$\varepsilon_e \frac{\partial c_e}{\partial t} = \frac{\partial}{\partial x}\left(D_e^{eff} \frac{\partial c_e}{\partial x}\right) + a(1 - t_+^0) j_r$	$\begin{cases} \left.\frac{\partial c_e}{\partial x}\right\|_{x=0} = \left.\frac{\partial c_e}{\partial x}\right\|_{x=x_p} = 0 \\ D_{e,sep}^{eff} \left.\frac{\partial c_e}{\partial x}\right\|_{x=x_{sep}^-} = D_{e,p}^{eff} \left.\frac{\partial c_e}{\partial x}\right\|_{x=x_{sep}^+}, \quad c_e\|_{x=x_{sep}^-} = c_e\|_{x=x_{sep}^+} \\ D_{e,n}^{eff} \left.\frac{\partial c_e}{\partial x}\right\|_{x=x_n^-} = D_{e,sep}^{eff} \left.\frac{\partial c_e}{\partial x}\right\|_{x=x_n^+}, \quad c_e\|_{x=x_n^-} = c_e\|_{x=x_n^+} \end{cases}$
Li-ion diffusion in the solid phase	$\frac{\partial c_s}{\partial t} = \frac{1}{r^2}\frac{\partial}{\partial r}\left(D_s r^2 \frac{\partial c_s}{\partial r}\right) = D_s\left(\frac{2}{r}\frac{\partial c_s}{\partial r} + \frac{\partial^2 c_s}{\partial r^2}\right)$	$D_s \frac{\partial c_s}{\partial r}\|_{r=0} = 0, \quad D_s \frac{\partial c_s}{\partial r}\|_{r=R_s} = -j_r$
Ohm's law of the electrolyte phase	$\kappa^{eff} \frac{\partial \phi_e}{\partial x} = -\frac{2RT\kappa^{eff}}{F}(t_+^0 - 1)\frac{\partial \ln c_e}{\partial x} - i_e$	$\begin{cases} \left.\kappa^{eff} \frac{\partial \phi_e}{\partial x}\right\|_{x=x_n^-} = \left.\kappa^{eff} \frac{\partial \phi_e}{\partial x}\right\|_{x=x_n^+}, \quad \left.\kappa^{eff} \frac{\partial \phi_e}{\partial x}\right\|_{x=x_{sep}^-} = \left.\kappa^{eff} \frac{\partial \phi_e}{\partial x}\right\|_{x=x_{sep}^+} \\ \phi_e\|_{x=x_n^-} = \phi_e\|_{x=x_n^+}, \quad \phi_e\|_{x=x_{sep}^-} = \phi_e\|_{x=x_{sep}^+} \end{cases}$
Ohm's law of the solid phase	$\sigma^{eff} \frac{\partial \phi_s}{\partial x} = -i_s$	$\begin{cases} \left.\sigma^{eff} \frac{\partial \phi_s}{\partial x}\right\|_{x=0} = -i, \quad \left.\sigma^{eff} \frac{\partial \phi_s}{\partial x}\right\|_{x=x_p} = -i \\ \left.\sigma^{eff} \frac{\partial \phi_s}{\partial x}\right\|_{x=x_n} = 0, \quad \left.\sigma^{eff} \frac{\partial \phi_s}{\partial x}\right\|_{x=x_{sep}} = 0 \end{cases}$
Charge conservation equation	$\begin{cases} i_s + i_e = i \\ \frac{\partial i_e}{\partial x} = a i_s = aF j_r \\ \frac{\partial i_s}{\partial x} = -aF j_r \end{cases}$	$\begin{cases} i_e\|_{x=0} = 0, \quad i_e\|_{x=x_p} = 0 \\ \left.\frac{\partial i_e}{\partial x}\right\|_{x=x_n} = 0, \quad \left.\frac{\partial i_e}{\partial x}\right\|_{x=x_{sep}} = 0 \end{cases} \quad \begin{cases} i_s\|_{x=0} = i, \quad i_s\|_{x=x_p} = i \\ \left.\frac{\partial i_s}{\partial x}\right\|_{x=x_n} = 0, \quad \left.\frac{\partial i_s}{\partial x}\right\|_{x=x_{sep}} = 0 \end{cases}$
Butler–Volmer kinetic equation	$\begin{cases} j_r = i_0\left(e^{\frac{\alpha_a F}{RT}\eta} - e^{-\frac{\alpha_c F}{RT}\eta}\right) \\ i_0 = k_s c_e^{\alpha_a}\left(c_{s,max} - c_{e-s}\right)^{\alpha_a} c_{e-s}^{\alpha_c} \end{cases}$	
Output voltage	$U_t = \phi_s\|_{x=x_p} - \phi_s\|_{x=0}$	

Equivalent circuit models (ECM)

Equivalent circuit models depict the operation of a battery cell by proposing an electrical circuit acting analogously to the real cell behaviour. The battery terminal voltage can be divided into two parts: static and dynamic. The static part represents the open circuit voltage (OCV) (equilibrium voltage) and the hysteresis voltage. The dynamic part represents the fast and slow changing voltage components related to ohmic polarization, the mass transport, and reaction kinetics. The equivalent circuit models are not meant to describe the structure of the cell, as for the physics-based models, rather they are designed such that basic circuit elements such as voltage sources, resistors, capacitors can imitate the behaviour of the internal processes of the battery upon being subjected to the same external stimuli [49].

Figure 5-3 represents a typical equivalent circuit model of a battery consisting of n-RC networks, the model is made of 3 parts [50]:

- Voltage source U_{OC} indicates the equilibrium voltage of the battery.
- Internal Ohmic resistance R_i indicates the cumulative static resistance inside the cell such as: contact resistance of the battery, electrode material resistance, and electrolyte resistance.
- Network RC indicates the dynamic characteristics of the battery including mass transport losses, and polarization losses.

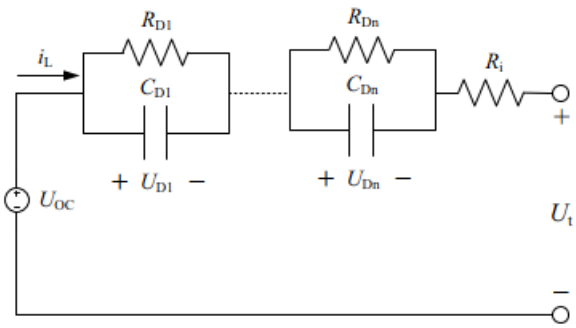

Figure 5-3 Typical ECM consisting of N-RC

ECM utilize data collected from cell lab tests or manufacturer's data sheets to optimize the model behaviour such that the current voltage behaviour matches that of the real cell. Since ECM employs curve fitting techniques, they are bounded by the curve fitting features. For instance, ECM tend to make the best predictions when interpolating inside the data set used when the model was created; however, they do not tend to behave correctly upon extrapolating.

ECM can only predict input/output current and voltage behaviour only and occasionally temperatures when combined with complementary empirical equations. Nevertheless, ECM yield fast and robust simulations.

5.2. Inverter modelling

The common power converter used in BESS is the voltage source converter (VSC) that converts DC voltage from the battery side to AC voltage and vice versa through fast switching of IGBT valves. The output voltage is controlled through the switching signal (Modulating amplification signal) P_M which arrives from the controller. In a linear PWM control mode the output, at fundamental frequency, is as follows [51]:

$$U_{ACr} = \frac{\sqrt{3}}{2\sqrt{2}} \cdot P_{Mr} \cdot U_{DC}$$

$$U_{ACi} = \frac{\sqrt{3}}{2\sqrt{2}} \cdot P_{Mi} \cdot U_{DC}$$

Where U_ACr and U_ACi represent the real and imaginary part of the ac voltage, $P_Mr$and P_Mi represent the real and imaginary part of the modulation amplification signal, and U_DC represent the DC side voltage. In order to remain operating bidirectionally in all scenarios, the DC voltage must satisfy the inequality:

$$U_{DC} \geq \frac{2\sqrt{2}}{\sqrt{3}} \cdot abs(U_{AC})$$

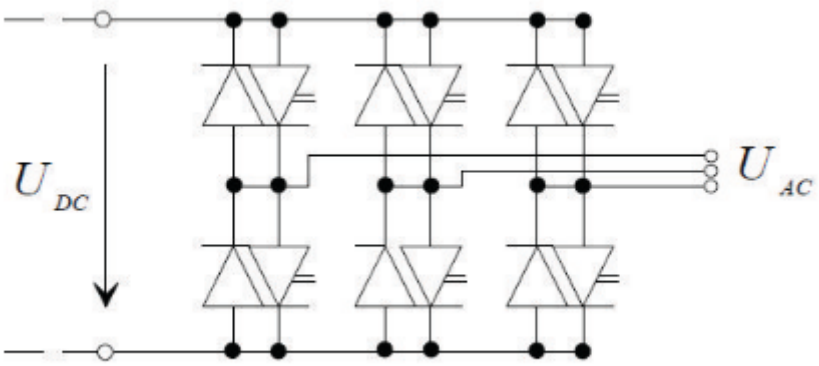

Figure 5-4 Equivalent circuit of PWM converter.

VSC in BESS allow full four quadrant control on the active and reactive power independently inside the limits of the IGBT (Figure 5-5). This implies that the real power current flow direction can represent either charging or discharging state and the reactive power current direction can represent either absorbing or supplying independently from each other and simultaneously.

The control scheme of the inverter during operation is usually done in dq frame of reference which would deeply simplify the signal processing, explained in detail in the final section in this chapter. The output of the inverter model is restricted by the TESEO modelling environment since it must accept real and reactive current injections.

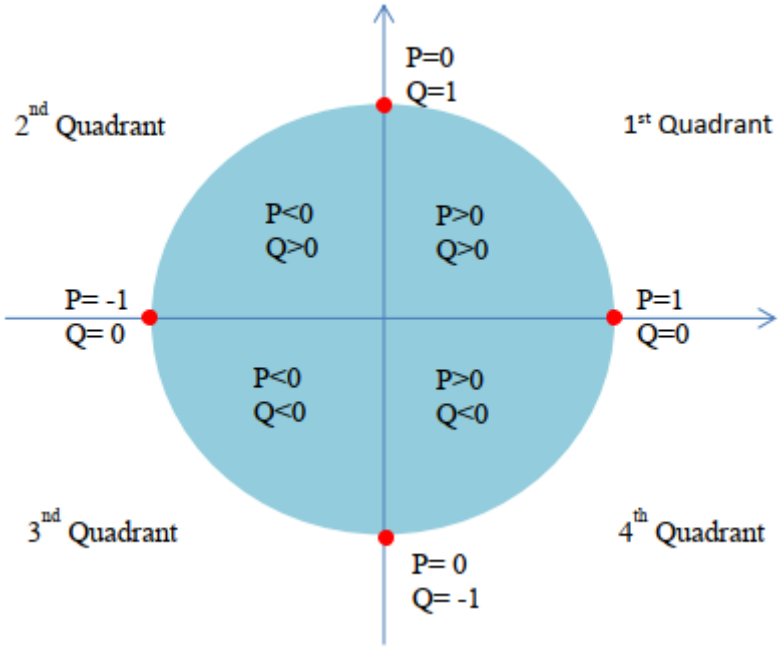

Figure 5-5 BESS full quadrants operation

5.3. Available models

This section will demonstrate some of the available BESS models in the commercial simulation softwares, their advantages, and their shortfalls.

5.3.1. DIgSILENT Model

DIgSILENT GmbH is an independent software and consulting company in the electrical power systems field. DIgSILENT's PowerFactory is one of the internationally most utilized power system analysis software mainly used for planning, operation, and optimisation of power systems [52].

Figure 5-6 DIgSILENT Logo

In the report [53], developers at DIgSILENT have examined the ability of their developed BESS model in providing primary frequency reserve in a test network. The main objective was to develop a model that was accurate enough without much computational complexities and adopt the parameters of manufacturers properly into the model.

Some assumptions were adopted to facilitate the modelling task, the important ones are listed below.

Regarding the battery cell model:

- The target technology of the model was more leaning towards lead acid batteries.
- Concerning the battery cell model equivalent circuit model was adapted, shown in Figure 5-7.

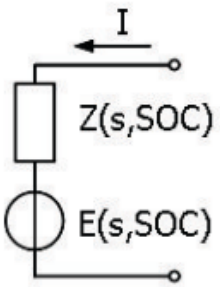

Figure 5-7 ECM used in DIgSILENT's model

- The battery could only operate in the state of charge (SOC) range of 20% to 80%.
- In the ECM, the resistance was considered constant.
- The voltage source was considered a linear function of the state of charge.
- The battery's capacity is function of the current setpoint according to Peukert's law.
- The SOC was calculated using an integrator.

Regarding the inverter model:

- A bidirectional VSC is utilized which is controlled in sinusoidal PWM mode.
- The converter will only work in the linear PWM amplification factor zone.
- The control input signals to the inverter are (I_d and I_q) which are the current phasors transformed in the dq frame of reference.
- The model has an internal control circuit which transforms the input signals to actual modulation signals.

For the control scheme the control of the model is divided into three parts:

- Frequency controller: Which operates in a single band droop control mode. The droop controller reads the frequency deviation from the nominal value and computes the corresponding output power to help stabilize the grid.
- Active/Reactive power Controller: The controller generates two reference signals, id and iq, representing the active/reactive power input setpoints. This controller operates in the dq frame of reference.
- Charge controller: The controller is responsible for achieving the assumptions/boundaries set. The inputs id, iq, and SOC, the controller checks the SOC of the battery and the apparent power limit of the inverter and based on it gives an operating signal. The controller prioritizes active power over reactive power.

The final scheme of the BESS model is shown in Figure 5-8.

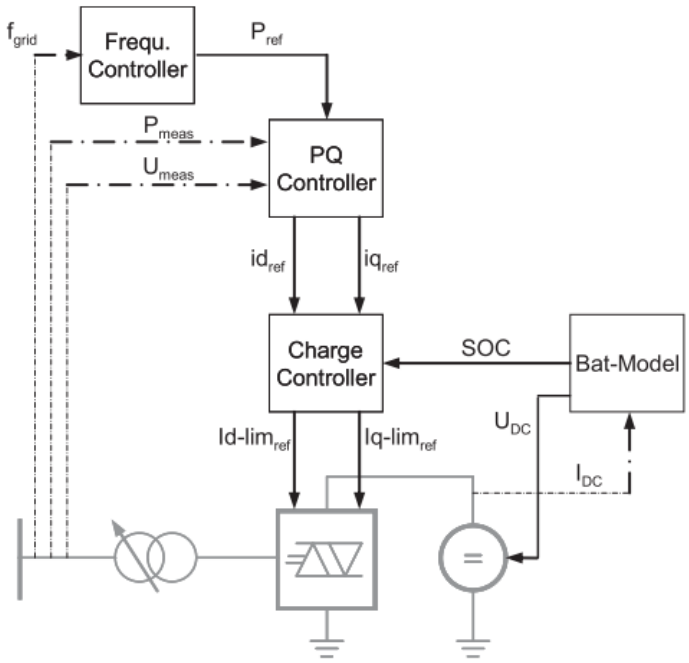

Figure 5-8 Final Model structure for DIgSILENT.

The model was tested in a small grid where it has improved the frequency response of the grid. Despite the model's successfulness in the test grid but it has some serious drawbacks:

- The model is not in a standard from; if the technology is changed or operation mode the model will be changed.
- The battery cell model technology is based on an obsolete technology, Lead acid.
- The parameter insertion of the battery cell model cannot fit most manufacturer's datasheets.

5.3.2. Siemens PSS®E model

Similar to DIgSILENT, PSS®E is a power system simulation and analysis software developed by Siemens. It is intensively used worldwide to perform many analysis like: power flow, dynamic, short circuit, transient stability, voltage stability, and much more [54].

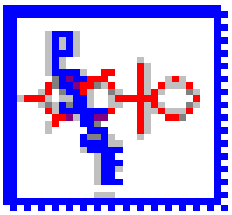

Figure 5-9 PSS®E logo

PSSE has adopted a different pathway than DIgSilent where its aim was developing a more standard model for BESS. The model developed by PSSE is based on WECC generic renewable electrical control models. In the following points the main aspects of the model will be explained [55], [56]:

- The WECC models are non-proprietary which are accessible without the need of non-disclosure agreements.
- The models are intended to provide a reasonably good representation of the dynamical performance of a BESS at the point of connection with the electrical power system.
- The model is suitable for studying system response to electrical disturbances but not dynamical battery cell disturbances (i.e., battery voltage is assumed constant and the capacity of the model is constant).
- The inverter is considered ideal without any losses from the DC side to the AC side.
- The simulations made using these models are typically in the range of 20-30 seconds.
- The models focus mainly on positive sequence currents.
- The models are initialized from a solved power flow.

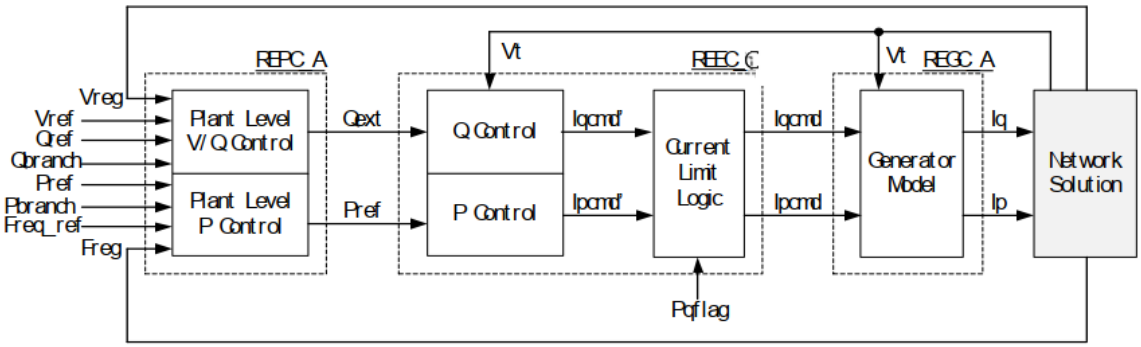

Figure 5-10 Architecture of PSSE BESS model

- REPC: This module represents the plant controller. It sets the plant reference signals where it computes voltage/reactive power output signals based on measures voltage/reactive power and computes active power output signal based on the measured frequency/active power.
- REEC: This module is an augmented version from the typical REEC_A/REEC_B modules which are used to represent the electrical control loops of the inverter. This module acts on the active/reactive power setpoints provided from REPC_A with feedback from the terminals of the BESS. Then it provides active and reactive power setpoints (Id and Iq) to the REGC_A block. The main difference of this module from the generic renewable ones is the added SOC constraint which is shown in Figure 5-11. The block limits the output current of the battery based on the SOC.
- REGC: This module is used to describe the BESS/inverter interface with the grid. It processes the real and reactive power commands and outputs real and reactive power injections.

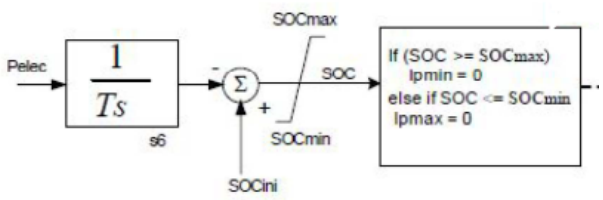

Figure 5-11 SOC constraint added by PSSE on WECC PV Module

The model was reported to have worked effectively in frequency containment situation and was able to respond to both generation and load loss events. However, the model suffers from the same limitation that the generic renewable energy modules suffered from such as [57]:

- They are intended for usage in frequency range 0.1Hz – 3Hz, simulations outside this range will give in accurate results such as switching transients of harmonics.
- The models focus only on the positive sequence stability software programs.
- The converter phase locked loop PLL was neglected for most of the parts.
- The models are not suitable for usage in weak networks with low short circuit current ratio at point of interconnection.

For the BESS specific case:

- The battery's inner reactions are not captured.
- The models are not suitable for modelling low rated (Energy/Power) batteries as the SOC might affect the battery output.
- Mid-term simulations involving high power applications might not represented well.

6. Developed BESS Model

The aim of this study is to develop a standardized model of the BESS using OpenModelica, which should follow the directives of the Common Grid Model Exchange Standard (CGMES) project. Thus, the model should adopt a standard architecture backbone and at the same time would allow fine tuning to suit specific battery vendors' specifications. The study will only focus on the primary/fast frequency response control scheme as a start, since it has been shown in the previous chapters the positive stability impact BESS can offer to the grid along with the new remuneration policies adopted worldwide that gave BESS higher return on investment than before.

The model is constructed as follows:

I. A Standard backbone: The main backbone component is adapted from the WECC PV modules. This component aims to providing a standard tool to simulate BESS' dynamic response regardless of the availability of the manufacturers' parameters as only few vendors offer them.
II. A Fine-tuning element: This component enables the user to enter specific manufacture's parameters if available therefore giving a more thorough picture of the BESS dynamic response and extending the mode of operation to include mid-term simulations.
III. Auxiliary functions: These functions facilitate the modelling of the system and assist the previous blocks to reach the final goal easily. They include phase locked loop and Park-Clarke transformation.

The suggested construction will allow the model to acquire the following characteristics:

- Having a modular format which makes adding features and functionalities easier since the main model structure is adopted from the WECC approved EPRI renewable modules.
- The model is suitable for studying system response to electrical disturbances.
- The simulations made using the model will increase the range of 20-30 seconds imposed by the WECC modules.
- The model focuses on positive sequence currents.
- The model is initialized using a power load flow.
- A better dynamic representation of the battery response is achieved with the ECM.

- The Peukert's law utilization allows a more realistic capacity representation.
- The ECM adopted will present medium-accuracy results without much computational complexities and can be operated for modelling several minutes.
- The ECM model can adopt the parameters of manufacturers easily using a simple UI.
- The services provided are active power control, reactive power control, and primary frequency regulation control.
- The inverter is considered ideal without any losses from the DC side to the AC side.
- All the control functionalities are operated in the dq axis.

As most models the introduced assumptions limit the operating conditions, for the BESS model these are:

- The model is not equipped with fault ride through logic.
- Only positive sequence is modelled.
- The individual cells interactions and full dynamics are not captured.
- High power long period simulations may not give accurate data due to lack of temperature dependence.
- Transformer and inverter losses are not introduced.

The model operates as a single DC-AC unit and is based on a three -phase inverter with the control unit operating in the dq axis frame of reference. The guidance of WECC report recommends the usage of per unit values inside the model for a more generic model development where the characteristic grid base values are supplied as input to the model. The dynamic simulation starts from the steady state solution results provided from TESEO environment as reference: active power, reactive power, voltage, and frequency. The final model structure is depicted in Figure 6-1 where the detailed is structure is depicted in the following sections. The OpenModelica interface is shown in Figure 6-2 and the input and output signals are described in Table 6-1.

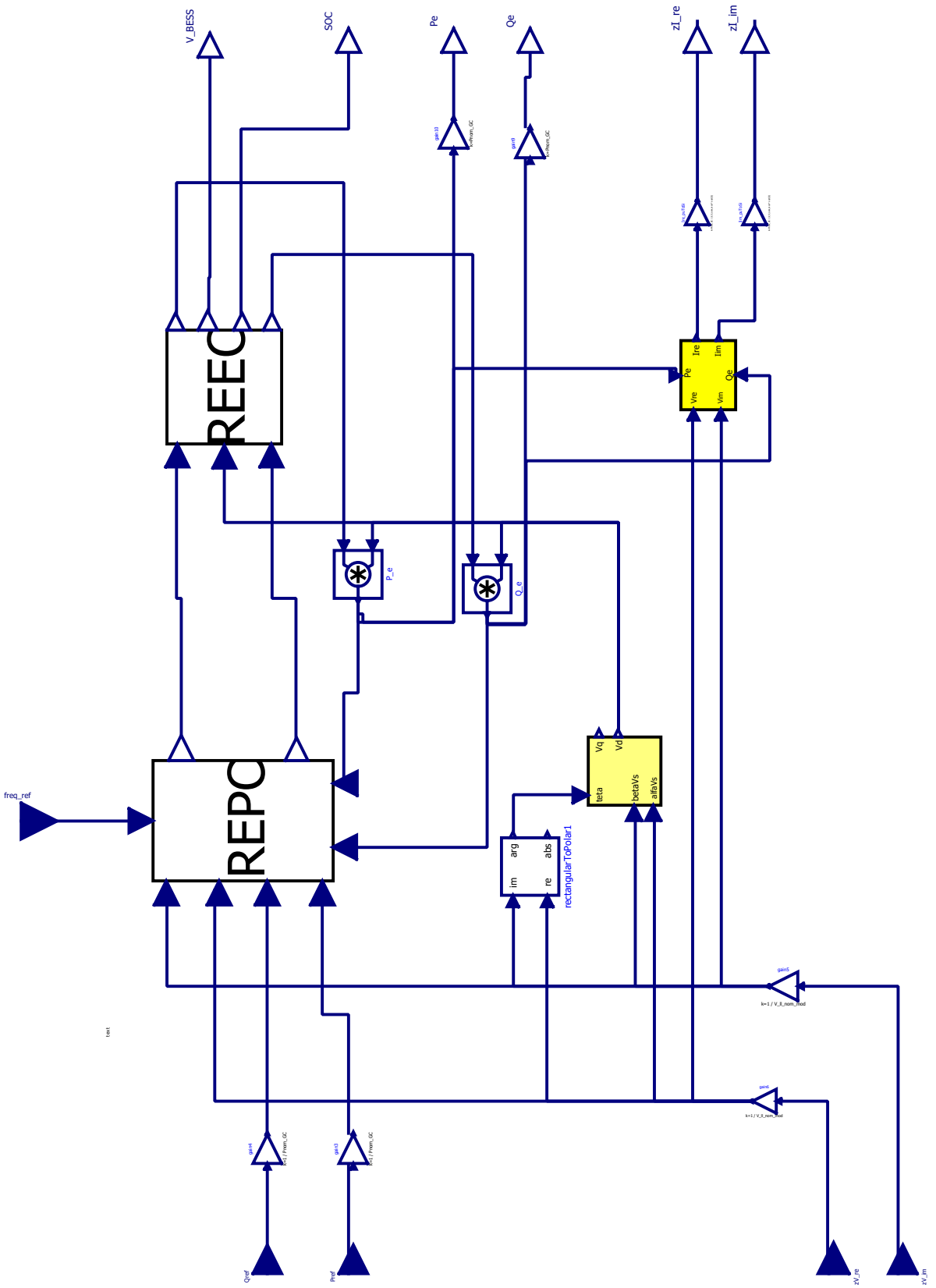

Figure 6-1 BESS final model structure

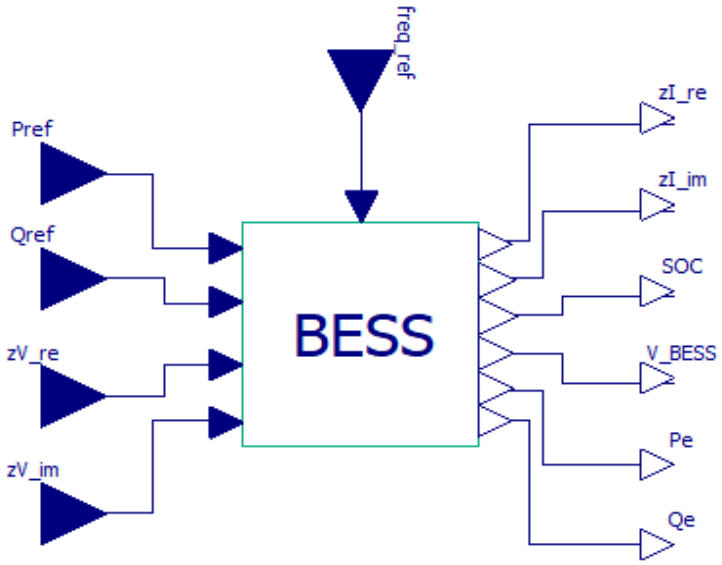

Figure 6-2 BESS final model OpenModelica interface

The BESS model parameters, described in the following sections, can be easily changed using a simple user-friendly parameters window, a portion of the scrollable window is depicted in Figure 6-3.

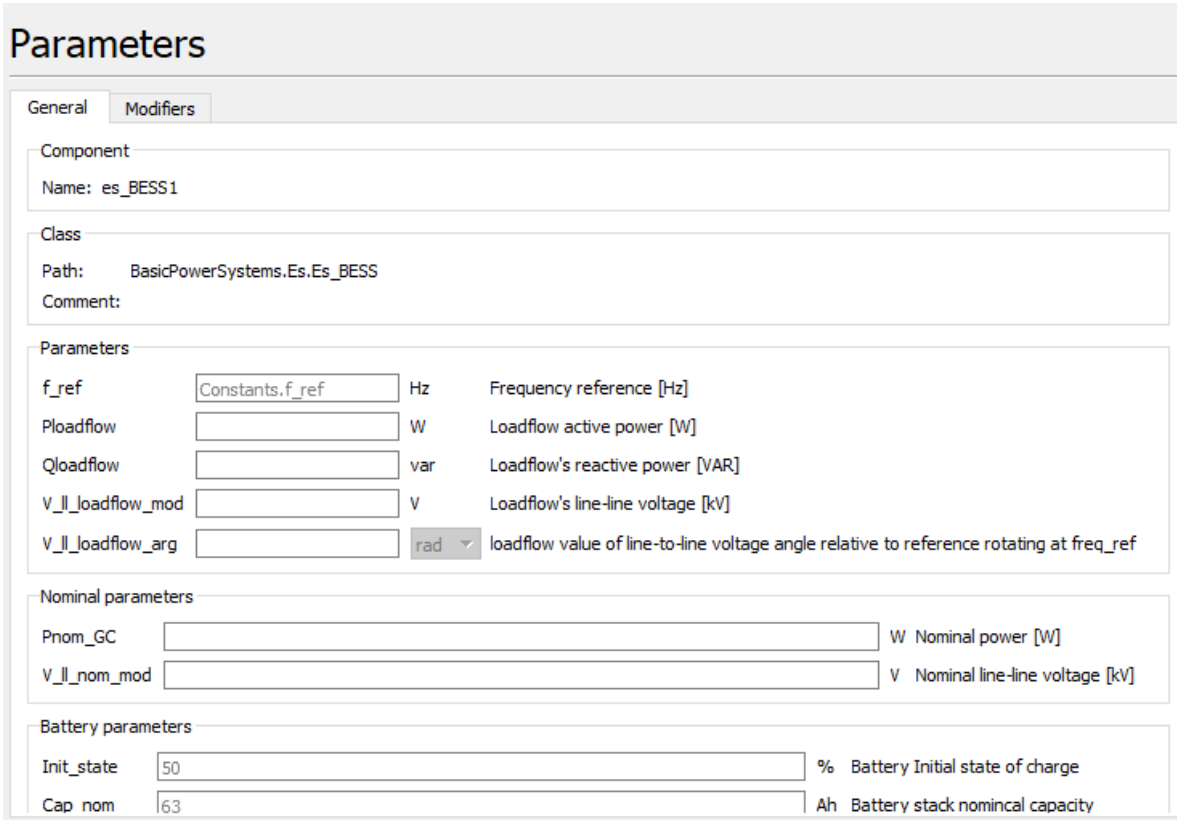

Figure 6-3 Model's parameters insertion window

Table 6-1 BESS model signals.

Signal	Type	Units	Description
Freq_ref	Input	pu	Initial frequency from steady state solution.
Pref	Input	Watt	Initial active power from steady state solution.
Qref	Input	Var	Initial reactive power from steady state solution.
zV_re	Input	kV	Initial real Voltage from steady state solution.
zV_im	Input	kV	Initial imaginary Voltage from steady state solution.
V_BESS	Output	Volts	Battery stack DC voltage output.
SOC	Output	Percent	State of charge of the battery stack.
Pe	Output	Watt	Output active power of the battery.
Qe	Output	Var	Output reactive power of the battery.
zI_re	Output	kA	Output real current of the battery.
zI_im	Output	kA	Output imaginary current of the battery.

6.1. Auxiliary functions

Park-Clarke(dq) transformation

The auxiliary functions described in this chapter define the instruments needed to set up the simulation environment or facilitate the control process in the model. The Park-Clarke transformation was introduced to easily analyse rotating machines. The transformation referred the stator variables to a frame of reference fixed in the rotor which subsequently eliminates all time varying inductances from the voltage equation hence facilitating strongly the analysis [58].

In this work the Park-Clarke transformation is used to refer the inverter AC side three phase quantities (abc) to a new rotational axis (dq0 axis) that rotate at the same velocity as the angular frequency (ω) of the AC side. The following equation represents the transformation of the quantities between the two frames of references:

$$f_{dq0} = \frac{2}{3} \cdot \begin{bmatrix} \cos \omega t & \cos \omega t - \frac{2\pi}{3} & \cos \omega t - \frac{4\pi}{3} \\ \sin \omega t & \sin \omega t - \frac{2\pi}{3} & \sin \omega t - \frac{4\pi}{3} \\ \frac{1}{2} & \frac{1}{2} & \frac{1}{2} \end{bmatrix} f_{abc}$$

Figure 6-4 illustrates graphically the transformation process of the quantities between the αβ and dq coordinate systems where the αβ coordinate is simply the projection of the phase variables on the two-stationary axis αβ. Once synchronism occurs as a result of the dq coordinates rotation at the same angular speed of the projected quantities on the αβ axis, the quantities which seemed as time varying in the abc coordinate systems now appear as DC quantities in the dq coordinate and simple control techniques can be utilized to achieve the desired values and then reverse the transformation to return back to the abc frame of reference.

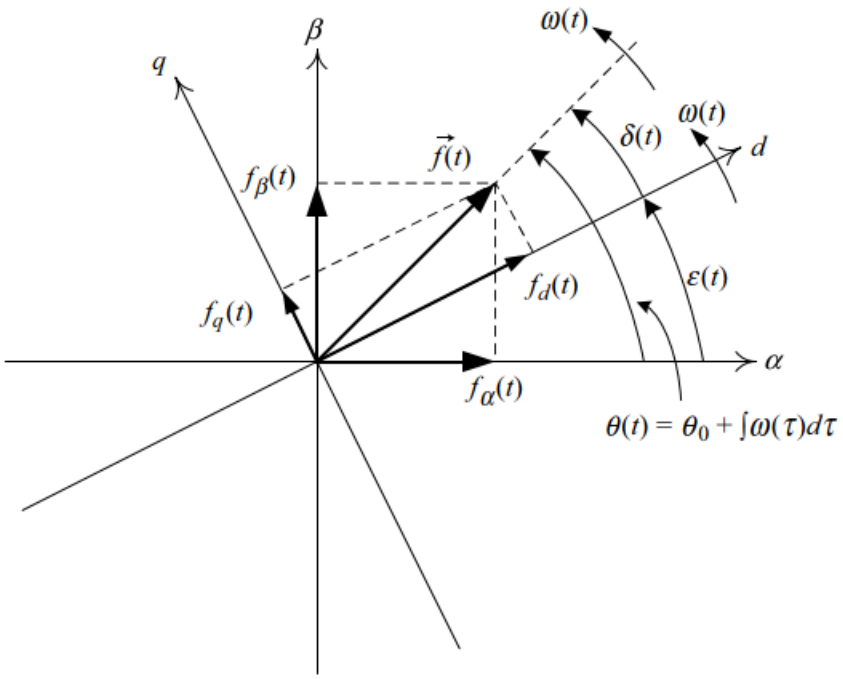

Figure 6-4 αβ and dq coordinate systems illustration.

The active and reactive power in the dq frame of reference are expressed as:

$$P(t) = \frac{3}{2}\left[v_d(t)i_d(t) + v_q(t)i_q(t)\right]$$

$$Q(t) = \frac{3}{2}\left[-v_d(t)i_q(t) + v_q(t)i_d(t)\right].$$

Which are time varying DC values therefore simplifying the analysis. Once synchronism is achieved it can be combined with a particular function called phase locked loop (PLL) where the quantity d-component is aligned with the d-axis and the q component is aligned with the q-axis, as shown in Figure 6-4. The q-value (F_q) gets zeroed and the active and reactive power from the previous expression are decoupled as follows:

$$P = \frac{3}{2} v_d\, i_d$$

$$Q = \frac{-3}{2} v_d\, i_q$$

In the network interface the inputs are provided in real and imaginary form (αβ coordinates) to transform to the dq coordinates the process is applied on two steps as shown in Figure 6-5: first the input voltage is inserted in the ideal PLL block where the angle (ωt) is provided then

the input voltage along with the produced angle value is used as input to block (αβ to dq) to get the value in the dq coordinates. The two blocks were provided by CESI from the library "BasicPowerSystems".

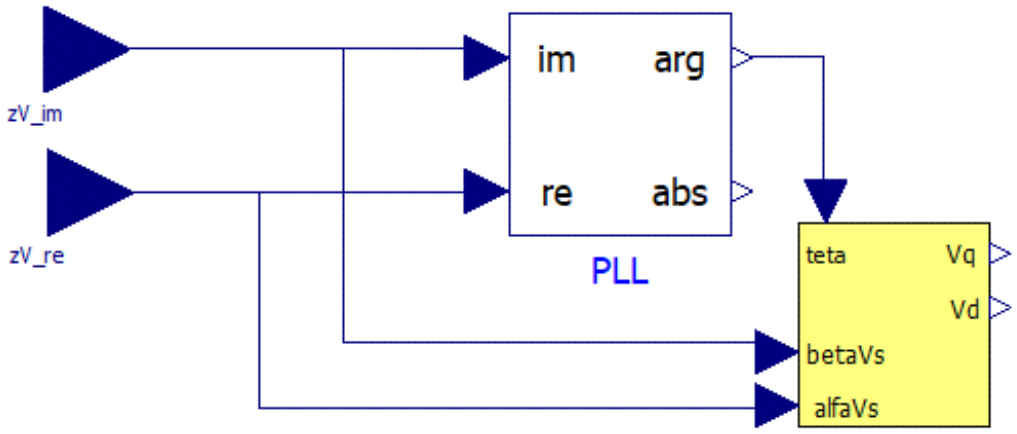

Figure 6-5 αβ to dq transformation

6.2. Battery Cell Model; Fine Tuning component

The battery cell modelling is implemented to overcome some short backs introduced by the PSSE standard WECC modules based model: capturing the voltage profile of the battery, limitation to short term simulation, and the inaccurate results for low rated systems (Energy/Power). It is also important for making user able to insert his/her battery specifications according to the parameters available.

Equivalent Circuit Model technique was chosen to represent the battery cell output dynamics because of its robustness and fast computational capabilities which shall meet the accuracy level need for transient stability analysis serving as a middle ground between computational efficiency and accuracy. It has been reported in [59]–[61] that a single RC circuit, n-RC was shown in Figure 5-3, is usually enough to accurately simulate the voltage/current output/input dynamics of lithium-ion batteries. Unfortunately, battery manufacturers often provide the open circuit voltage of the battery as a function of the state of charge or depth of discharge which would increase the difficulty for the user to insert the battery's data. Therefore, an adapted Thevenin circuit is used, shown in Figure 6-6 in which the current is an input set by the controller. The user can easily enter the OCV and internal resistance "R" data function of SOC in the battery cell model by utilizing a simple data extractor tool from the manufacturer's datasheet.

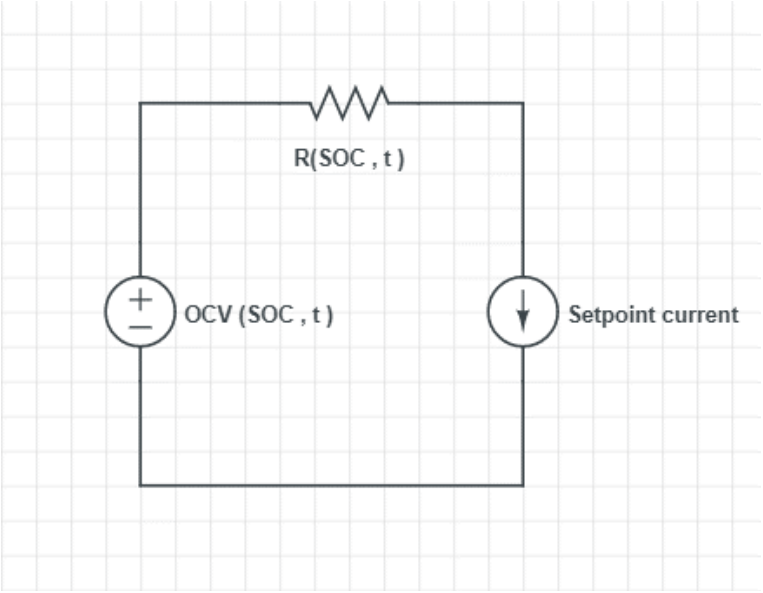

Figure 6-6 The Adapted ECM applied

Some important assumptions were made to facilitate the modelling:

- The temperature of the battery pack remains constant within the simulation interval because of the lack of temperature dependence information in the datasheets. This assumption can hold at small simulation time intervals as batteries' temperature can be slow [62] however for long time periods this assumption may give inaccurate result.
- The available commercial battery data does not entail an insight on the alignment of the cell in the pack hence [63] suggested an approximate remedy for this challenge where the complete pack dynamics can be referred to a single cell dynamics referring with the state of charge, C-rate, and E-rate. This assumption provides inaccuracies but helps overcoming the missing information impose by manufacturers challenge.
- To overcome the DAE looping error in OpenModelica constant pack voltage is utilized in calculating the current setpoint from the power setpoint yielding the C-rate equal to the E-rate.
- The aging effect/state of the battery is considered constant during the operational simulation interval where it can be introduced as an input affecting the accessible extractable capacity at the beginning of each simulation.
- To avoid fading capacity and polarization effects, [64] suggests battery packs is ought to operate in the range of 15% –– 85% SOC.
- The internal resistance will be constant in the operational time range it is constant for each temperature in the range of 15% – 85% SOC range for the specific case of the commercial battery used. It will be considered an input to the model according to the assumed constant temperature operation.
- The pack voltage is a function of the cell voltage through using the maximum dc voltage as a reference and the operating range ratio as an amplification ratio, as demonstrated in Table 6-2. This allow a prediction of the operating DC pack voltage while overcoming the lack of cells/modules alignment information.

The following equations are implemented for calculations:

Table 6-2 Utilized simulation equations

Equation	Description
$C-rate=\frac{I}{Cnom}$	The c-rate is calculated by dividing the operating current by the nominal capacity 63Ah
$E-rate=\frac{P}{Enom}$	The e-rate is calculated by dividing the operating power by the nominal energy 233 Wh
$V_{dc}^{cell}=OCV-I*R_{int}$	The output cell voltage is open circuit voltage subtracted by the internal resistance voltage drop.
$(V_{pack}^{max}-V_{pack}^{out})=$ $(V_{cell}^{max}-V_{cell}^{out})*$ $(\frac{operating\ pack\ range}{operating\ cell\ range})$	The output pack voltage is a linear function of the of the cell voltage using the maximum allowable voltage as a reference and the operating ratio as an amplification factor.

The final structure of the cell model is shown Figure 6-7.

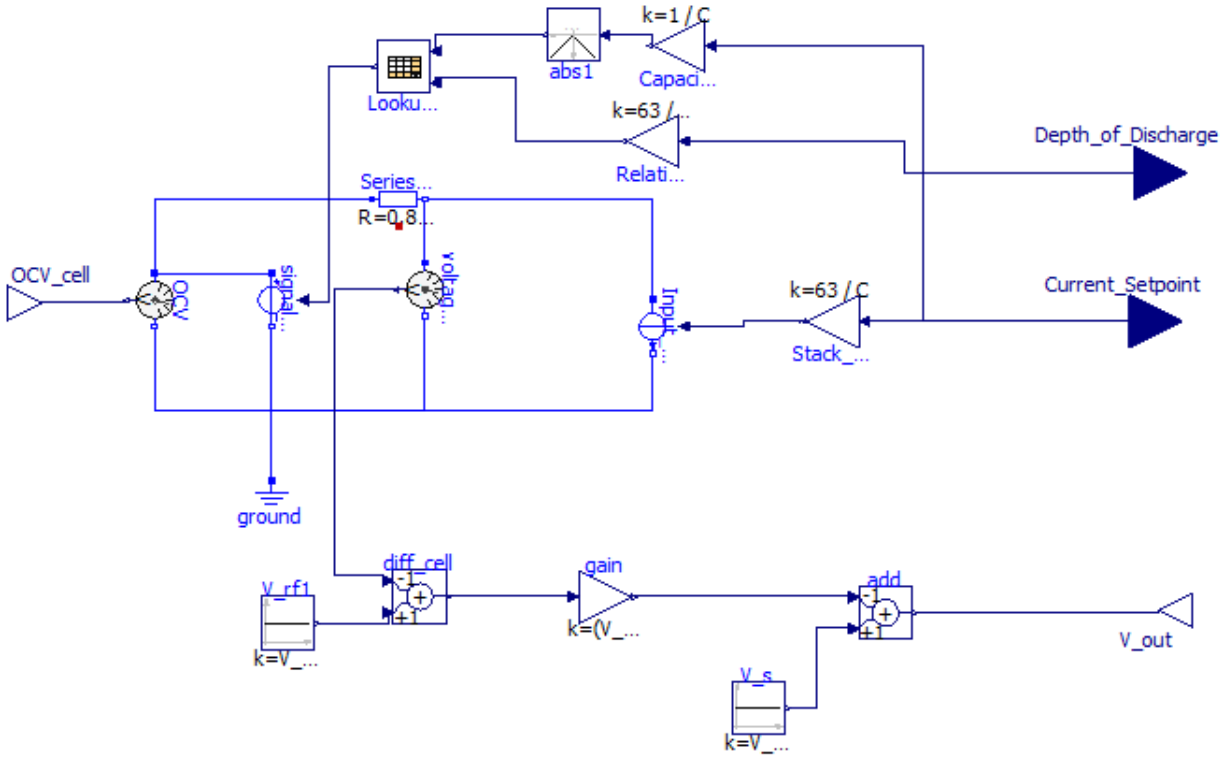

Figure 6-7 Battery cell OpenModelica model

The open circuit voltage of the battery is obtained from a commercial battery with the profile shown in Figure 6-8 and the parameters are set in Table 6-3 Cell model parameters.

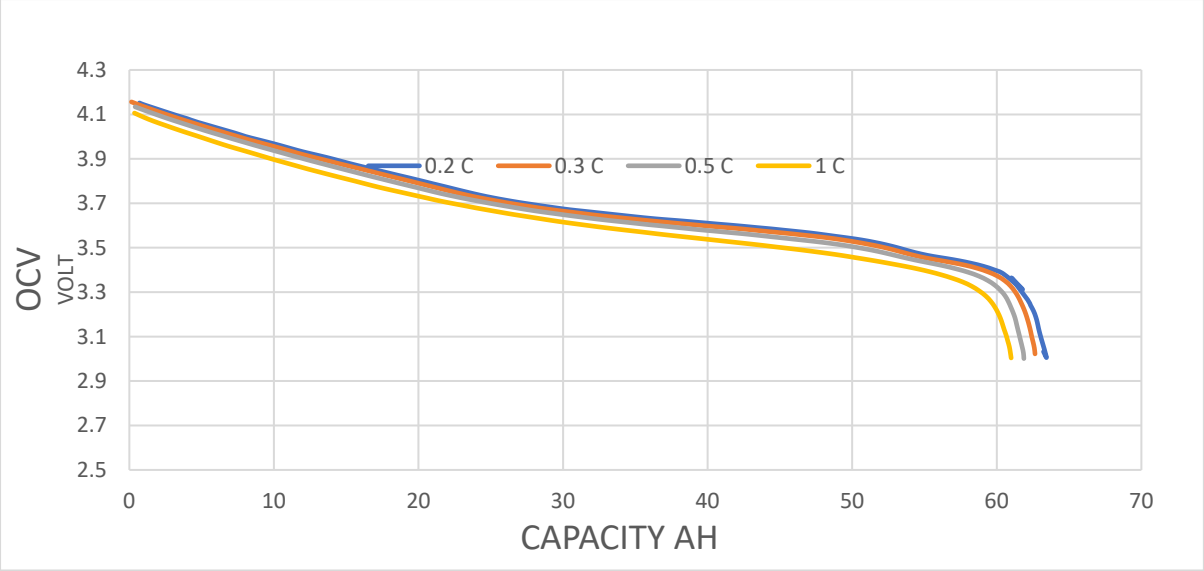

Figure 6-8 Commercial battery data

Table 6-3 Cell model parameters

Parameter	Value	Units	Description
Init_state	50	%	Initial state of charge of the battery cell
lim_max	85	%	Maximum state of charge of the battery cell
lim_min	15	%	Minimum state of charge of the battery cell
R_int	0.83	$m\Omega$	Battery cell internal resistance at 35 C

Since ECM could deliver inaccurate data when extrapolating, the maximum E-rate/C-rate of the battery is bounded by the maximum found in the datasheet of the manufacturer.

Regarding the SOC of the battery cell, it is computed using a simple integrator with an initial state option, the default initial state is set to 50% similar to Figure 5-11. In the case of the commercial battery utilized an extra adjustment is performed to calibrate the system behaviour to meet the real data supplied in the datasheet. Table 6-4 is supplied in the datasheet of the battery indicating the extractable energy as a function of the charging/discharging current supplied to the battery.

Table 6-4 Energy available at varying charging/discharging rates

C-rate (constant power)	0.2	0.3	0.5	1
Energy (%)	100	97.5	94.9	89.5

For the SOC customized calculation, Table 6-4 is utilized combined with Peukart's law that states $Q_p = I^k t$ where:

- Q_p is the nominal energy of the battery at specified rate
- I is the operation current.
- t is the discharge time.
- k is Peukart's constant.

For the model in this work, Peukart's law is utilized using a look-up table prior to the SOC integrator as in Figure 6-9.

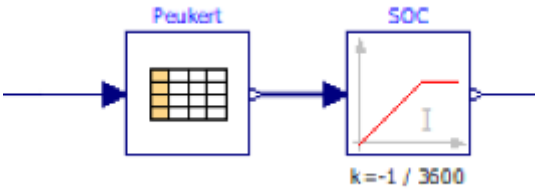

Figure 6-9 Peukart law utilization

6.3. WECC Adapted Modules

Since the standard backbone structure is adopted from the WECC generic renewable energy modules, the structure will be similar to that of PV as done by PSSE thus grasping the standardized advantage of that model. This will allow the final model to have a standard structural formula that can simulate any battery type or vendor. The models of the WECC library utilize simple PI controllers to regulate the reference quantities with the measured ones. To mimic the measurement time delay simple lag blocks are used with appropriate setting adopted from WECC's simulation and CESI's previous work [65]–[68].

This part is constructed as follows:

6.3.1. REPC Renewable Energy Plant Controller model

The plant controller module processes voltage, active/reactive power, and frequency to control the power plant objectives of active and reactive power injection. In the BESS mode the REPC block acts as the supervisory control units which provides the ancillary service chosen, primary/fast frequency response, based on the inputs from the network and then provides the active and reactive power setpoint to the next block REEC the electrical control module. The active and reactive power control loops are operated independently as in Figure 6-10 . The reactive power is controlled over the measured output and the setpoint reactive power. The active power can be controlled by either a setpoint power or by frequency measured as in the main objective of the model primary frequency control.

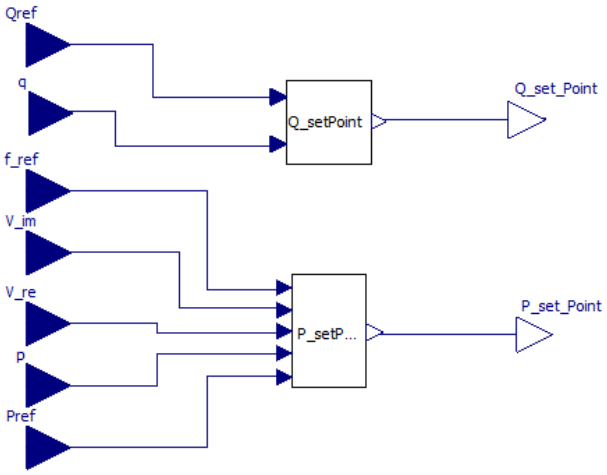

Figure 6-10 REPC_a block

Active Power Setpoint

The active power control block provides a setpoint active power which is controlled by reference power input, frequency measurement, or both. The block is based on the reference module provided in Figure 6-11 left panel. The power setpoint is regulated through a PI controller which has an input signal:

$$P_{signal} = P_{droop} + P_{reference} - P_{measured}$$

“Psignal” is limited by an error limiter block. The measured power is the electrical active power at the output of the model where a lag time constant “Tpe” is employed to emulate the measurement delay. The frequency is measured through the input voltage signals where the output frequency is used to activate the static droop power signal block. The frequency flag functionality is not utilized in the model. The final employed OpenModelica components of the block are shown in Figure 6-11 right panel. The final output of the block is limited by the battery pack capability which in this scenario is limited by the manufacture’s datasheet.

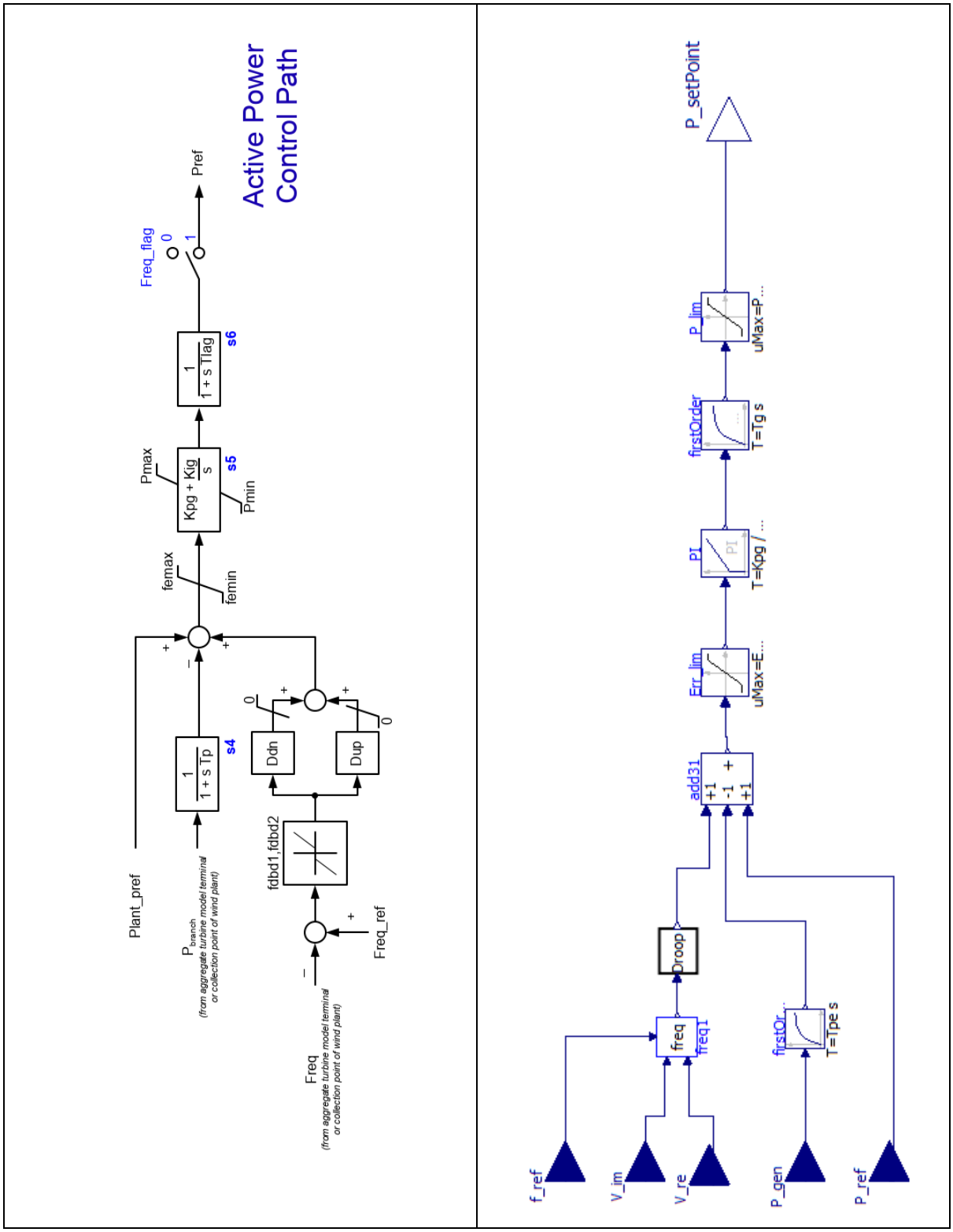

Figure 6-11 Concept vs Implemented Active power setpoint block

The primary/fast frequency response is carried using a static droop block shown in Figure 6-12 where the parameters of the droop will be adapted from the Italian codes and the battery will emulate the response of a hydrothermal unit which will use 100% of its power for frequency regulation.

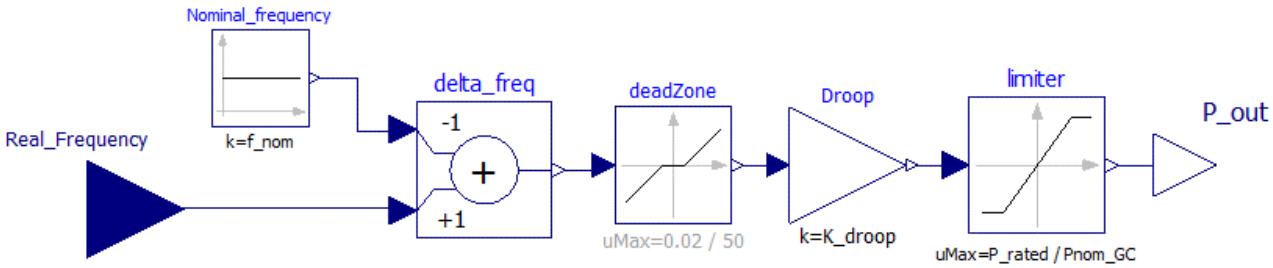

Figure 6-12 Static Droop block

The final parameters utilized in the Active Power control "P_setPoint" block are shown in Table 6-5. The parameters were adopted from the WECC documents along with CESI's previous work concerning PV modelling.

Table 6-5 Active Power set point block parameters

Parameter	Value	Units	Description
K_{pe}	1	*[p.u.]*	Active power measurement filter gain
T_{pe}	0.02	*s*	Active power measurement filter time constant
Pmax	1	*[p.u.]*	Maximum active power limit
Pmin	-1	*[p.u.]*	Minimum active power limit
Err_max	1	*[p.u.]*	Maximum power error
Err_min	-1	*[p.u.]*	Minimum Power error
K_{pg}	1	*[p.u.]*	Proportional gain for PI power control
K_{ig}	8	*[p.u.]*	Integral gain for PI power control
K_pg	1	*[p.u.]*	Filter gain for power controller
T_g	0.1	*s*	Filter lag time constant for power controller
Droop_const	5	%	Droop constant value
P_rel	1	*[p.u.]*	Active regulation power relative to total power
Freq_ded	0.004	*[p.u.]*	Frequency measurement dead band

Reactive Power Setpoint

The reactive power control block provides a reactive power setpoint to the REEC block. The block is a reduced version of the reference block in Figure 6-13 left panel**.** The reactive power setpoint is regulated through a PI controller which has an input signal:

$$Q_{signal} = Q_{reference} - Q_{measured}$$

"Qsignal" is limited by an error limiter block. The measured reactive power is the electrical reactive power at the point of interconnection of the model where a lag time constant "T_qe" is employed to emulate the measurement delay along the lag time constant "Tg" that emulates the communication delay among between the plant controller and subsequent equipment. The output signal is limited to ensure inverter safe operation. The final implemented OpenModelica block is shown in Figure 6-13 right panel. The value of the parameters in this block were adopted from WECC simulation values and CESI's previous work in "BasicPowerSystem" library, depicted in Table 6-6.

Table 6-6 Reactive power setpoint block parameters

Parameter	Value	Units	Description
K_qe	1	*[p.u.]*	Reactive power measurement filter gain
T_qe	0.02	*s*	Reactive power measurement filter time constant
Qmax	1	*[p.u.]*	Maximum reactive power limit
Qmin	-1	*[p.u.]*	Minimum reactive power limit
Dbd1	0	*[p.u.]*	Upper threshold of reactive power control deadband
Dbd2	0	*[p.u.]*	Lower threshold of reactive power control deadband
emax	1	*[p.u.]*	Upper limit of deadband output
emin	-1	*[p.u.]*	Lower limit of deadband output
Kp	0.9	*[p.u.]*	Proportional gain for PI reactive power control
Ki	5	*[p.u.]*	Integral gain for PI reactive power control
Tft	0	*s*	Filter lead time constant
Tg	0.2	*s*	Filter lag time constant

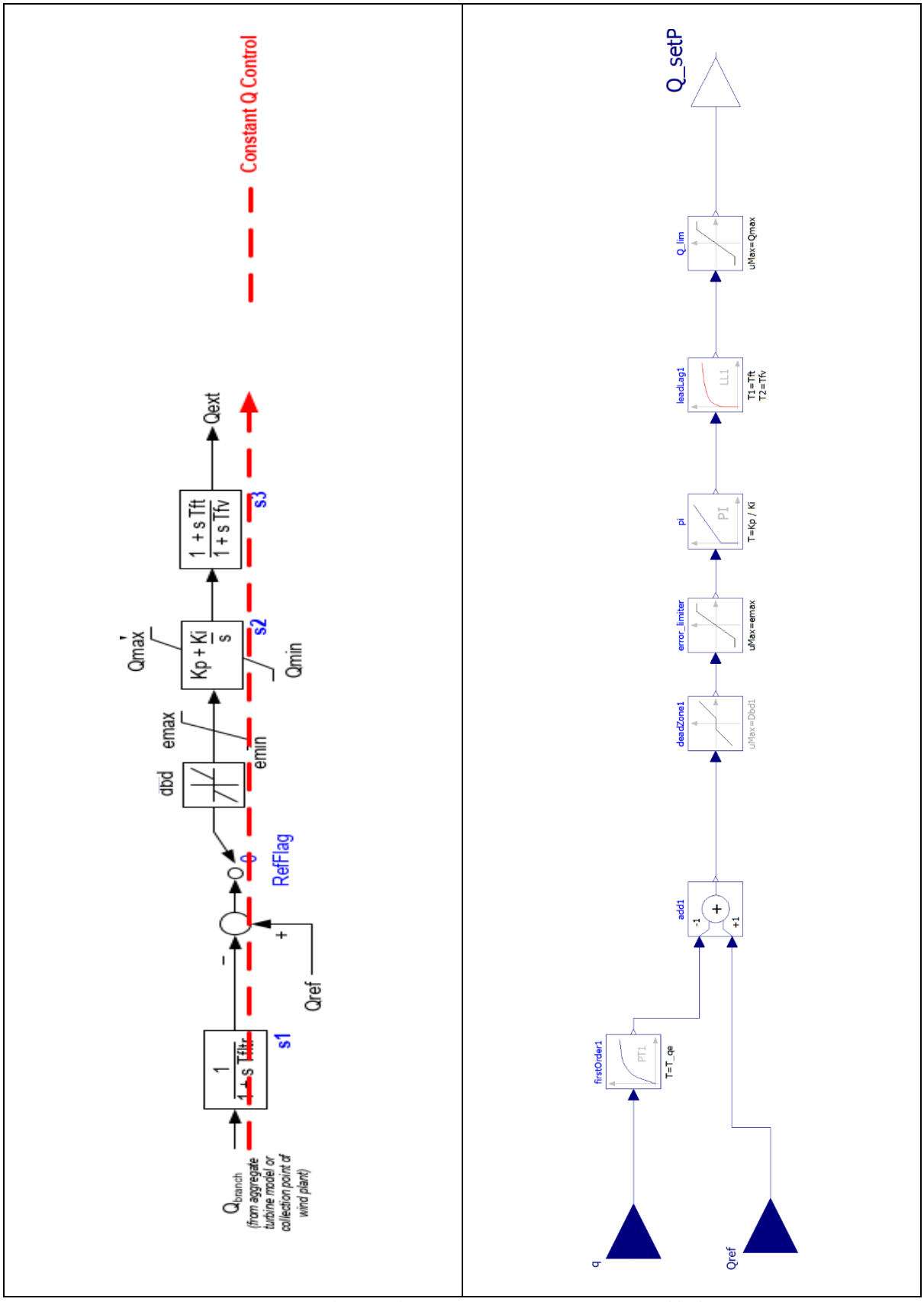

Figure 6-13 Implemented vs concept reactive power setpoint block.

6.3.2. REEC Renewable Energy Electrical Controller model

The REEC model is the responsible component for the inverter control and in the case of the BESS the charge control. It takes active/reactive power setpoints from the previous model REPC accompanied by feedback signals from the point of delivery of the inverter and provides active and reactive current setpoints (I_d and I_q) in the dq frame of reference. In addition to the inverter functionalities of the REEC, the charge controller functionality is added for the specific case of BESS. The charge controller calculates the charging state of the BESS and protects the system from over charging or deep discharging. For the specific case where the user has the battery parameters the battery cell model is incorporated inside the charge controller function. The usage of dq frame of reference and PLL allows the control of the active and reactive power to be done independently where each quantity is controlled by an independent block. The three main blocks of the module are:

- Active current command setpoint block "I_d_Setpoint".
- Reactive current command setpoint block "I_q_Setpoint".
- Battery charge controller block "Charge_Ctrl".

The Charge Controller

The charge controller is responsible for keeping the battery operating in the admissible range of voltage and state of charge. The block also incorporates the battery cell model if the battery parameters are available. The controller receives the power setpoint as input and provides the state of charge or the complementary depth of charge, and the operating command to the BESS. The operating command is based on a simple if conditions where the battery is not allowed to operate in two conditions:

- If the SOC is maximum and the active power setpoint is discharging.
- If the SOC is minimum and the active power setpoint is charging.

The allowable SOC operating range is 15% -- 85% after reviewing the available commercial battery datasheet. The charge controller block is shown in Figure 6-14.

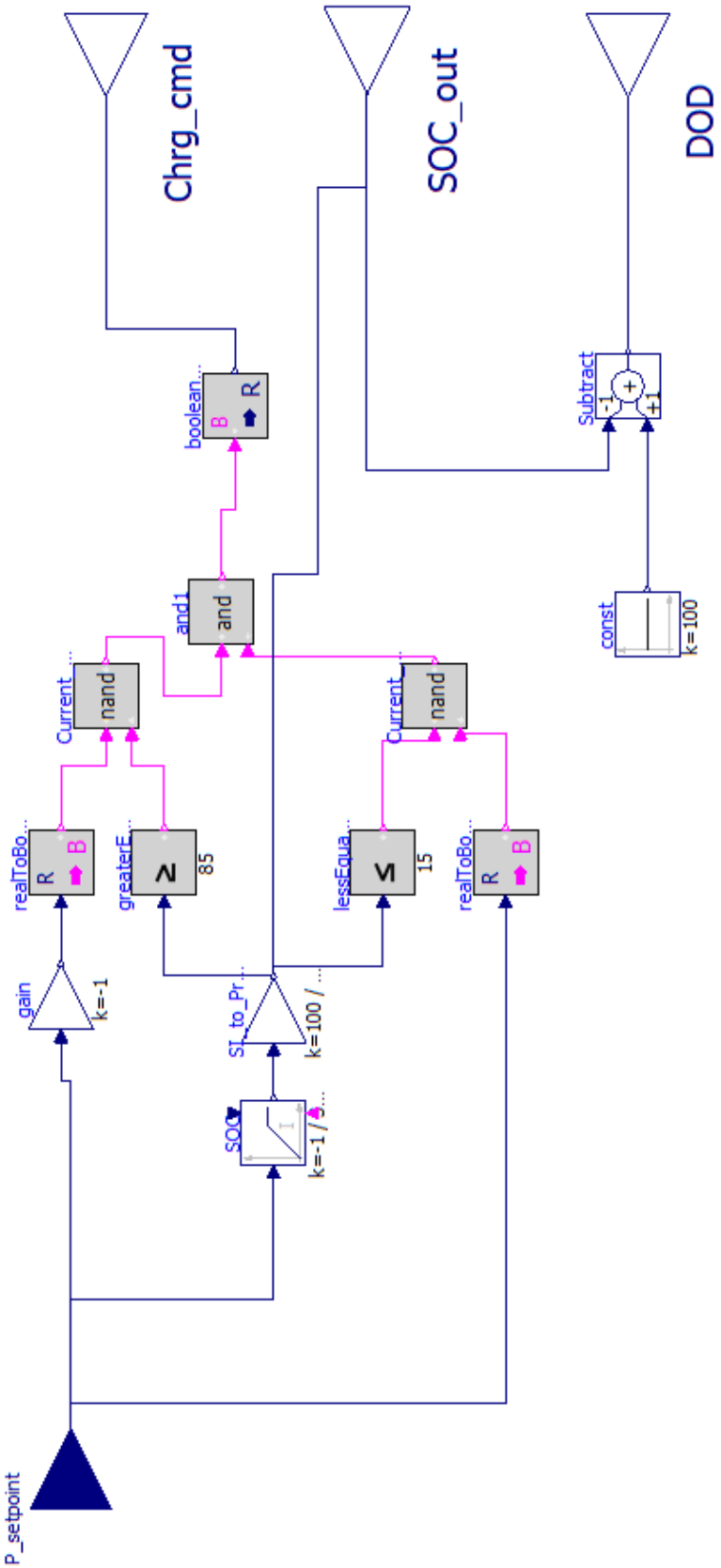

Figure 6-14 Charge Controller block

The Active Power Current Controller

The active power current controller block develops the "*Ipcmd"* current which, after the utilization of the dq frame of reference and the PLL discussed earlier, can be easily computed using the equation:

$$P = \frac{3}{2} V_d \, I_p$$

The model is depicted in Figure 6-15 where the input power setpoint received from the REPC block is multiplied by the operating command from the charge controller block. Furthermore, lag filters were utilized which would mimic the lag associated with the measurement process. The value of the parameters in this block were adopted from WECC simulation values and CESI's previous work in "BasicPowerSystem" library, they are depicted in Table 6-5.

Table 6-7 Active current setpoint block parameters

Parameter	Value	Units	Description
Krv	1	*[p.u.]*	Voltage measurement filter gain
Trv	0.02	*s*	Voltage measurement filter time constant
Ipmax	1	*[p.u.]*	Maximum active power current limit
Ipmin	-1	*[p.u.]*	Minimum active power current limit
dPmax	500	*[p.u./s]*	Maximum rise slew rate
dPmin	-500	*[p.u./s]*	Minimum fall slew rate
T_dp	0.001	*[p.u.]*	Derivative time constant for slew rate
Kpord	1	*[p.u.]*	Proportional gain for power filter
Tpord	0.02	*[p.u.]*	Integral gain for power filter
Pmax	1	*[p.u.]*	Maximum active power limit
Pmin	-1	*[p.u.]*	Minimum active power limit

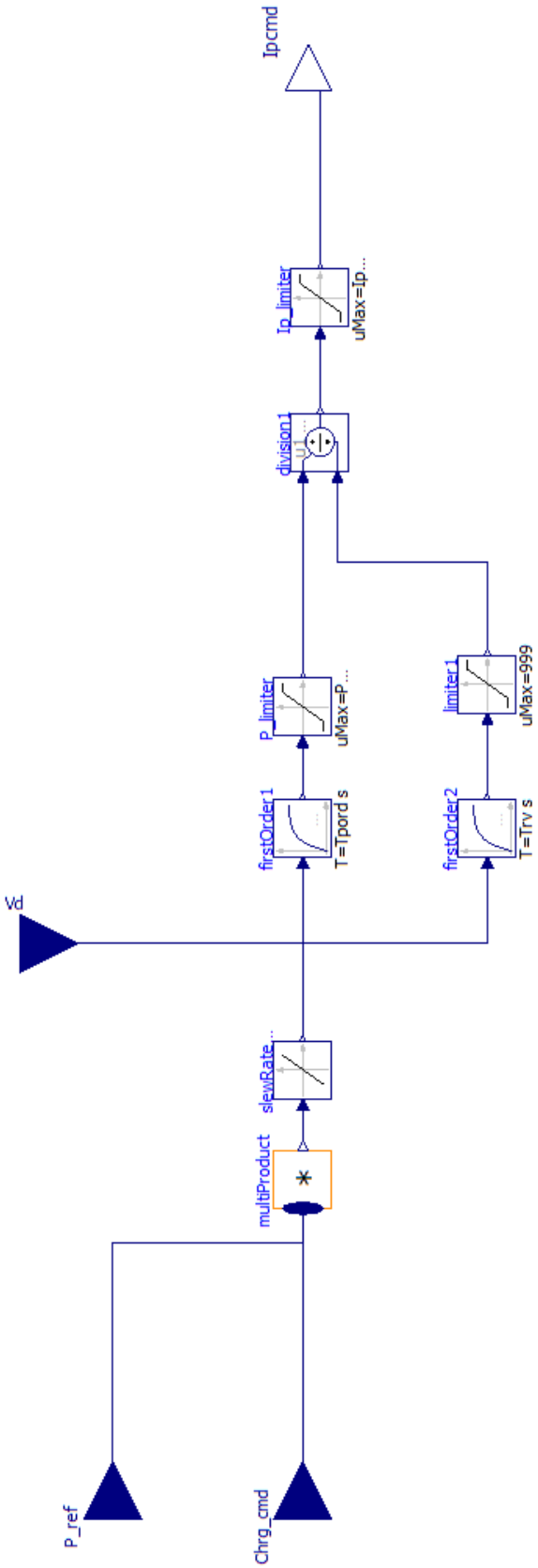

Figure 6-15 Active current setpoint block

The Reactive Power Current Controller

The reactive power current controller block develops the "*Iqcmd"* current which, after the utilization of the dq frame of reference and the PLL discussed earlier, can be easily computed using the equation:

$$Q = \frac{-3}{2} V_d \, I_Q$$

The model is depicted in Figure 6-16 where the input reactive power setpoint is received from the REPC. Additionally, lag filters were utilized which would mimic the lag associated with the measurement process. The value of the parameters in this block were adopted from WECC simulation values and CESI's previous work in "BasicPowerSystem" library, they are depicted in Table 6-8.

Table 6-8 Reactive Current setpoint block parameters

Parameter	Value	Units	Description
Krv	1	*[p.u.]*	Voltage measurement filter gain
Trv	0.02	*s*	Voltage measurement filter time constant
Iqmax	1	*[p.u.]*	Maximum reactive power current limit
Iqmin	-1	*[p.u.]*	Minimum reactive power current limit
Kiq	1	*[p.u.]*	Filter gain for reactive current power control
Tiq	0.02	*s*	Filter time constant for reactive current power control

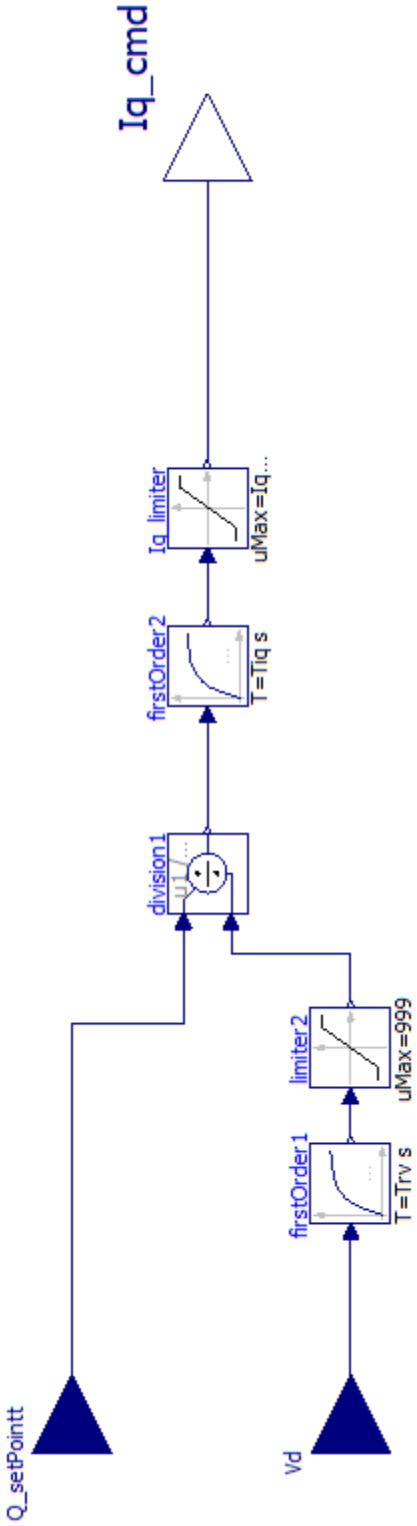

Figure 6-16 Reactive Current setpoint block

7. Model Testing and Validation in OpenModelica

An important step prior to assessing the model in its designated environment, DYANA tool, is testing the subsystems models and making sure that the theoretical assumptions and expected behaviour of the subsystems conform with the real simulated output signals. Hence the simulation process in this chapter is divided into two parts:

- Independent testing of the model's Subsystems in OpenModelica.
- Final dynamic simulation of the complete BESS model inside a test grid in TESEO/DYANA.

The first phase of the system testing, and validation process starts with an independent subsystems qualitative validation performed in OpenModelica. The main aim of this phase is to ensure that the implemented control loops and logical functions behave in a qualitative consistent way with the given test input. Since the subsystems are not yet connected to the test network, the feedback signals do not exist therefore appropriate feedback signals are implemented. The feedback signals are set to target every possible scenario the subsystem can endure and check if the output of the subsystems is coherent with the expected output qualitatively. The "Source" package in OpenModelica (Figure 7-1) was utilized to apply appropriate input signals and particularly the four main signals shown in Figure 7-2.

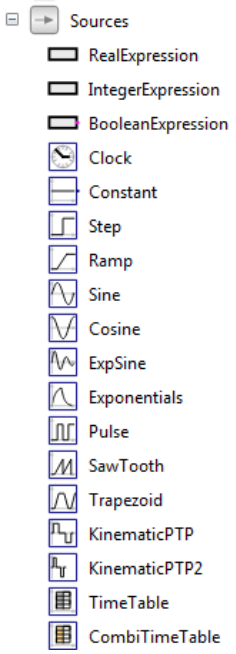

Figure 7-1 Source package in OpenModelica

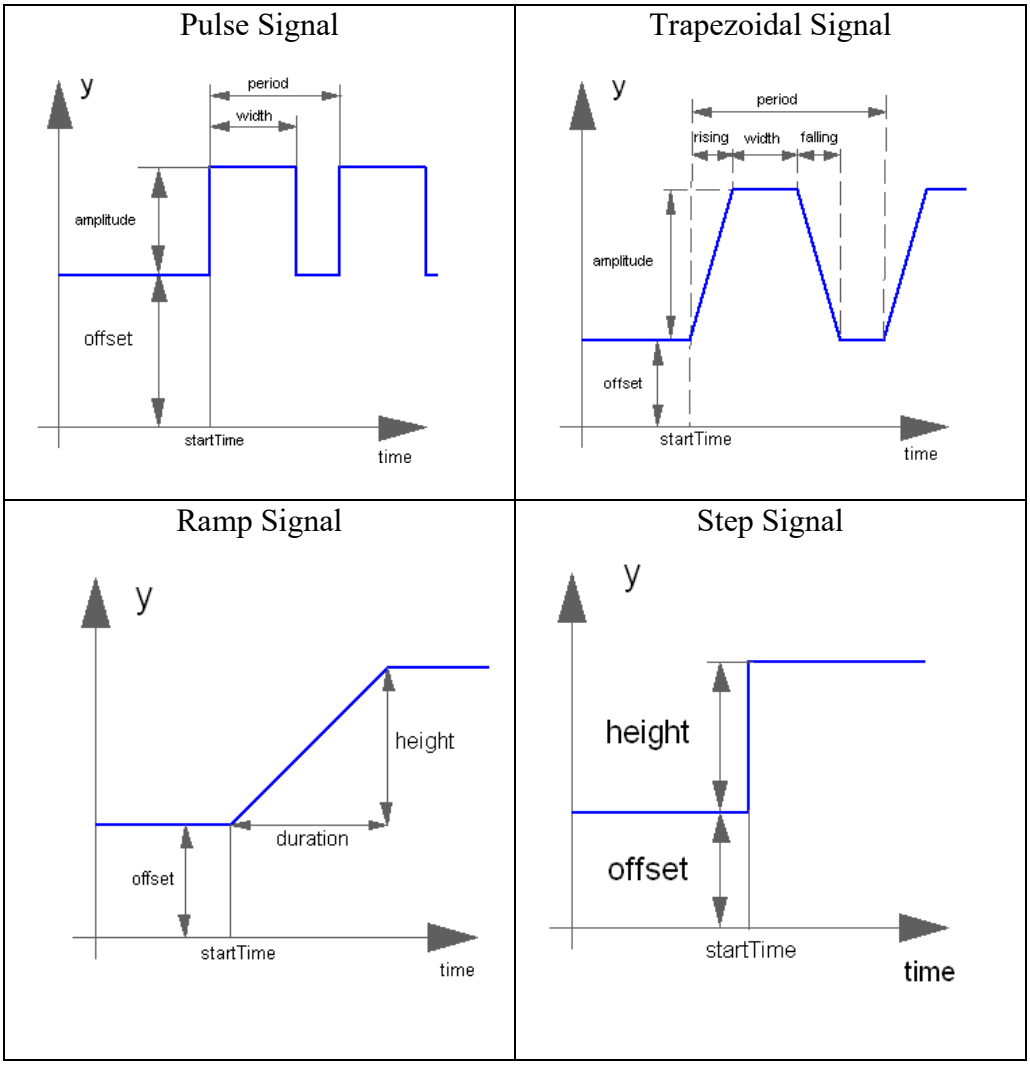

Figure 7-2 Utilized "Source" Package signals

7.1. REPC Reactive Power setpoint block

The reactive power setpoint block test is employed using the block structure shown in Figure 7-3, with input signals having ramp and step input. The setup is employed as to have the feedback signal “Q_meas” in three different states to study the three different behaviours of the block:

- Measured signal is smaller than the reference signal.
- Measured signal is equal to the reference signal.
- Measured signal is bigger than the reference signal.

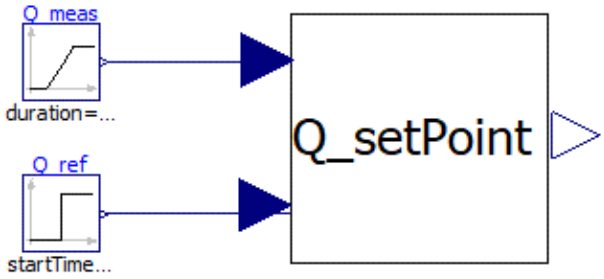

Figure 7-3 Reactive power setpoint block test structure

The characteristics of the input signals is represented in Table 7-1 in compliance with the description terminologies used in Figure 7-2.

Table 7-1 Reactive power setpoint block test signals' parameters

Signal	Name	Type	Description
Q_meas	Measured Reactive Power	Ramp	Height: 0.2 p.u. Duration: 3 sec Offset: 0.2 p.u. Start time: 3.5 sec
Q_ref	Reference Reactive power	Step	Height: 0.2 p.u. Offset: 0.2 p.u. Start time: 5 sec

The result of the test is shown in Figure 7-4. The behaviour of the output signal "Q_setpoint" is noticed and it goes through three states:

- A stable non changing state where the measured signal is equal to the reference signal in the intervals of 0 – 3.5 and 6.5 – 10 seconds.
- An increasing trend, where the measured signal is less than the reference signal in the interval 5 – 6.5 seconds.
- A decreasing trend, where the measured signal is greater than the reference signal in the interval of 3.5 – 5 seconds

Additionally, a small lag can be noticed in the setpoint signal behaviour which is due to the lag filters applied to mimic the measurement process delay.

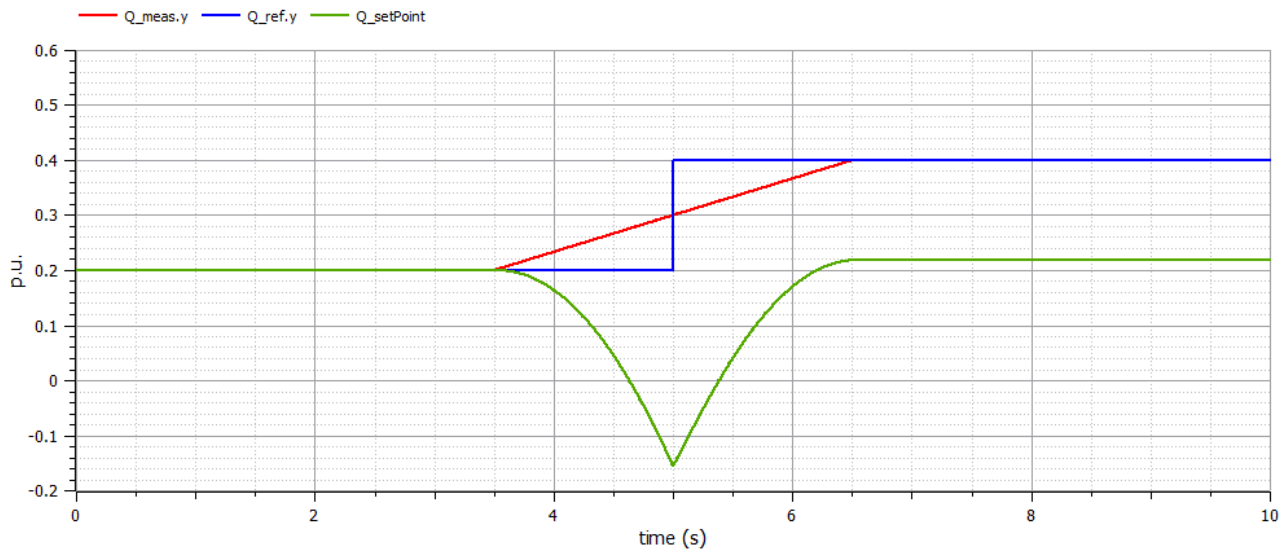

Figure 7-4 Reactive power setpoint result

7.2. REPC Active Power setpoint block

The REPC Active power setpoint block will be tested in two setups: the first setup is similar to the reactive power setpoint block where the behaviour of the PI controller with the feedback loop is tested using a reference power and the second setup will test the static droop block functionalities.

7.2.1. Reference Active Power input

The first active power setpoint block test is employed using the block structure shown in Figure 7-5, with input signals having ramp and step input. The setup is employed as to have the feedback signal "P_meas" in three different states to study the three different behaviours of the block:

- Measured signal is smaller than the reference signal.
- Measured signal is equal to the reference signal.
- Measured signal is bigger than the reference signal

The characteristics of the input signals is represented in Table 7-2 in compliance with the description terminologies used in Figure 7-2.

Table 7-2 Active power setpoint block first test signals' parameters

Signal	Name	Type	Description
P_meas	Measured Active Power	Ramp	Height: 0.2 p.u. Duration: 3 sec Offset: 0.2 p.u. Start time: 3.5 sec
P_ref	Reference Active power	Step	Height: 0.2 p.u. Offset: 0.2 p.u. Start time: 5 sec
f_ref	Reference Frequency	Constant	1 p.u.
V_im	Imaginary Voltage part	Constant	0.1 p.u.
V_re	Real Voltage part	Constant	1 p.u.

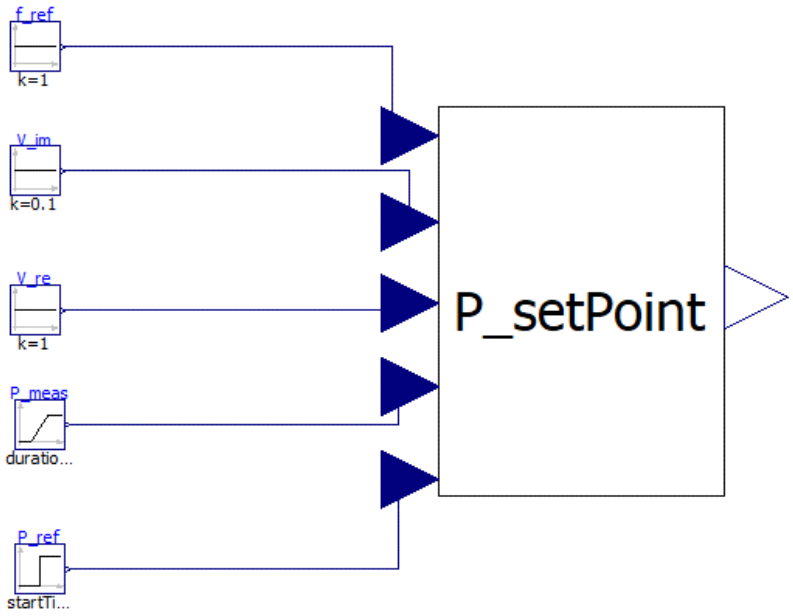

Figure 7-5 Active power setpoint block first test structure

The result of the test is shown in Figure 7-6. The behaviour of the output signal “P_setpoint” is noticed and it goes through three states:

- A stable non changing state where the measured signal is equal to the reference signal in the intervals of 0 – 3.5 and 6.5 – 10 seconds.
- An increasing trend, where the measured signal is less than the reference signal in the interval 5 – 6.5 seconds.
- A decreasing trend, where the measured signal is greater than the reference signal in the interval of 3.5 – 5 seconds

Additionally, a small lag can be noticed in the setpoint signal behaviour which is due to the lag filters applied to mimic the measurement process delay.

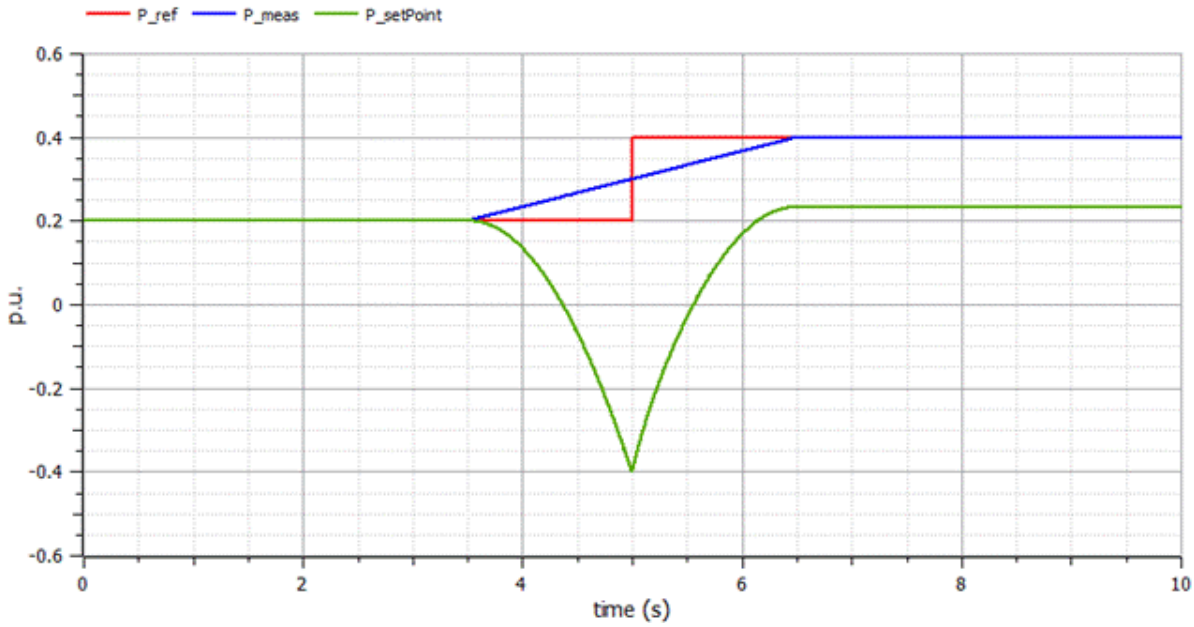

Figure 7-6 Active power setpoint controller test result

7.2.2. Static Droop Controller

In this section, the functionality of the static droop controller will be first demonstrated followed by the simulation of the complete block as a response to a frequency change. The frequency drop setup is shown in Figure 7-7 the frequency rise setup is similar with the real and imaginary voltage signals switched.

A frequency change is emulated through a change in the real and imaginary parts of the measured voltage. An increase in the real voltage part will emulate a drop in in measured frequency will an increase in the imaginary will emulate a rise in measured frequency. In Figure 7-8 and Figure 7-9 the frequency change is shown on the upper panel and the static droop block reaction is previewed on the lower panel. It is observed that a negative frequency drop (underfrequency) triggers a power injection while a positive frequency rise (overfrequency) triggers a power withdrawal.

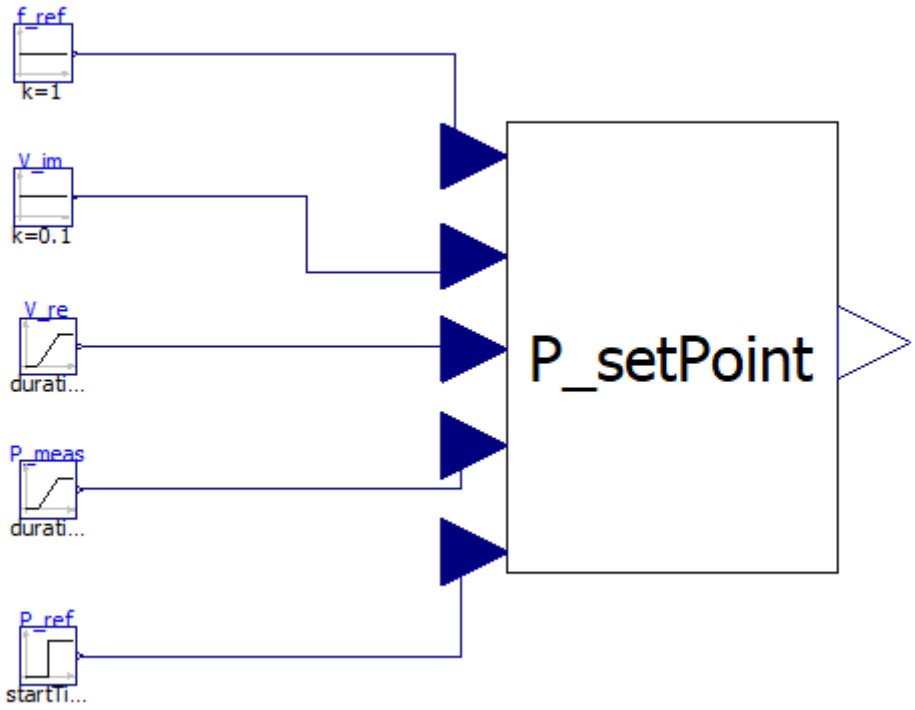

Figure 7-7 Static droop block in frequency drop case setup

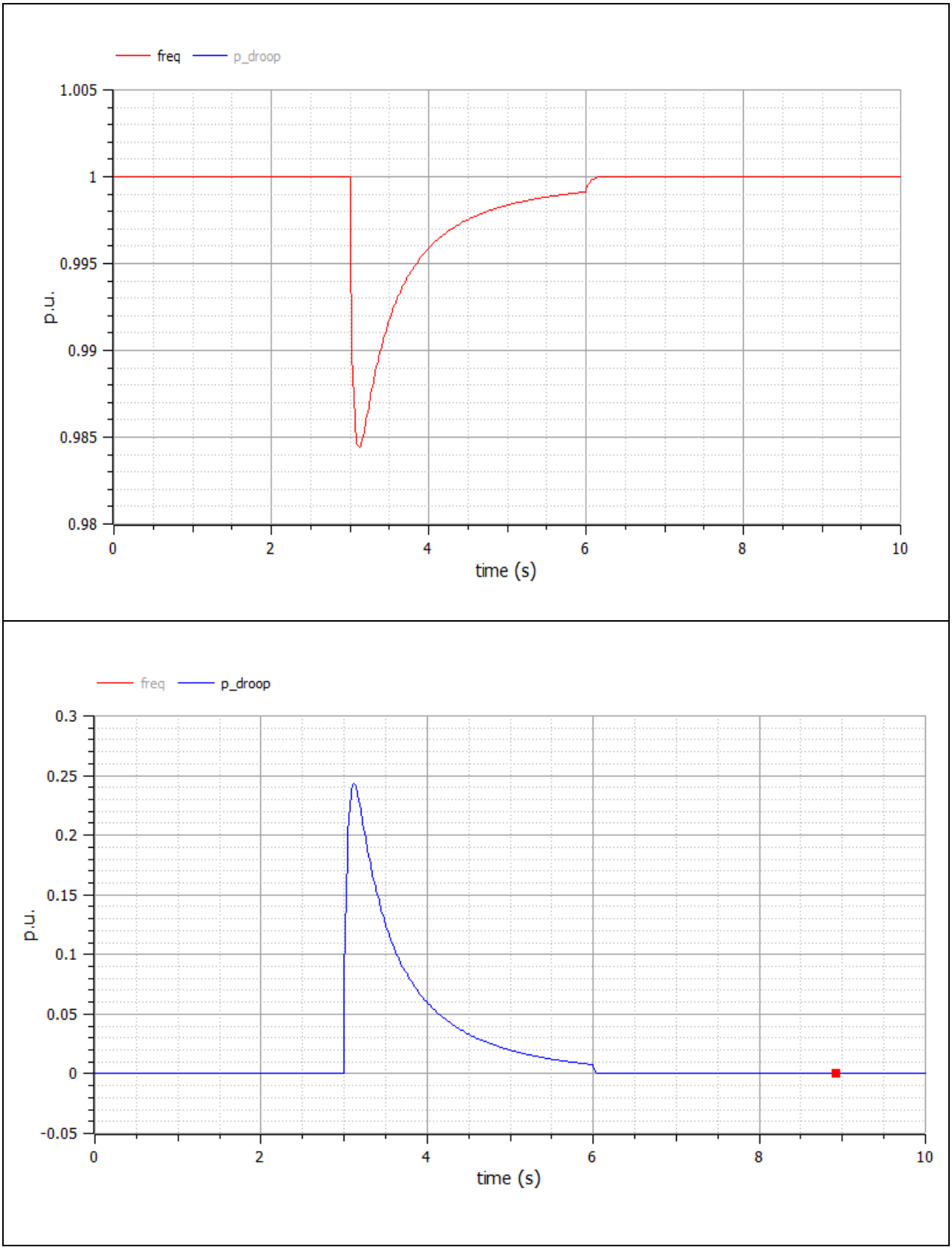

Figure 7-8 Static droop block reaction to negative frequency change

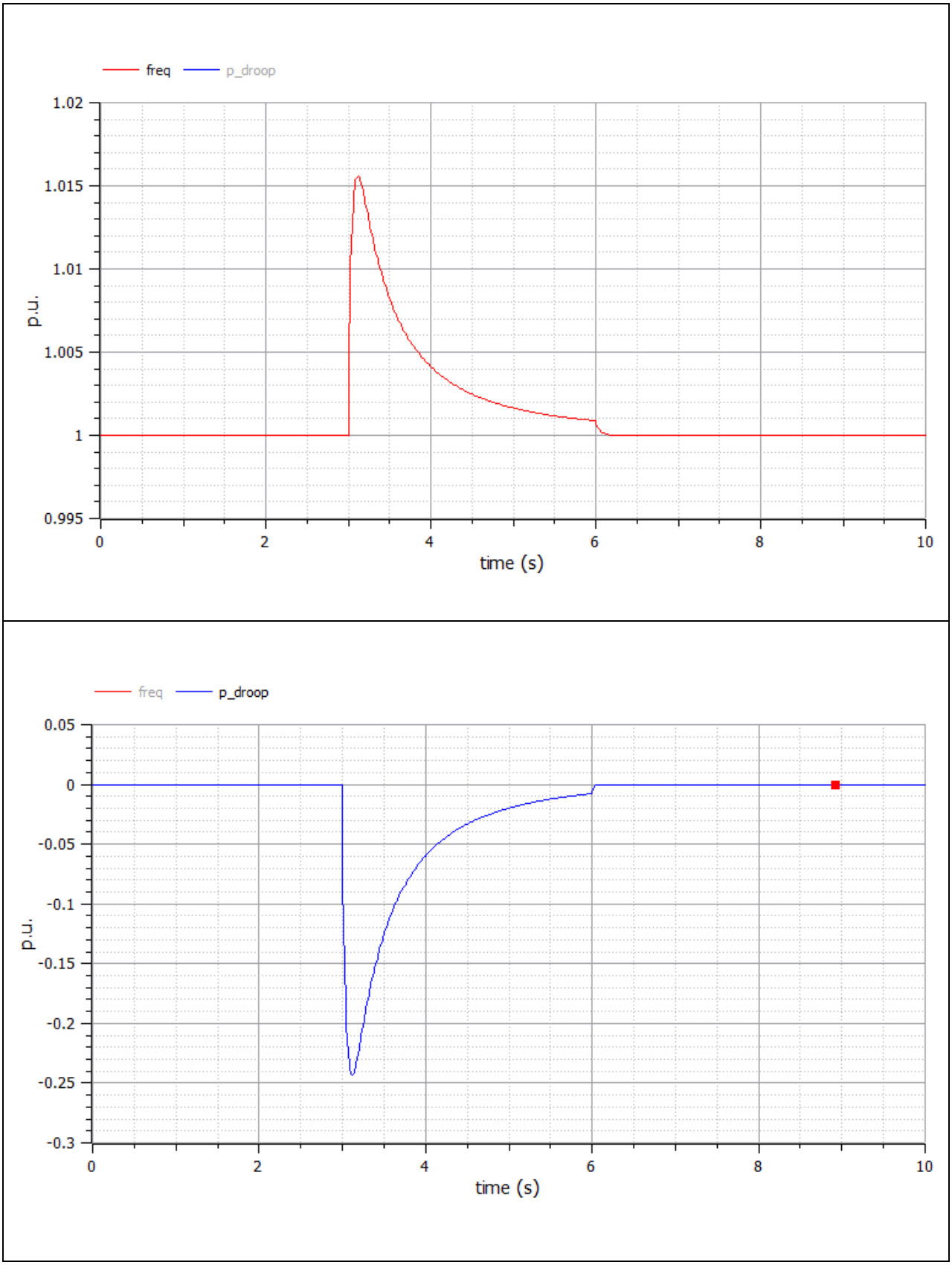

Figure 7-9 Static droop block reaction to positive frequency change

The signals' parameters of the test setup in both cases is shown in Table 7-3 in compliance with the description terminologies used in Figure 7-2.

Table 7-3 Active power setpoint static droop block test signals' parameters

Signal	Name	Type	Description
P_meas	Measured Active Power	Ramp	Height: 0.2 p.u. Duration: 4 sec Offset: 0.2 p.u. Start time: 4 sec
P_ref	Reference Active power	Step	Height: 0.2 p.u. Offset: 0.2 p.u. Start time: 5 sec
f_ref	Reference Frequency	Constant	1 p.u.
V_im	Imaginary Voltage part	Case 1 Constant Case 2 Ramp	**Case 1** 0.1 p.u. ***Case* 2** Height: 3 p.u. Duration: 3 sec Offset: 1 p.u. Start time: 3 sec
V_re	Real Voltage part	Case 1 Ramp Case 2 Constant	**Case 1** Height: 3 p.u. Duration: 3 sec Offset: 1 p.u. Start time: 3 sec **Case 2** 1 p.u.

In Figure 7-10 case 2 results are presented where the "P_ref_new" is the new reference signal adding the reference signal "Pref" with the static droop signal "p_droop". The results agree with the design anticipated goal.

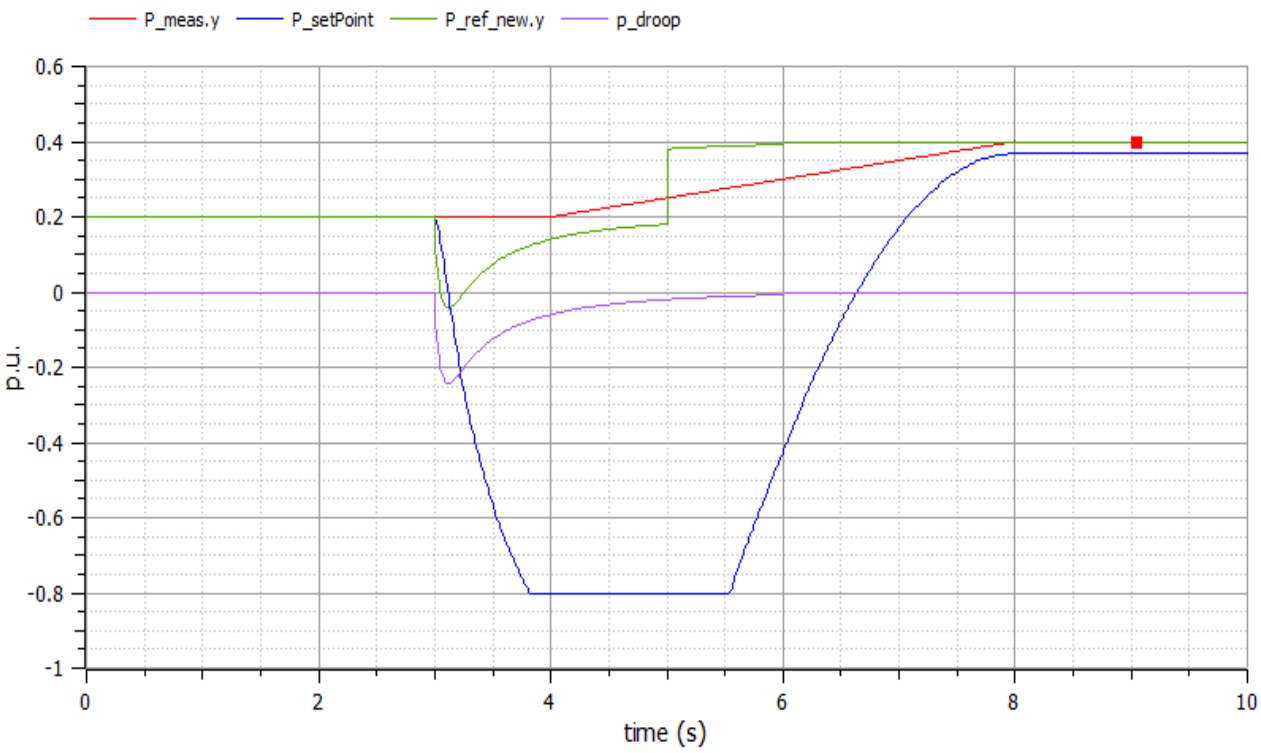

Figure 7-10 Active power controller with Droop test result

7.3. REEC Reactive Current command block

The purpose of this test is to check if the reactive current command controller block operates properly. A Reactive power step signal is used as an input with a constant d-axis voltage. The test setup is shown in Figure 7-11. While the signals' parameters are in Table 7-4. Results of the simulation are shown in Figure 7-12 where the reactive current command follows the setpoint received from the REPC block.

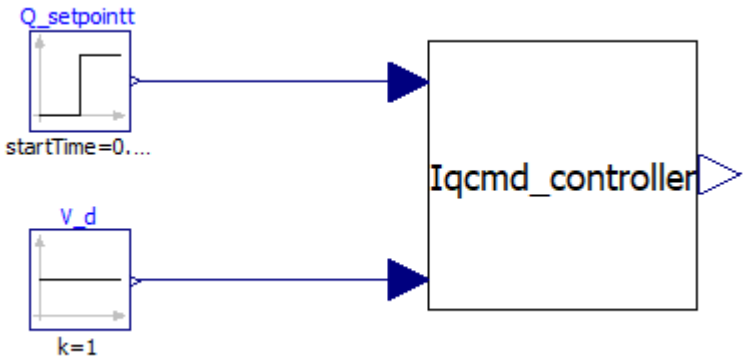

Figure 7-11 Reactive current control block test

Table 7-4 Reactive current control block signals' parameters

Signal	Name	Type	Description
V_d	d Component voltage	Constant	1 p.u.
Q_setPOint	Setpoint Reactive power	Step	Height: 0.4 p.u. Offset: 0.2 p.u. Start time: 0.5 sec

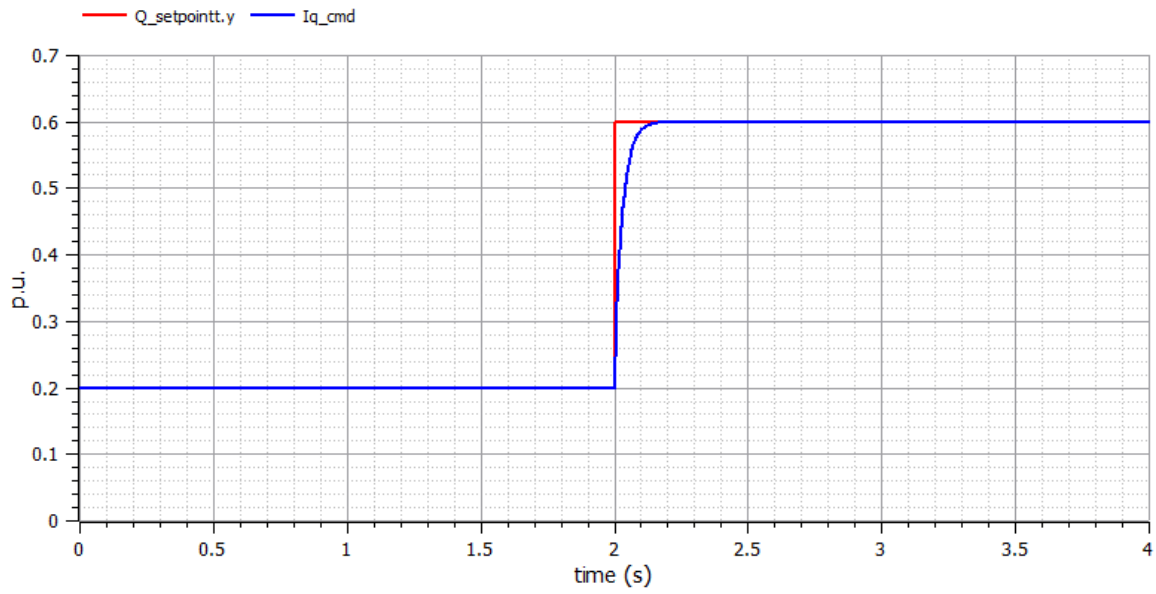

Figure 7-12 Reactive current control block test results

7.4. REEC Active Current command block

The purpose of this test is to check if the active current command controller block operates properly. An active power step signal is used as an input with a constant d-axis voltage. The test setup is shown in Figure 7-13 Active current control block test. While the signals' parameters are in Table 7-5. Results of the simulation are shown in Figure 7-14 where the active current command follows the setpoint received from the REPC block.

Table 7-5 Active current control block signals' parameters

Signal	Name	Type	Description
V_d	d Component voltage	Constant	1 p.u.
P_setpoint	Setpoint Active power	Step	Height: 0.4 p.u. Offset: 0.2 p.u. Start time: 0.5 sec

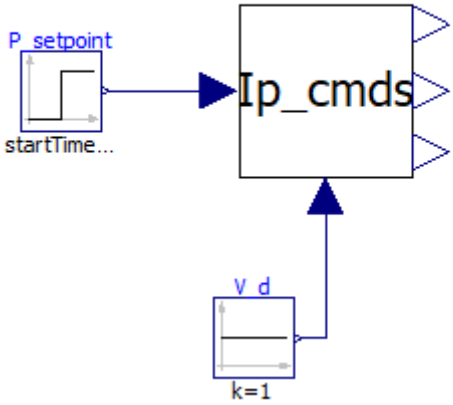

Figure 7-13 Active current control block test

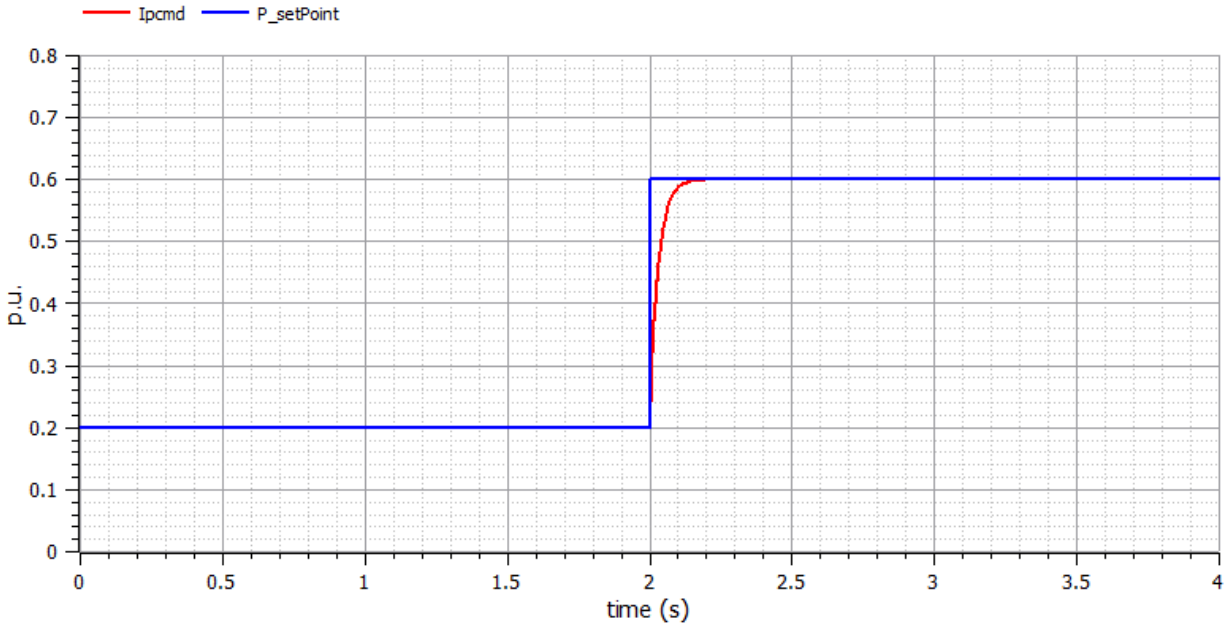

Figure 7-14 Active current control block test results

7.5. REEC Battery Model test

In this section the purpose of the simulation is to test the battery cell model setup coupled with the charge controller model and validate the theoretical expectations. The setup, shown in Figure 7-14, is similar to the "Ipcmd" test setup but with a change in the input signals to serve the aims of this test.

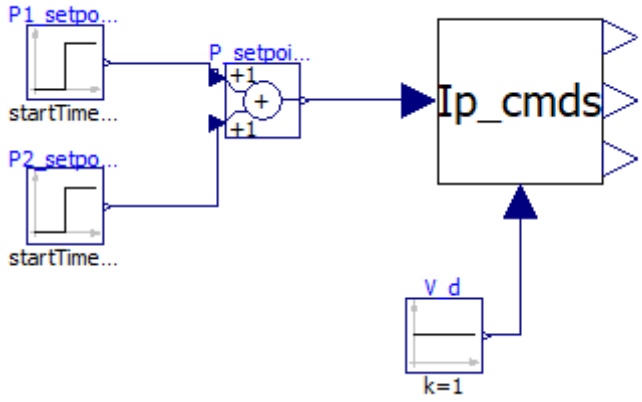

Figure 7-15 REEC Battery model test setup

The time scale of the simulation will be in minutes to explore the BESS capability of operating over a long time period and allowing the BESS to fully discharge. The input signals' parameters are described in Table 7-6. First the setpoint signals will emulate a discharging command followed by a charging command to check the model's capability in performing in both directions, then a deep discharge will be performed to check the charge controller precise functionality.

Table 7-6 Battery model test signals' parameters.

Signal	Name	Type	Description
V_d	d Component voltage	Constant	1 p.u.
P1_setpoint	Setpoint Active power 1	Step	Height: 1.1 p.u. Offset: -0.2 p.u. Start time: 10 mins
P2_setpoint	Setpoint Active power 2	Step	Height: -1.9 p.u. Offset: 0 Start time: 36 mins

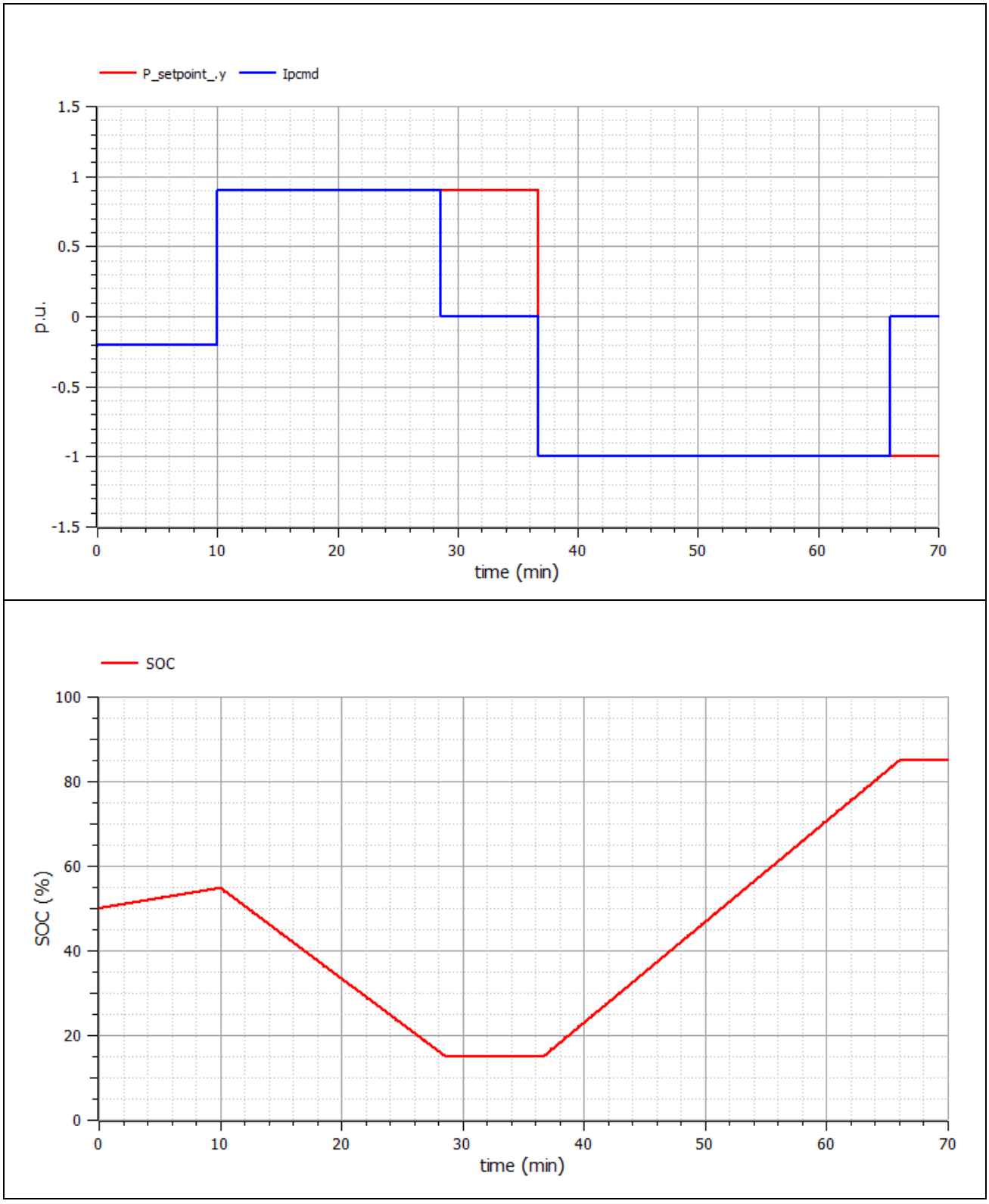

Figure 7-16 REEC Battery model test result 1

In Figure 7-16 the input power setpoint is compared with the output “Ipcmd” signal. It can be observed that around minute 28 the battery is fully discharged, hence the charge controller activates the stopping command and the output signal “Ipcmd” drops to zero even though the power setpoint signal is still positive. At minute 36 when the “P2_setpoint” signal is activated to charge the battery at maximum current the “Ipcmd” signal changes from zero to a negative value. At minute 66 the battery is fully charged to the admissible limit and again the charge controller is activated to change the output signal to zero even though the power setpoint signal is still negative.

In Figure 7-17, the per unit voltage of the battery is compared with the state of charge. It can be deducted that:

- During charging periods, the voltage of the battery increases.
- During discharging periods, the voltage of the battery decreases.
- The charge controller keeps the battery voltage inside the admissible limits.
- At no operation periods, the battery voltage remains constant.

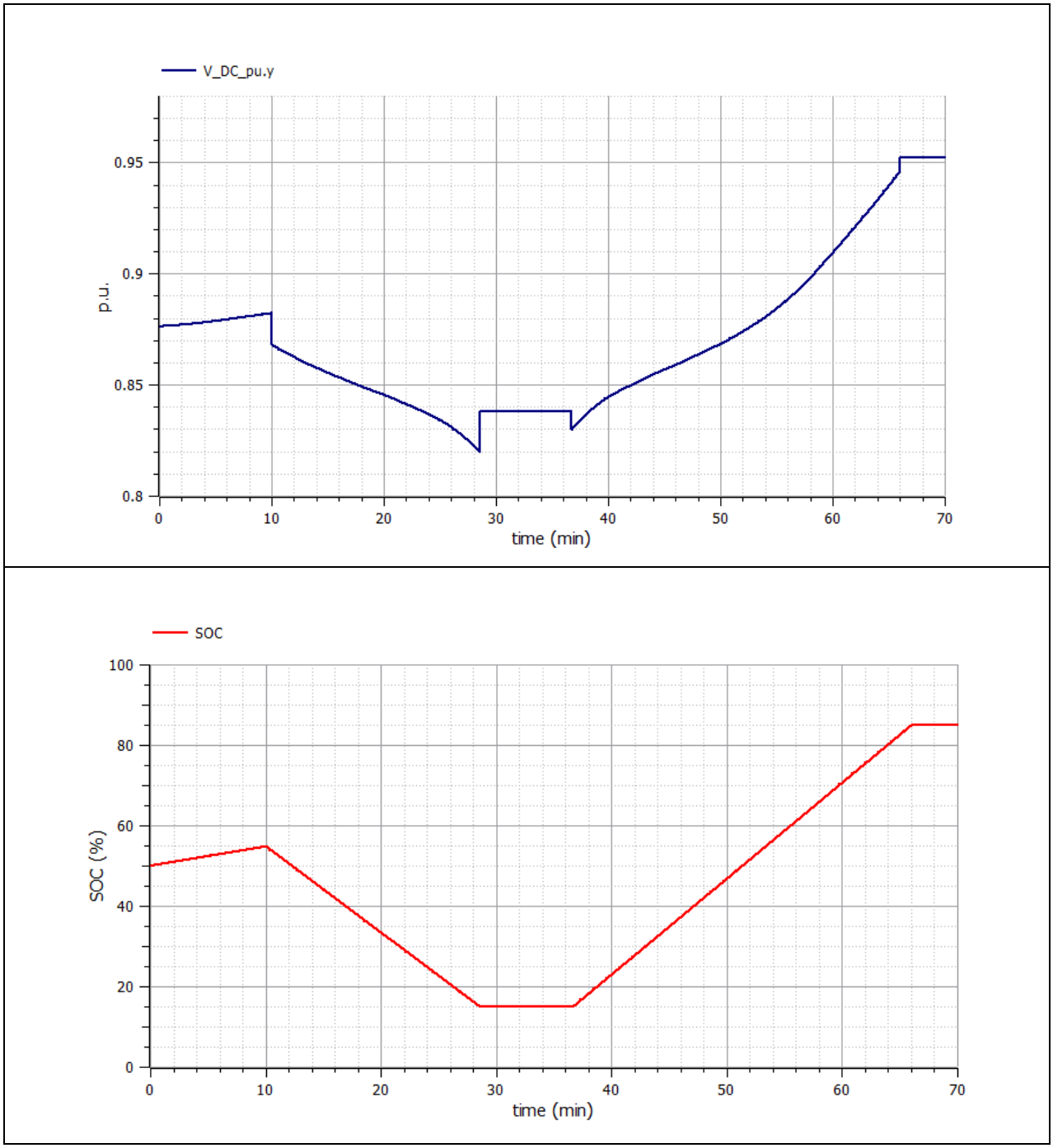

Figure 7-17 REEC Battery model test result 2

In Figure 7-18 the voltage profile of a single battery cell is shown where the open circuit voltage of the cell is compared with the output voltage of the cell. Several observations can be described, which conform with the theoretical background, such as:

- During discharging, the output voltage of the cell is lower than the open circuit voltage.
- During charging, the output voltage of the cell is higher than the open circuit voltage.
- During no operation periods, the output voltage is equal to the open circuit voltage.
- As the charging rate increases the voltage difference between the output voltage and open circuit increases due to the voltage drop in the internal resistance.

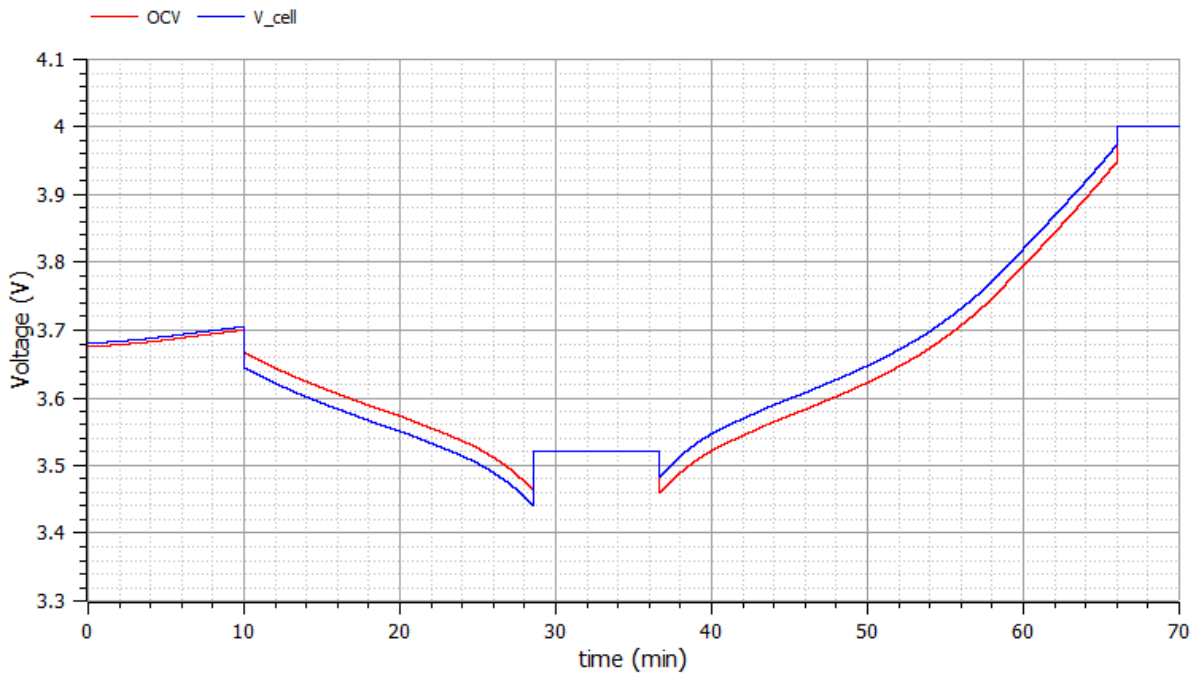

Figure 7-18 REEC Battery model test result 3

7.6. Frequency variability test

In this section the behaviour of the BESS DC side without feedback is investigated where the droop behaviour of the system is assessed through a variable frequency signal. The variable frequency data is obtained from an old data set form a network in the UK. The frequency signal is for 7 days and is shown in Figure 7-19. The maximum and minimum frequency recorded are 50.261 Hz and 49.6940 Hz respectively, while the average frequency is 50.0012 Hz.

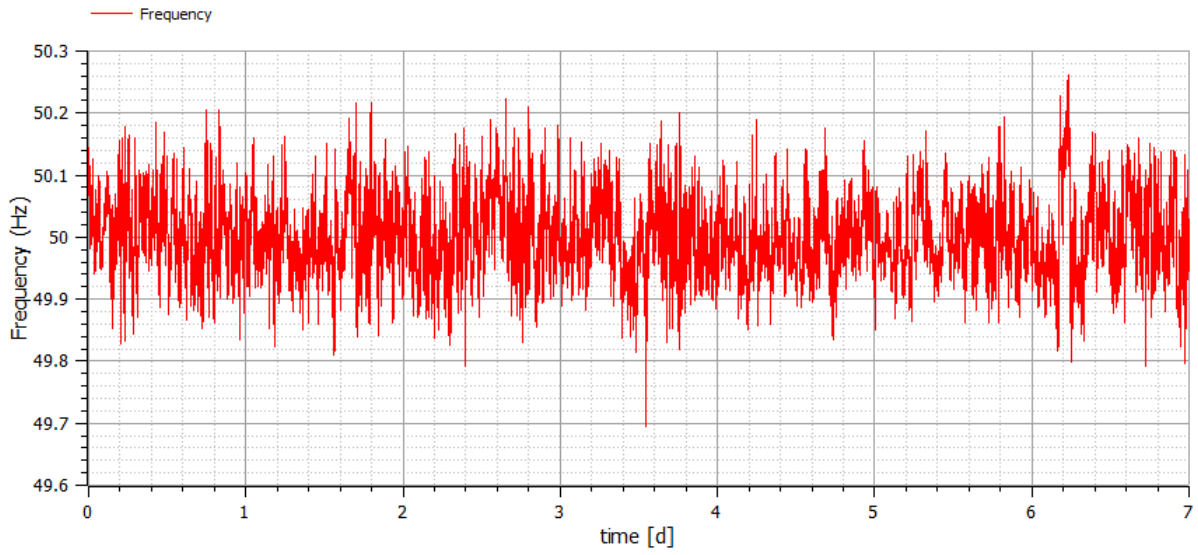

Figure 7-19 Variable frequency data

A Storage system of parameters in Table 7-7 was used in the test based on the cell data shown in Figure 6-7, the maximum power of the battery is assumed 5 MW to avoid extrapolation. The test setup is shown in Figure 7-20 assuming the static droop power controller is the only active component thus allowing full utilization of the nominal 5 MW power in PFR regulation.

Table 7-7 Battery system values

Parameter	Name	Value
E_nom	Nominal Energy of the Battery system	5 MWh
V_nom	Nominal DC voltage of the Battery system	20 kV
V_min	Minimum DC voltage of the Battery system	16.25 kV
V_max	Maximum DC voltage of the Battery system	22.25 kV

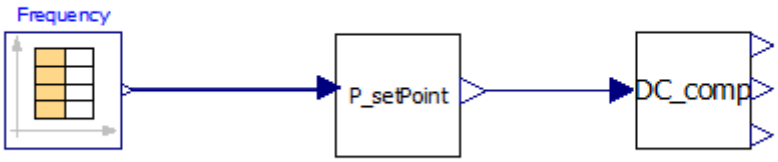

Figure 7-20 Variable frequency test setup

The simulation results through the whole week are shown in Figure 7-21 as the system starts at 50% SOC. It is observed that the trend of SOC is analogous to the output DC voltage since in Figure 6-7 through the interval 50%-70% the relation can be assumed linear.

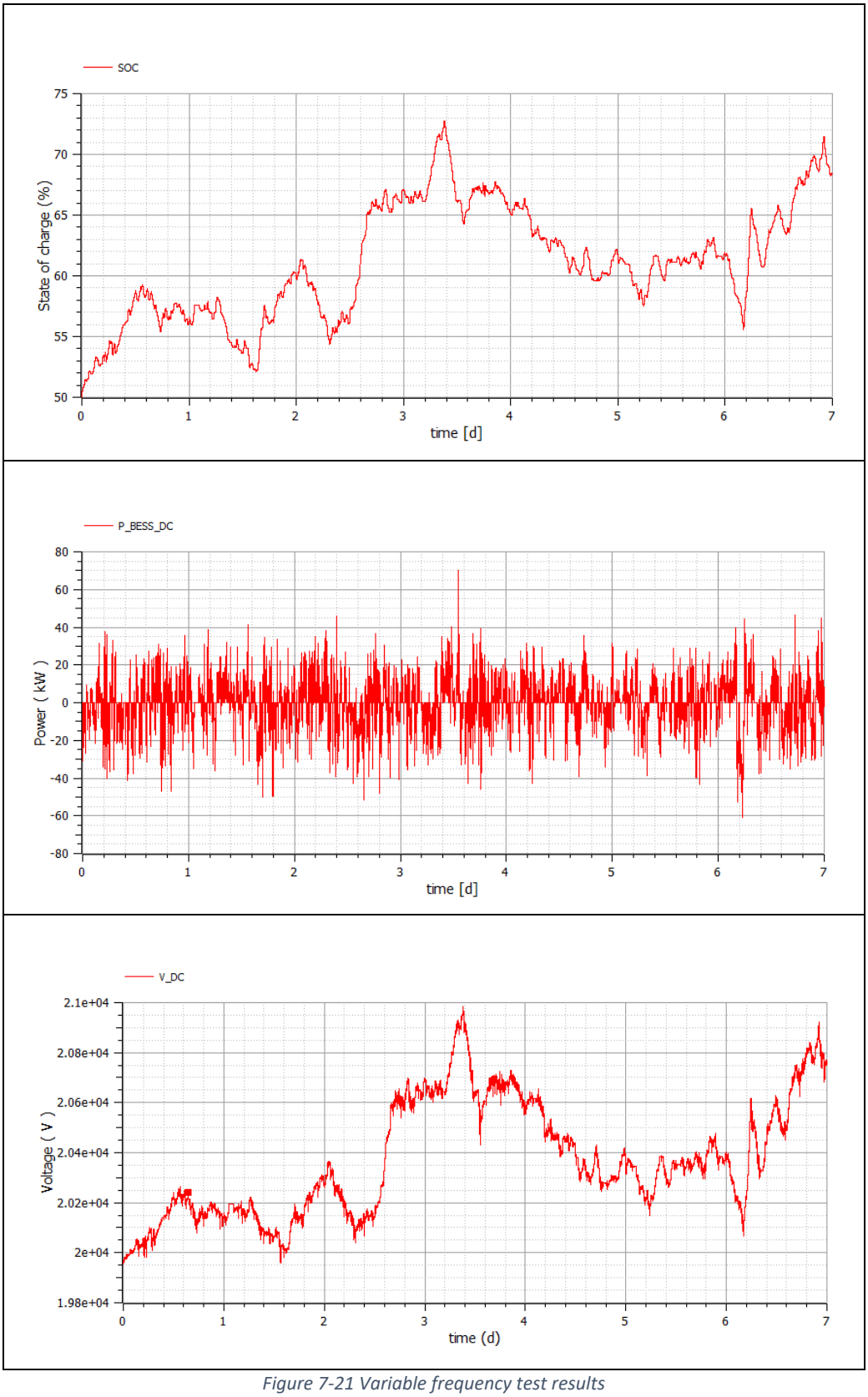

Figure 7-21 Variable frequency test results

8. Model Testing and Validation in TESEO

After testing the subsystems models in OpenModelica and assessing their behaviour qualitatively in some functions and quantitively in other, the final important step is to assess ana validate the model in its designated environment TESEO/DYANA software. This step is important for:

- Testing the model for its main aim; functioning in a dynamic simulation.
- Testing and calibrating the PI controllers and lag constants.

The forthcoming tests are carried out in a 16-bus isolated sample network supplied by CESI. The network consists of two main primary substations Brussels and Amsterdam, Amsterdam substation is shown in Figure 8-1. Three voltage levels exist: extra high voltage (red), high voltage (blue and green), and medium voltage (yellow).

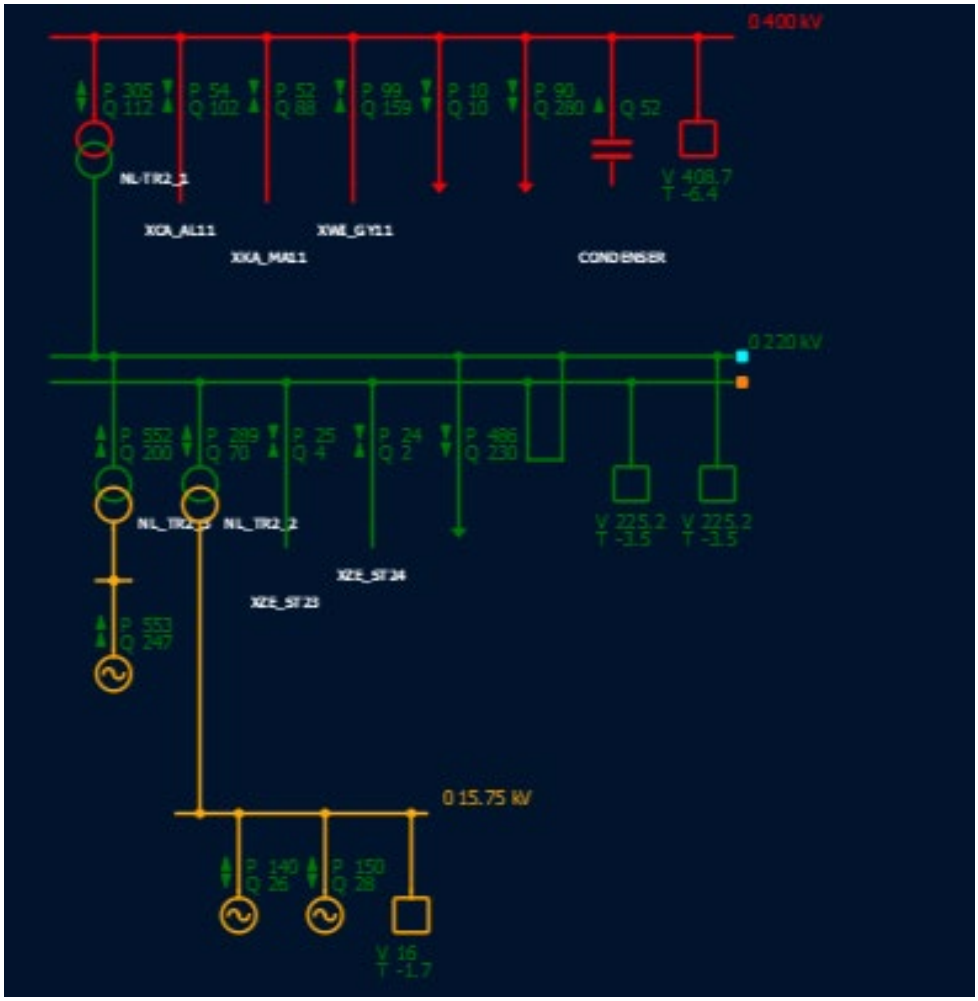

Figure 8-1 Amsterdam primary substation of sample grid

A summary of the network elements in the initial steady state condition is shown in Table 8-1 and Table 8-2. All the generators employed in the network are not equipped with Secondary frequency regulation control as this functionality is not yet introduced in DYANA. The total load and generation are 986 MW and 1050 MW respectively with losses of 64 MW.

Table 8-1 Test network 1 generators description.

Equipment	Type	Substation	Power factor	Active power [MW]	Voltage [kV]	Primary regulation parameters
Generator 1	Thermal	Amsterdam	0.90	140	16.03	Droop =5% Power = 100 MW
Generator 2	Thermal	Amsterdam	0.90	150	16.02	Droop =5% Power = 100 MW
Generator 3	Thermal	Amsterdam	0.90	553	16.02	Droop =5% Power = 400 MW
Generator 4	Thermal	Brussels	0.85	118	21.99	Droop =5% Power = 80 MW
Generator 5	Thermal	Brussels	0.85	90	10.81	Droop =5% Power =80 MW
Generator 6	BESS	Brussels	1	–	21	Droop =5% Power =5 MW

Table 8-2 Test network 1 loads description.

Equipment	Type	Substation	Active power [MW]	Reactive power [MVAR]	Current [A]	Voltage [kV]
Load 1	PQ	Amsterdam	486	230	1379	225.2
Load 2	PQ	Amsterdam	10	10	20	408.7
Load 3	PQ	Amsterdam	90	280	416	408.7
Load 4	PQ	Brussels	200	50	531	224.3
Load 5	PQ	Brussels	200	90	1096	115.5

The BESS was chosen based on a commercial battery of 5 MWh based on the same data of Figure 6-8. As discussed in previous chapters the ECM do not extrapolate correct data hence the power limit of the battery was set to 5 MWh. The BESS is connected to the medium voltage level at the Brussels substation with thumbnail of generator as shown in Figure 8-2.

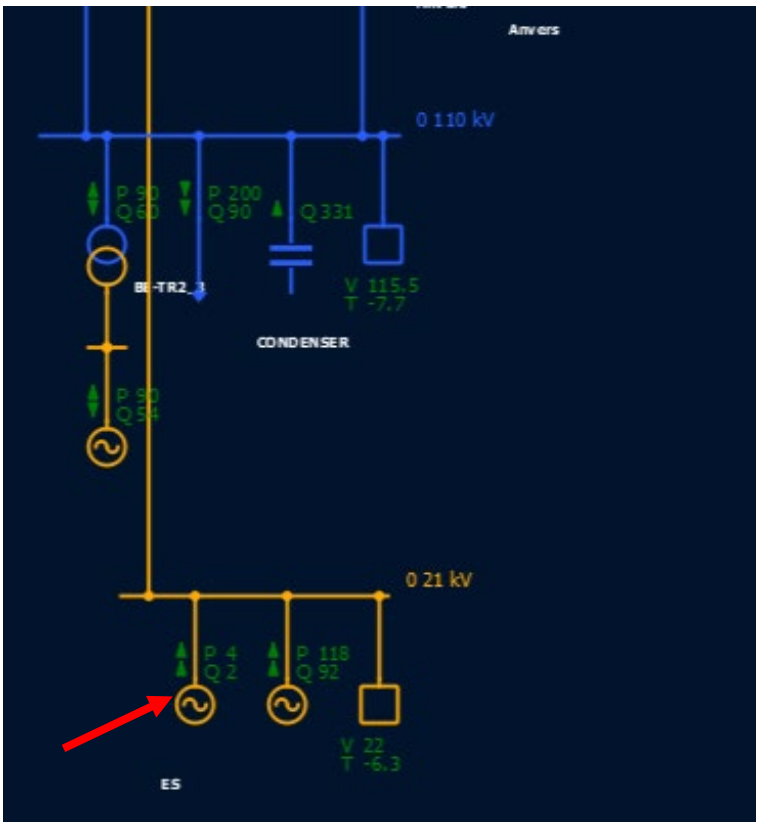

Figure 8-2 BESS connection to the grid, pointed by the red arrow.

Before running a dynamic simulation, the solver's parameters must be set. CESI's own solver was used which is based on Adam-Moulton algorithm, the parameters are shown in Figure 8-3.

Figure 8-3 Solver's parameters used in this test.

Prior to performing the dynamical simulation, a power flow is carried out to initialize the system variables. All the upcoming tests are assumed to be initiated with the conditions stated in Table 8-1 and Table 8-2 unless stated otherwise.

8.1. Stable grid conditions

The first test is for checking the BESS stability during a constant conditions system. Active and reactive power setpoint of 5 MW and 2 MVAR were initialized independently. The results are in Figure 8-4 where the system remains stable in both conditions.

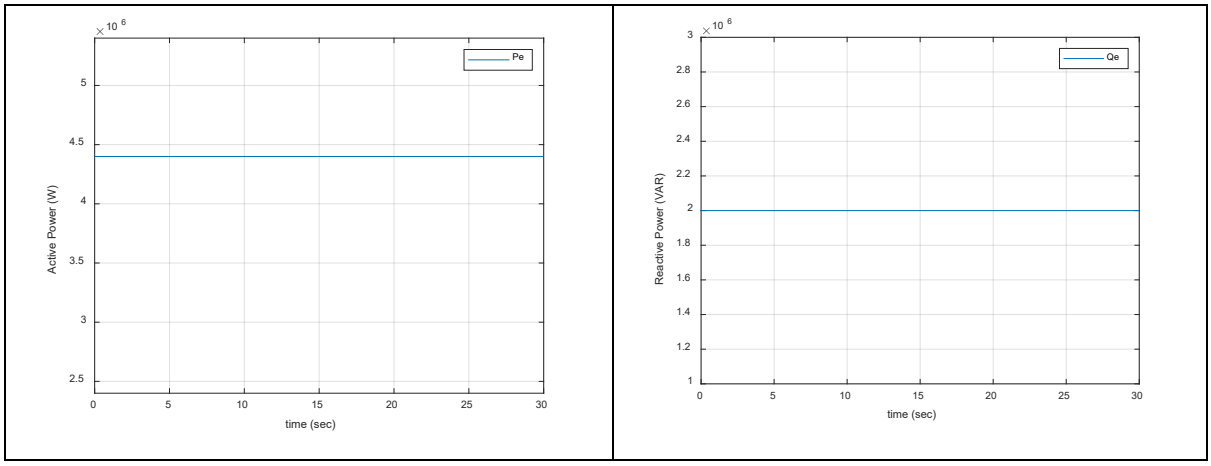

Figure 8-4 Stable system operation.

8.2. Power Injection mode.

Throughout this section two main goals are sought; to provide a validation on the performance of the BESS by tracking a reference active/reactive power setpoint and calibrating the controllers to emulate real behaviour correctly. In Figure 8-5 an active power setpoint of 2 MW is triggered at second 5, it can be interpreted that the system reaches steady state after 700 milliseconds a value close to real data.

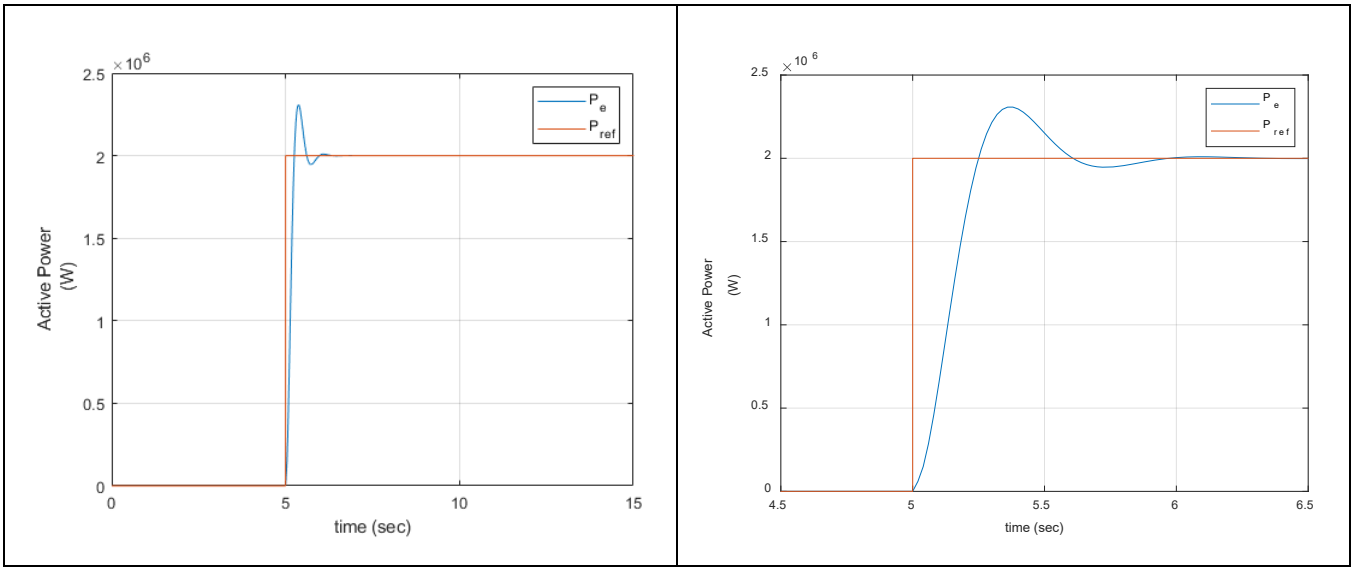

Figure 8-5 Active power setpoint test

A similar is setup is performed for the reactive power setpoint where a step signal of 1.5 MVAR is triggered at second 5. The result is shown in Figure 8-6 with a closer look in the right panel the settling time of about 1 second which a value close to real data .

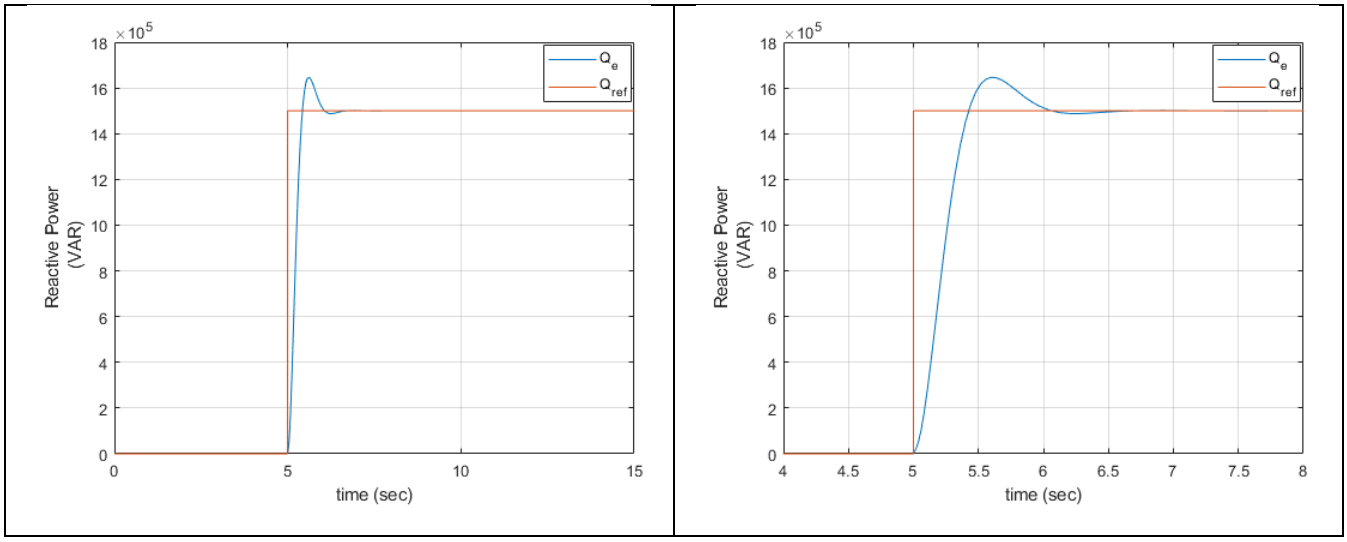

Figure 8-6 Reactive power setpoint test

8.2.1. State of Charge estimation

The SOC estimation of the BESS was tested using a step input reference point of 5 MW at time 0 sec and the SOC of the BESS is at 50%. The theoretical calculations using look-up Peukart's law predicts a battery discharge at time 1128 seconds which corresponds with the result obtained from the DYANA simulation in Figure 8-7.

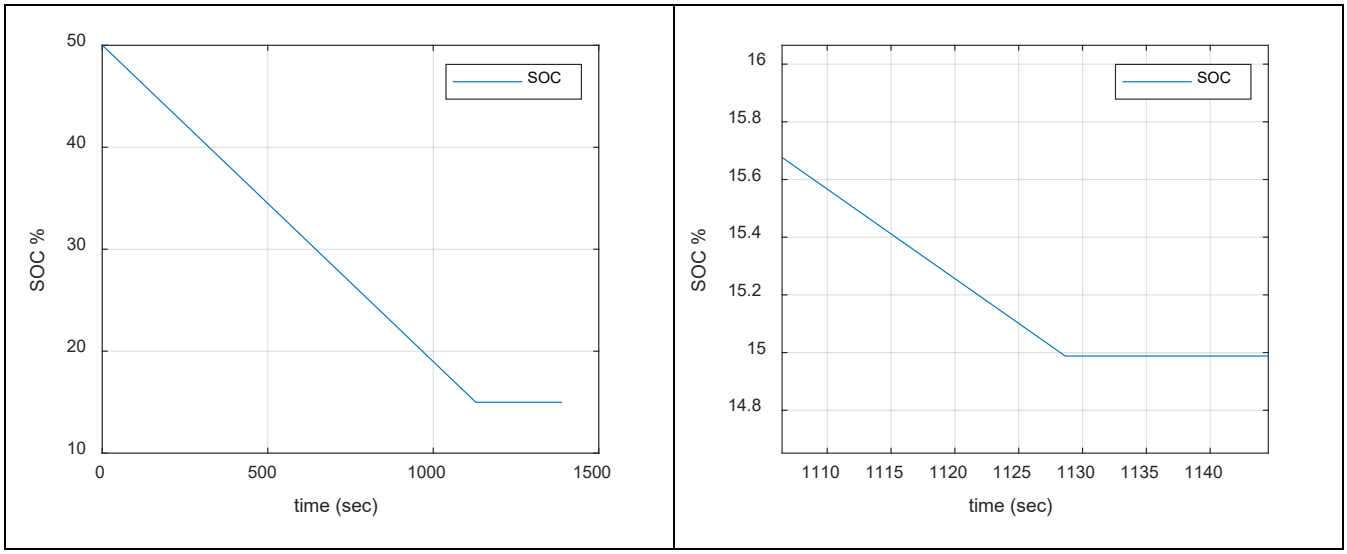

Figure 8-7 SOC DYANA estimation

8.3. Loss of generation mode.

In this test a generation loss of generation power was simulated were at t=10 sec a generator of 50 MW was disconnected. In Figure 8-8 the BESS reaction to the loss of generation is presented where the reactive power setpoint was previously set to 0. The behaviour of the battery conforms with the theoretical behaviour since the adopted droop constant was 20 $p.u.$ where the measured frequency dip provides a power injection of 93.6 kW. An important observation can be made in this test that the SOC does not change significantly through the whole minute operation therefore low implications on the battery dynamics as suggested by EPRI. According to the previous observation it can be assumed for small time period simulations the standard model without circuit model can be used for less computational effort. This assumption however falls short at high power long period simulations.

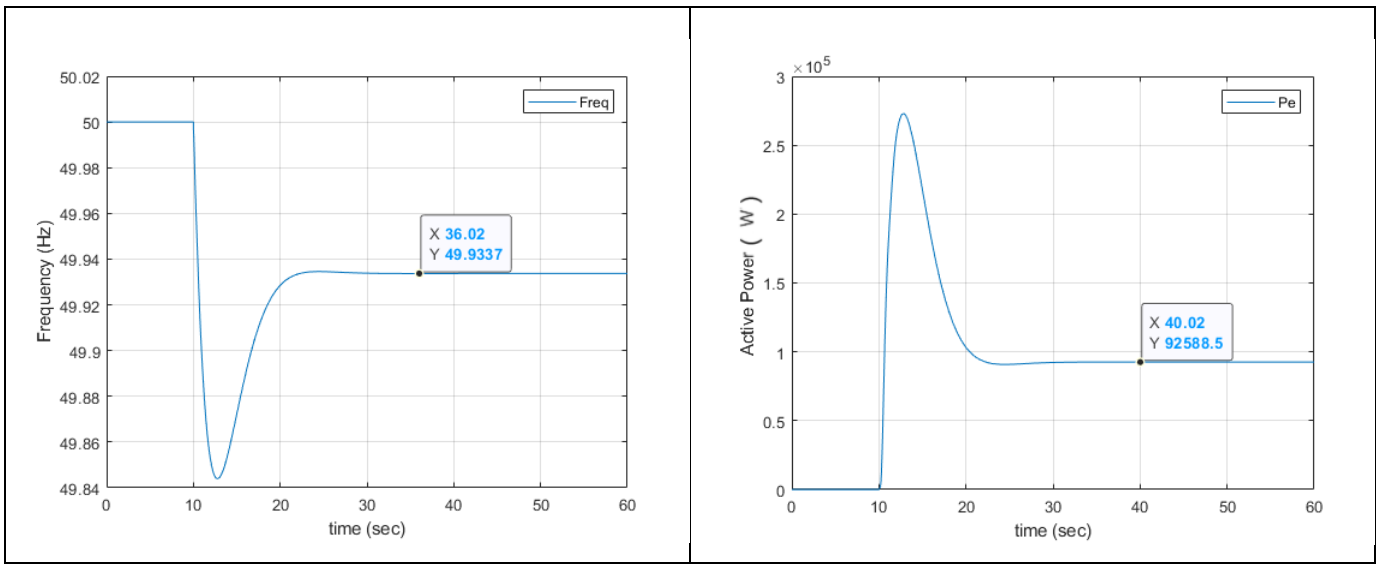

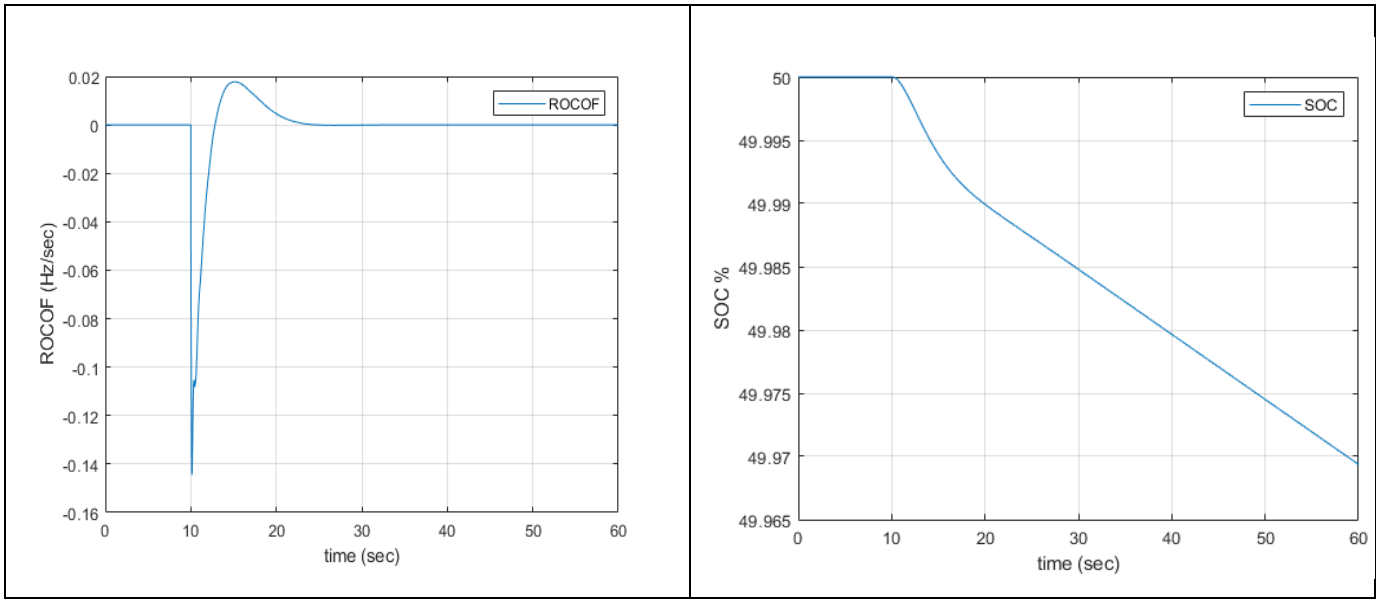

Figure 8-8 Loss of generation mode results

The effect of different droop setting was investigated were the droop constant was set to 25 $p.u.$ and the same generation loss was simulated. The result is shown in Figure 8-9 conforming with the theoretical result of 0.1157 MW.

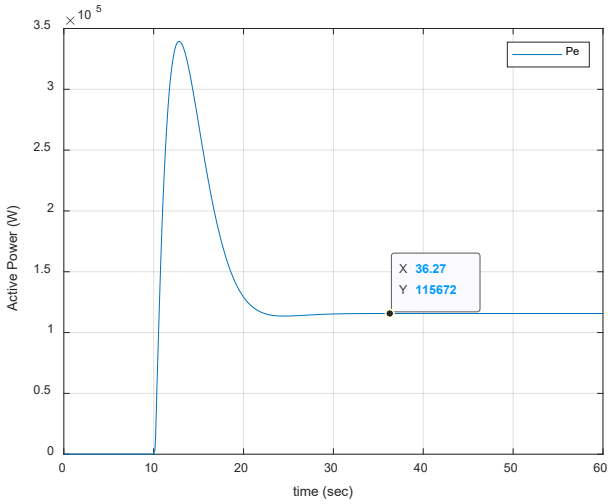

Figure 8-9 Effect of changing droop constant

8.4. Loss of load mode

In this test a generation loss of load power was simulated were at t=10 sec a load of 100 MW was disconnected.

In the Figure 8-10 BESS reaction to the loss of load is presented where the reactive power setpoint was previously set to 0. The behaviour of the battery conforms with the theoretical

behaviour since the adopted droop constant was 25 $p.u.$ where the measured frequency dip provides a power withdrawal of 0.28 kW.

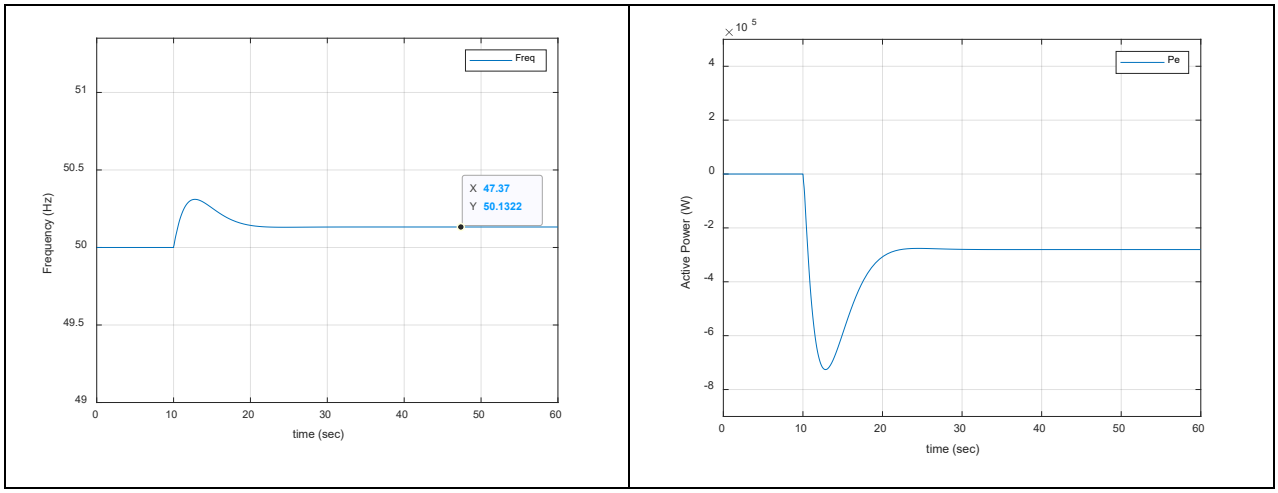

Figure 8-10 Loss of load test

8.5. Charge Controller operation

In this test the operation of the charge controller is tested where the power limiting functioning ability is observed and the operation near the full discharge limits. In the first the BESS is operating at a previous setpoint of 4.4 MW and a loss of generation of 50 MW occurring at a nearby bus. The result is shown in Figure 8-11 where the charge controller of the battery successfully limits the output power of the BESS.

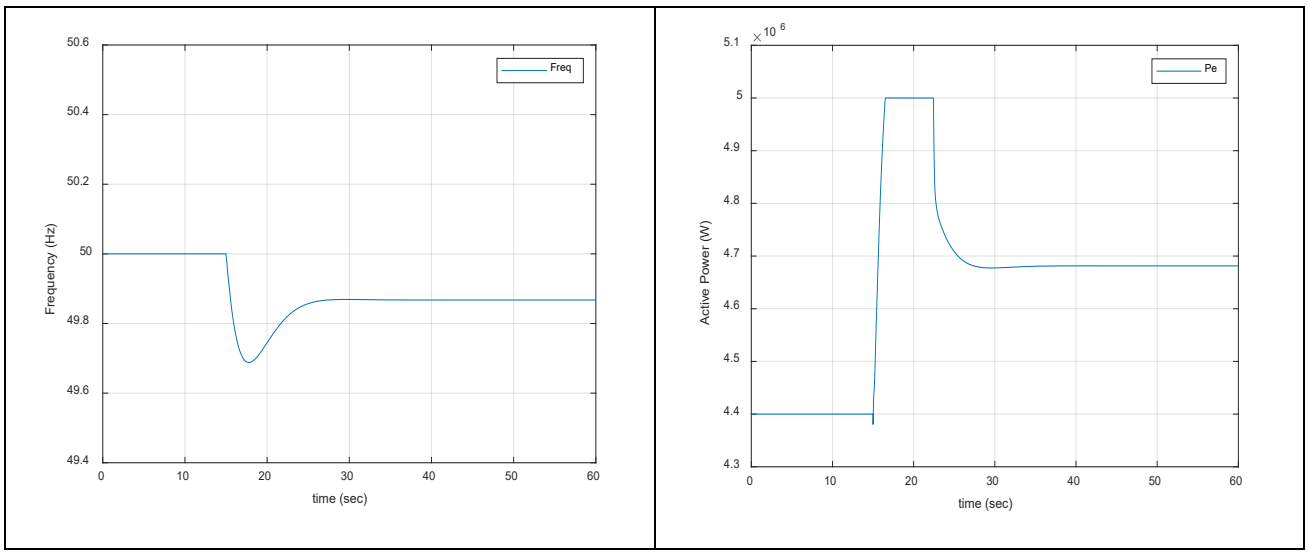

Figure 8-11 Charge controller test; power limit.

The second test involves the BESS operating near the deep discharge limit to address two important issues risen by SONI [38] which are the capacity limited ramp rate and the activation of the BESS when it is near its limit. The test aims first at observing the operation of the charge controller near the operational limit then study the effect of the BESS abrupt disconnection on the bulk power system. In the test the BESS was supplying a network suffering a loss of generation event through primary frequency response control, in the network codes the PFR service should remain at least for 15 consecutive minutes from the activation signal. In the test the activation signal is at time 0 sec and the BESS was operating near the capacity limit. After approximately two and half minutes two important observations can be made from Figure 8-12. The first is the correct operation of the charge controller where it disconnects the battery when the deep discharge limit is reached. The second and more important is the effect of the disconnection on the BESS on a distress grid where the grid has already suffered from a loss of generation and with the battery disconnection further imbalance occurs which may worsen the network's safety and stability.

This situation rises concerns on the regulations concerned with the BESS since the limited capacity ramp rate was not addressed by the expert group and neither the relation between the battery SOC and the activation of grid services as traditional regulations addressed power headroom but there is no mention of energy headroom regarding BESS case.

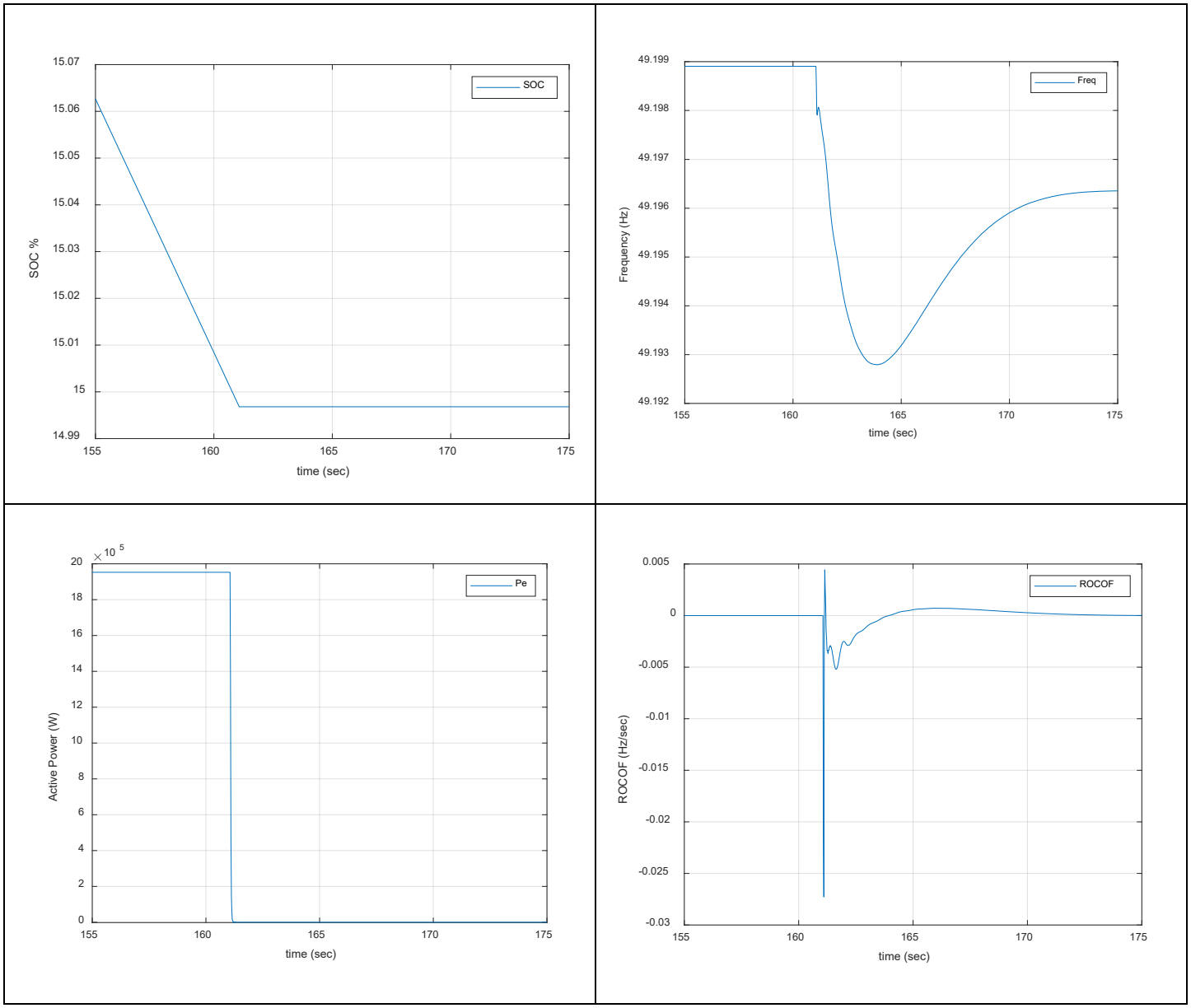

Figure 8-12 Charge controller test operating near SOC limit.

8.6. Variable frequency test

A variable frequency test similar to the one conducted in OpenModelica was performed in TESEO. To create a variability in the network's frequency DYANA has stochastic loads feature which is based on OpenModelica random noise function block where the base load is multiplied with the random noise signal having standard deviation of 0.7 p.u. and time constant of 3.5 seconds. An example of load ins stochastic mode is shown in Figure 8-13 where the base load is 210 MW. This stochastic behaviour induces a variability in the network's frequency as in Figure 8-14.

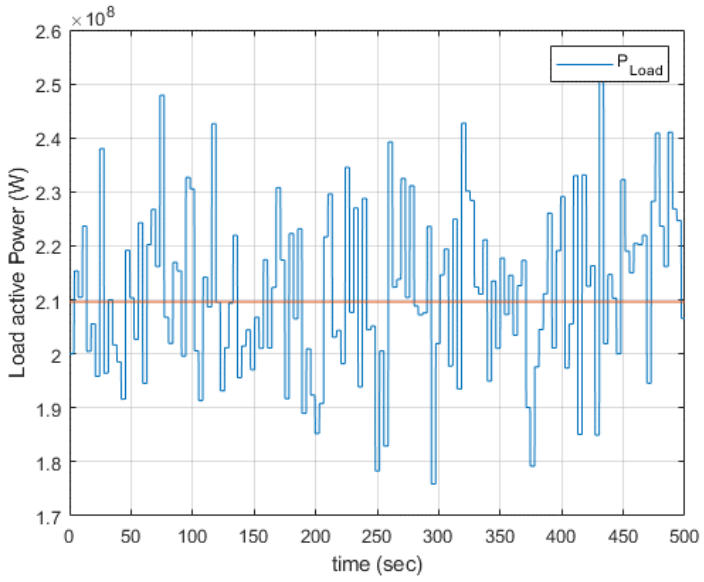

Figure 8-13 Stochastic load feature in DYANA

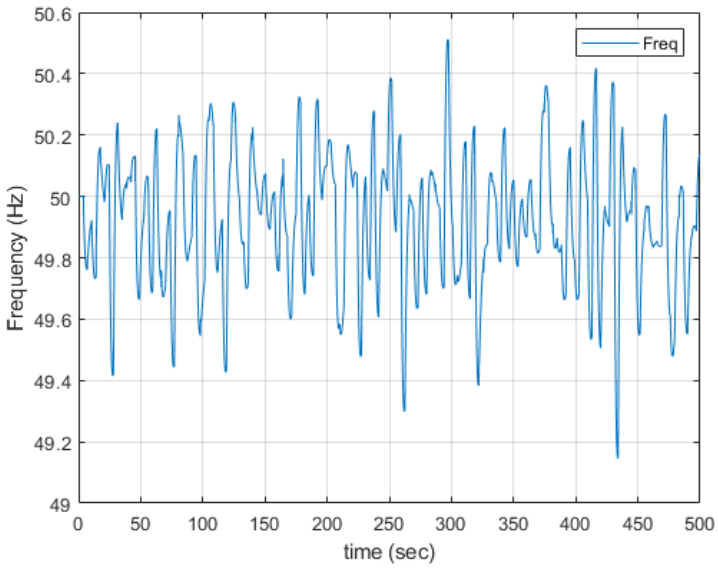

Figure 8-14 Variable network frequency

The behaviour of the BESS is demonstrated in Figure 8-15 and Figure 8-16 where the state of charge of the battery is decreasing over the simulation time period which conforms with the fact that the network frequency is 49.91 Hz and the BESS active power output is 0.16 MW.

The variable frequency test highlights the computational advantage of the model where it can simulate a variable load for a time window of hours, with the BESS droop response activated, on a standard personal computer in few minutes without any complexity.

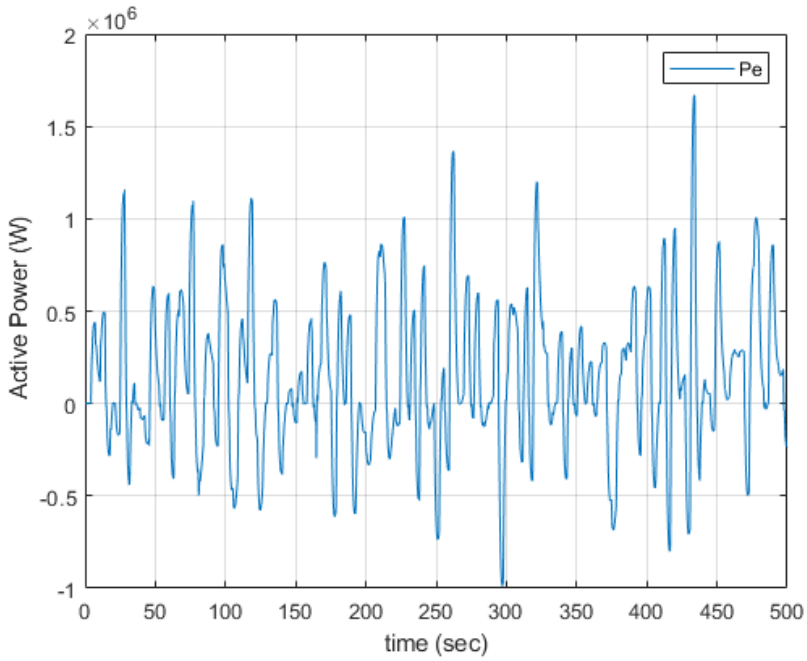

Figure 8-15 BESS Active power output at variable frequency test

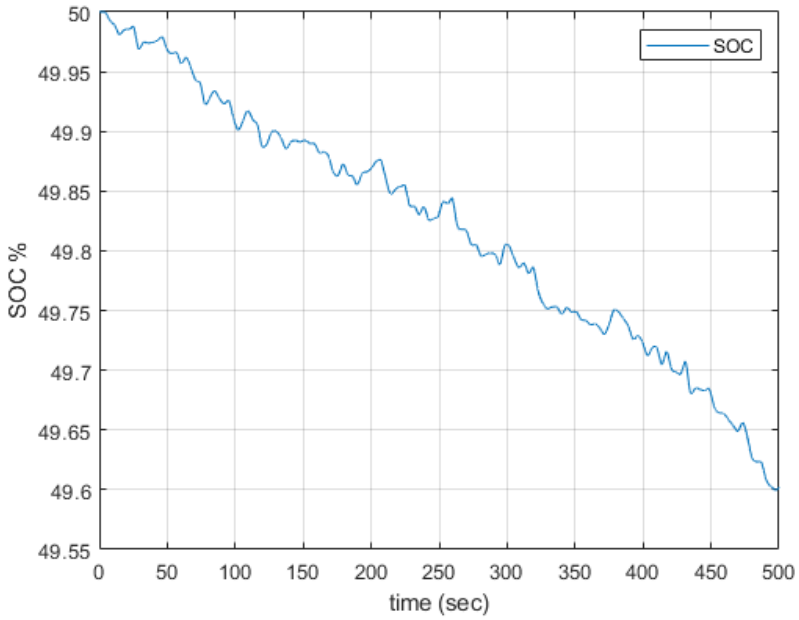

Figure 8-16 BESS SOC at variable frequency test

8.7. Microgrid with RES penetration

The aim of this scenario is to test the operation of the BESS in a relatively small microgrid with RES penetration. With the increasing penetration of RES, the overall kinetic energy stored in the rotating masses of the thermal units decreases hence decreasing the system inertia. The significant loss of the system's inertia can affect the frequency response. The microgrid utilized in this test is similar in structure to the previous one but the loads and generators are modified. as shown in Table 8-3 and Table 8-4. No secondary frequency regulation is activated, and the BESS droop "K" constant is increased. The generator inertia constant is 3.75 seconds.

Table 8-3 Test network 2 load specifications

Equipment	Type	Substation	Active power [MW]	Reactive power [MVAR]	Current [A]	Voltage [kV]
Load 1	PQ	Amsterdam	186	130	577	227.2
Load 2	PQ	Amsterdam	10	10	20	409
Load 3	PQ	Amsterdam	90	280	416	409
Load 4	PQ	Brussels	200	50	531	224.3
Load 5	PQ	Brussels	200	90	1096	115.5

Table 8-4 Test network 2 generators specifications

Equipment	Type	Substation	Power factor	Active power [MW]	Voltage [kV]	Primary regulation parameters
Generator 1	Wind	Amsterdam	0.80	30	16.03	–
Generator 2	Wind	Amsterdam	0.80	30	16.02	–
Generator 3	Thermal	Amsterdam	0.90	632	175	Droop =5% Power = 400 MW
Generator 4	Wind	Brussels	0.80	30	21	–
Generator 5	Wind	Brussels	0.80	30	10.81	–
Generator 6	BESS	Brussels	1	–	21	Droop =2% Power =5 MW

In this test a loss of 20 MW generation is simulated and the effect on the system is observed with and without BESS. Prior to performing the dynamical simulation, a power flow is carried out to initialize the system variables. The upcoming test is initiated with the conditions stated in Table 8-3 and Table 8-4

The generation loss is simulated in two cases with and without BESS connected. The results are shown in Figure 8-17 and Figure 8-18. It can be observed that the presence of BESS improves the network frequency response with a lower frequency drop and damping the ROCOF. This conforms with [17] proposal of utilizing BESS in fast frequency response for better performance in the frequency arresting period and decreasing the nadir. The FFR service will complement PFR and not substitute it. The static droop is only a single control suggestion for PFR a ROCOF based or combination can be utilized in this scheme.

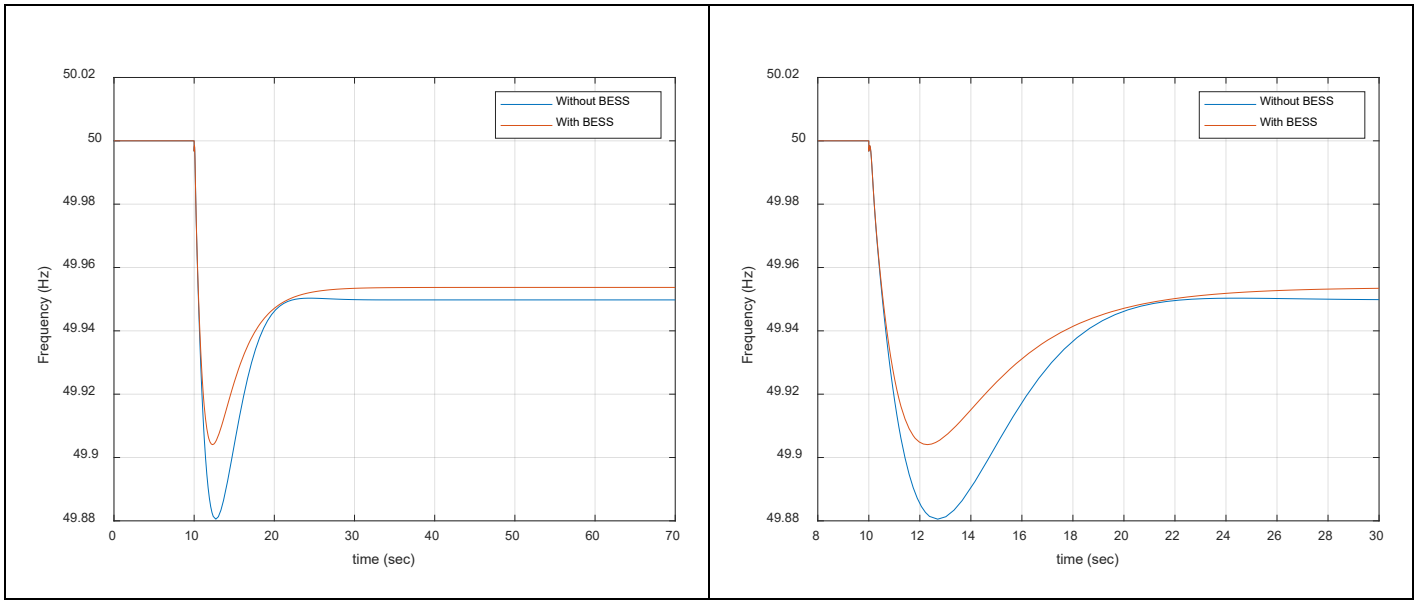

Figure 8-17 Frequency drop in the two cases

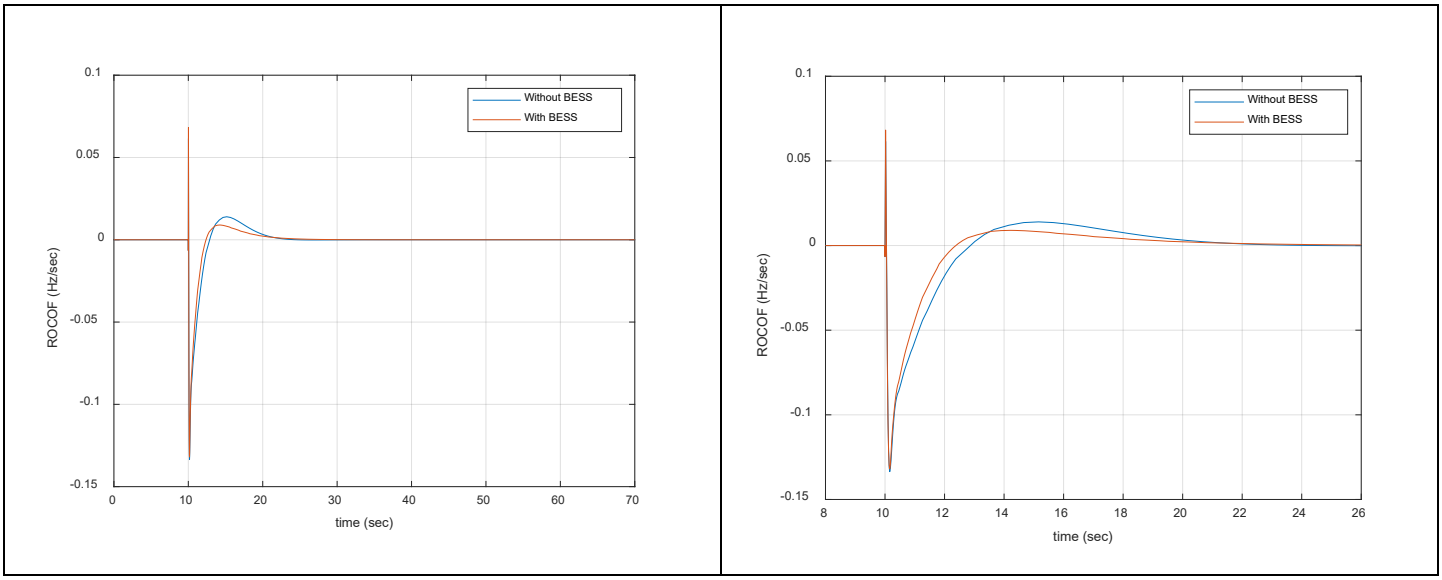

Figure 8-18 ROCOF in the two cases

Conclusion

BESS are the key enabling technologies for facing the upcoming challenges concerning utility scale services. BESS will allow easier merger of RES and facilitate the path for smarter grid hence an accurate model representation will produce reliable results upon executing power system performance studies. This work is collaboration between Politecnico di Milano and CESI S.p.A to develop a standard BESS dynamical model in OpenModelica. The model is to be utilized in the proprietary network analysis tool TESEO developed by CESI for the Italian TSO TERNA. A BESS modified standard model foundation is proposed in his study, developed in OpenModelica to comply CGMES standard. The model is based on WECC approved modular EPRI's generic renewable energy system models combined with an add-on feature of battery cell modelling using lithium-ion technology-based ECM with user defined real data. The model can perform in a steady state simulation as well as dynamic simulation through active/reactive power control along with frequency regulation services. The model was tested in OpenModelica and in a sample network in TESEO and found to match the theoretical expectations of the commercial battery data utilized, transient behaviour of battery systems, and the Italian grid code specifications regarding frequency regulation. The fine-tuning add-on was found to push few of the EPRI model limitations concerning long period simulations, BESS with high rated power/energy ratio, DC voltage monitoring, and SOC with operating current adjustment. BESS specific grid codes are now of great importance since it has been observed in few scenarios that BESS can deteriorate the bulk power system stability rather than supporting it in particular, the capacity limited ramp rate and capacity limited ancillary services activation where the system's ROCOF was obviously affected.

The model developed in this thesis project will be proposed to ENTSO-E as a foundation for BESS embracing the CGMES standard. Prior to the proposal the model performance can be improved in the upcoming work by realizing additional control features like fault ride through and local voltage control.

References

[1] I. R. E. Agency, *Renewable Power Generation Costs in 2018*. 2018.

[2] International Energy Agency, “Renewables Information 2020,” *IEA Stat.*, p. 497, 2020.

[3] B. V. A. Boicea, “Energy Storage Technologies : The Past and the Present,” vol. 102, no. 11, pp. 1777–1794, 2014.

[4] EU, “Directive (EU) 2018/2001 of the European Parliament and of the Council on the promotion of the use of energy from renewable sources,” *Off. J. Eur. Union*, vol. 2018, no. L 328, pp. 82–209, 2018.

[5] A. R. Dehghani-Sanij, E. Tharumalingam, M. B. Dusseault, and R. Fraser, “Study of energy storage systems and environmental challenges of batteries,” *Renew. Sustain. Energy Rev.*, vol. 104, no. November 2018, pp. 192–208, 2019.

[6] A. Poullikkas, “A comparative overview of large-scale battery systems for electricity storage,” *Renew. Sustain. Energy Rev.*, vol. 27, pp. 778–788, 2013.

[7] F. Nadeem, S. Member, and S. M. S. Hussain, “Comparative Review of Energy Storage Systems , Their Roles and Impacts on Future Power Systems,” *IEEE Access*, vol. PP, no. c, p. 1, 2018.

[8] A. R. Dehghani-Sanij, E. Tharumalingam, M. B. Dusseault, and R. Fraser, “Study of energy storage systems and environmental challenges of batteries,” *Renew. Sustain. Energy Rev.*, vol. 104, no. January, pp. 192–208, 2019.

[9] F. Nadeem, S. M. S. Hussain, P. K. Tiwari, A. K. Goswami, and T. S. Ustun, “Comparative review of energy storage systems, their roles, and impacts on future power systems,” *IEEE Access*, vol. 7, no. c, pp. 4555–4585, 2019.

[10] U. Energy Information Administration, “Battery Storage in the United States: An Update on Market Trends,” no. July, 2020.

[11] IRENA, “Utility-Scale Batteries,” p. 7, 2019.

[12] A. Eller, “Commissioned By Ifc and Esmap,” *Energy storage trends Oppor. Emerg. Mark.*, p. 2009, 2017.

[13] Terna, “Partecipazione Alla Regolazione Di Frequenza e Frequenza-Potenza - allegato

A15," *Allegato A15*, 2008.

[14] European Network of Transmission System Operators for Electricity (ENTSO-E), "LOAD-FREQUENCY CONTROL AND PERFORMANCE A1 – Appendix 1 : Load-Frequency Control and Performance [E]," *Control*.

[15] NERC, "Frequency Response Initiative Report NERC's Mission," p. 212, 2012.

[16] S. Rossi, "Electricity Balancing Market and Balancing Platfoms European way to the electricity market design European way to the electricity market design," 2019, no. November, pp. 1–11.

[17] NERC Inverter-Based Resource Performance task Force (IRPTF), "Fast Frequency Response Concepts and Bulk Power System Reliability Needs," no. March, pp. 1–23, 2020.

[18] Terna, "Fast Reserve: Accompanying note on the public consultation," pp. 1–9, 2019.

[19] D. Moneta, "Ancillary service markets & Distributed resources : UVA-X pilot projects • Day Ahead Market • Intraday Market," no. December, pp. 1–30, 2019.

[20] E. E. L. Approvazione, D. E. L. Regolamento, and A. I. S. Della, "2020 200/2020/r/," pp. 1–9, 2020.

[21] EDSO, "Integrating electricity storage in distribution grids," no. May, 2016.

[22] S. Ugarte *et al.*, "Energy Storage: Which market design and regulatory incenctives are needed?," *Rep. Eur. Parliam. Com. Ind. Res. Energy*, no. 1, pp. 1–5, 2015.

[23] B. A. Babb and R. E. Emery, "April 2018," *Fam. Court Rev.*, vol. 56, no. 2, pp. 205–206, 2018.

[24] H. K. H. Burgess, "New York Battery and Energy Storage Technology (NY-BEST) Consortium," pp. 1–27, 2018.

[25] KPMG, "EFR tender resul ts KPMG Energy," no. September, pp. 1–3, 2016.

[26] U. K. P. Networks, L. Buzzard, M. W. Network, S. Facility, L. B. Green, and U. K. P. Networks, "' Next generation utility ' wins contract for UK ' s biggest battery," pp. 1–2, 2020.

[27] K. Fehrenbachor, "Tesla moves beyond electric cars with new California battery farm |

Guardian Sustainable Business | The Guardian," *Guard.*, pp. 1–4, 2017.

[28] A. Flusso, L. Scale, S. D. I. Difesa, B. Up, G. Congestioni, and L. Shifting, "Energy Intensive."

[29] A. Bräutigam, T. Rothacher, H. Staubitz, and R. Trost, "The Energy Storage Market in Germany," p. 6, 2017.

[30] B. Michelle and F. May, "Acciona begins operation of hybrid wind & storage plant Tell Us What You Think !," pp. 1–4, 2020.

[31] "Who Is ENTSO-E?" [Online]. Available: https://www.entsoe.eu/about/inside-entsoe/objectives/. [Accessed: 21-Oct-2020].

[32] "Grid Codes - Terna spa." [Online]. Available: https://www.terna.it/en/electric-system/grid-codes. [Accessed: 21-Oct-2020].

[33] ENTSO-E, "Phase 2 Storage Expert Group :," 2020.

[34] ENTSOE, "Phase 1 Storage Expert Group :," 2018.

[35] CEI Standard 0-16., "Reference technical rules for the connection of active and passive users to the HV and MV electrical Utilities," *Ital. Electrotech. Comm.*, 2019.

[36] CEI Standard 0-21., "Reference technical rules for the connection of active and passive users to the LV electrical Utilities," *IItalian Electrotech. Comm.*, 2014.

[37] EirGrid, "EirGrid Grid Code, version 8," *Comm. Regul. Util.*, no. July, pp. 1–349, 2019.

[38] D. Eirgrid and N. Ireland, "Battery ESPS Grid Code Implementation Note," no. June, 2020.

[39] "SONI GRID CODE 14 th February 2020," no. February, 2020.

[40] H. Bahar, Y. Abdelilah, F. Briens, K. Daszkiewicz, and T. Rinke, "Renewables 2019, Market analysis and forecast from 2019 to 2024," *Isbn 978-92-64-30684-4*, no. October 2019, pp. 1–7, 2019.

[41] B. M. T. Lawder *et al.*, "System (BESS) and Battery Management System (BMS) for Grid-Scale Applications," vol. 102, no. 6, 2014.

[42] EUR-Lex, "Directive 2006/66/EC of the European Parliament and of the Council of 6 September 2006 on batteries and accumulators and waste batteries and accumulators and

repealing Directive 91/157/EEC," *Off. J. Eur. Union*, vol. L 266, no. September 2006, pp. 1–14, 2006.

[43] S. Vazquez, S. M. Lukic, E. Galvan, L. G. Franquelo, and J. M. Carrasco, "Energy Storage Systems for Transport and Grid Applications," vol. 57, no. 12, pp. 3881–3895, 2010.

[44] F. J. Gomez, L. Vanfretti, and S. H. Olsen, "CIM-Compliant power system dynamic model-to-model transformation and modelica simulation," *IEEE Trans. Ind. Informatics*, vol. 14, no. 9, pp. 3989–3996, 2018.

[45] M. Otter, "Modelica Overview," p. 23, 2013.

[46] P. Fritzson, *Introduction to Modeling and Simulation of Technical and Physical Systems with Modelica*. 2012.

[47] P. Fritzson *et al.*, "The OpenModelica Integrated Modeling, Simulation, and Optimization Environment," *Proc. Am. Model. Conf. 2018, Oct. 9-10, Somb. Conf. Center, Cambridge MA, USA*, vol. 154, pp. 206–219, 2019.

[48] B. M. T. Lawder *et al.*, "System (BESS) and Battery Management System (BMS) for Grid-Scale Applications," vol. 102, no. 6, 2014.

[49] G. L. Plett, *Battery Management Systems, Volume II: Equivalent-Circuit Methods*. 2015.

[50] G. L. Plett, *Battery Management Systems, Volume I: Battery Modeling*. 2015.

[51] A. Y. R. Iravani, *Voltage-Sourced Converters in Power Systems: Modeling, Control, and Applications*. 2010.

[52] "Company - DIgSILENT." [Online]. Available: https://www.digsilent.de/en/company.html. [Accessed: 02-Oct-2020].

[53] DIgSILENT GmbH, "DIgSILENT PowerFactory Application Example Battery Energy Storing Systems," *Batter. Energy Storing Syst.*, pp. 1–28, 2010.

[54] "PSS®E – transmission planning and analysis | PSS® power system simulation and modeling software | Global." [Online]. Available: https://new.siemens.com/global/en/products/energy/energy-automation-and-smart-grid/pss-software/pss-e.html. [Accessed: 02-Nov-2020].

[55] PSSE SIEMENS, "Genrator Models CBEST."

[56] PSSE SIEMENS, “Generic Renewbale Electrical Control.”

[57] P. Pourbeik *et al.*, “Value and Limitations of the Positive Sequence Generic Models of Renewable Energy Systems,” pp. 1–10, 2015.

[58] P. Krause, O. Wasynczuk, S. Sudhoff, and S. Pekarek, Eds., *Analysis of Electric Machinery and Drive Systems*. Hoboken, NJ, USA: John Wiley & Sons, Inc., 2013.

[59] K. Sibi, “Generic Battery Model Covering Self-discharge and Internal Resistance Variation,” *2016 IEEE 6th Int. Conf. Power Syst.*, pp. 1–5, 2016.

[60] B. Enache, M. Ieee, E. Lefter, and C. Stoica, “Comparative Study for Generic Battery Models used for Electric Vehicles,” *2013 8TH Int. Symp. Adv. Top. Electr. Eng.*, no. 2, pp. 1–6, 2013.

[61] S. N. Motapon, A. Lupien-bedard, F. Member, H. Fortin-blanchette, K. Al-haddad, and F. Member, “IEEE TRANSACTIONS ON INDUSTRIAL ELECTRONICS A Generic Electro-Thermal Li-ion Battery Model for Rapid Evaluation of Cell Temperature,” vol. 0046, no. c, 2016.

[62] R. Xiong, *Battery management algorithm for electric vehicles*. 2019.

[63] G. L. Plett, “High-performance battery-pack power estimation using a dynamic cell model,” *IEEE Trans. Veh. Technol.*, vol. 53, no. 5, pp. 1586–1593, 2004.

[64] E. Raszmann, K. Baker, Y. Shi, and D. Christensen, “Modeling stationary lithium-ion batteries for optimization and predictive control,” *2017 IEEE Power Energy Conf. Illinois, PECI 2017*, no. February, 2017.

[65] Poyan Pourbik, “Specification of the Second Generation Generic Models for Wind Turbine Generators,” no. 23.01.2014, p. 36, 2014.

[66] WECC Renewable Energy Modeling Task Force, “WECC PV Power Plant Dynamic Modeling Guide,” no. X, pp. 1–26, 2014.

[67] EPRI, “Model User Guide for Generic Renewable Energy System Models,” p. 74, 2015.

[68] P. Pourbeik, “Proposed Changes to the WECC WT4 Generic Model for Type 4 Wind Turbine Generators,” no. X, p. 35, 2011.